

# Goal-oriented modelling-error estimation for hierarchical models of a different type

Proefschrift

ter verkrijging van de graad van doctor  
aan de Technische Universiteit Delft,  
op gezag van de Rector Magnificus prof.dr.ir. J.T. Fokkema,  
voorzitter van het College voor Promoties,  
in het openbaar te verdedigen op maandag 7 mei 2007 om 10:00 uur

door

Jelmer Mennolt CNOSEN,  
ingenieur Luchtvaart- en Ruimtevaarttechniek,  
geboren te Nijland.

Dit proefschrift is goedgekeurd door de promotoren:

Prof.dr.ir.drs. H. Bijl  
Prof.dr.ir. B. Koren  
Prof.dr.ir. P.G. Bakker

Samenstelling promotiecommissie:

Rector Magnificus,	voorzitter
Prof.dr.ir.drs. H. Bijl,	Technische Universiteit Delft, promotor
Prof.dr.ir. B. Koren,	Technische Universiteit Delft, promotor
Prof.dr.ir. P.G. Bakker,	Technische Universiteit Delft, promotor
Prof.dr.ir. P. Wesseling,	Technische Universiteit Delft
Prof.dr.ir. C. Lacor,	Vrije Universiteit Brussel
Prof.dr.ir. H. Deconinck,	Von Karman Institute for Fluid Dynamics
Dr.ir. B.I. Soemarwoto,	Nationaal Lucht- en Ruimtevaartlaboratorium NLR

Het onderzoek is gesteund door de Technologie Stichting STW onder projectnummer DMR.5670.

ISBN 978 90 8559 289 1

# Summary

Nowadays, computer simulations of physical systems (e.g. a propulsion system) or processes (e.g. combustion) play a very important role in science and engineering. For many physical systems or processes mathematical models have been derived (often in the form of partial differential equations) with different levels of sophistication and accuracy. The collection of models describing the same physical system or process is called a class of hierarchical models. The hierarchy is determined by the level of sophistication of the model. Considering two different models, the sophisticated model is referred to as ‘fine model’ and the approximating model as ‘coarse model’.

In many classes of hierarchical models, solving a fine model is computationally costlier than solving a coarse model. Using the coarse model however, introduces a so-called modelling error in the solution with respect to the fine model solution. A new trend in computer simulations to reduce computational time but to meet a certain required accuracy, is adaptive modelling. This means that a computer simulation is started with a coarse model which is adapted to a fine model when the required accuracy is not achieved. This accuracy is, in many engineering applications, the accuracy of a quantity of interest, such as the lift of an airfoil, instead of the local accuracy of the solution. To drive an adaptive modelling process in which the accuracy of a quantity of interest is the goal, an estimator of the modelling error in the quantity of interest is required. Such an estimator is called a goal-oriented modelling-error estimator.

An approach to derive a goal-oriented modelling-error estimator is the Dual-Weighted Residual (DWR) method. This requires the solution of an adjoint (or ‘dual’) problem that acts as weighting function for the modelling residual. So far, the DWR method has not been applied to classes of hierarchical models where the model equations are of different mathematical type. With different type is meant in this case, that the models require different boundary conditions. This can be caused by a different characterisation of the partial differential equations (parabolic, hyperbolic or elliptic)

or the order of the equations. When the fine and coarse models require different boundary conditions, a modelling residual arises on the boundary (called the ‘boundary residual’) in addition to the modelling residual on the inner domain. Therefore, the main question of this thesis is whether or not the DWR method is suitable for modelling-error estimation in classes of hierarchical models in which the model equations are of a different type.

Two approaches to apply the DWR method are followed: a linear differential approach and a variational approach. The first only applies to linear(ised) problems but is a straightforward approach. The variational approach, in which the model equations are considered in weak formulation, is more complex but allows the derivation of high-order terms in nonlinear problems. For successful use of the DWR method, it is found to be essential to incorporate boundary residuals explicitly in the error estimator. To achieve this for the variational approach the boundary conditions need to be imposed weakly.

An example of a class of hierarchical models where the model changes type is a (nonlinear) convection-diffusion problem in which the convection-diffusion equation is the fine model and the convection equation is the coarse model. Omitting the diffusion in the coarse model means that the order of the equation changes. Such a problem is known as a singular perturbation problem in which the modelling error does not have to vanish for a vanishing diffusion coefficient. The DWR method in the variational approach has been successfully applied to steady and unsteady linear convection-diffusion problems where the unsteady problem is solved by the Spectral Element Method.

For the nonlinear Burgers problem an analysis is made of high-order terms originating from the nonlinear convection term and from a nonlinear quantity of interest. The analysis reveals computable high-order boundary terms that can be of significant magnitude and should therefore be included in the error estimator. To investigate goal-oriented modelling-error estimator by means of the DWR method in the Burgers problem, computations are performed using the Finite Volume Method. Although the solution restrictions according to the variational approach are violated in case of a shock, the DWR performs well in the studied Burgers problems as well.

One can use the fine or the coarse dual solution as weighting function in the DWR method. Using the coarse dual solution is essential for the efficiency of the DWR method in adaptive modelling, since solving the fine primal and dual problems is equally expensive in a computational sense. Because of this, adaptive modelling becomes unusable to decrease computational time when using the fine dual problem. When the coarse dual problem is used however, an additional error is introduced in the error es-

imator. The cases studied show, as can be expected, that the quality of the coarse dual-weighted estimator is lower than the fine dual-weighted estimator. In all cases the estimator improves when the diffusion coefficient decreases.

Finally, a preliminary study is made of the DWR method in the linear differential approach, applied to a 2-D flow problem described by the Navier-Stokes equations (the fine model) and the Euler equations (the coarse model). From the cases studied, it is concluded that the DWR method is suitable for classes of hierarchical models in which the model equations are of a different type. The variational approach is preferred for nonlinear problems.



# Samenvatting

Computersimulaties van fysische systemen of processen spelen tegenwoordig een zeer belangrijke rol in wetenschap en techniek. Voor vele fysische systemen of processen zijn verschillende wiskundige modellen (in de vorm van partiële differentiaal vergelijkingen) afgeleid, vaak met een verschillend niveau van verfijning en nauwkeurigheid. De verzameling van modellen die hetzelfde fysische systeem of proces beschrijven, wordt een klasse van hiërarchische modellen genoemd. De hiërarchie wordt bepaald door het niveau van verfijning van het model. Wanneer twee modellen worden beschouwd, wordt het verfijnde model het ‘fijn model’ genoemd en het benaderende model het ‘grof model’.

In vele klassen van hiërarchische modellen is het oplossen van een fijn model duurder in termen van computertijd dan het oplossen van een grof model. Het gebruik van het grof model introduceert echter een modelleringsfout in de oplossing ten opzichte van de oplossing van het fijn model. Een nieuwe tendens in computersimulaties om rekentijd te verminderen maar een bepaalde vereiste nauwkeurigheid te behalen is adaptief modelleren. Dit houdt in dat een computersimulatie wordt gestart met een grof model welke wordt verfijnd naar een fijn model, wanneer de vereiste nauwkeurigheid niet wordt bereikt. In vele technische toepassingen is dit de nauwkeurigheid van een bepaalde grootheid, bijvoorbeeld de lift van een vleugelprofiel, in plaats van de gewenste lokale nauwkeurigheid van de oplossing. Voor het aansluiten van een adaptief modelleringsproces met als doel de nauwkeurigheid van een grootheid, is een schatter van de modelleringsfout in de grootheid vereist. Een dergelijke schatter wordt een doelgerichte modelleringsfout-schatter genoemd.

Een aanpak om een doelgerichte modelleringsfout-schatter af te leiden is de zgn. Dual-Weighted Residual (DWR) methode. Hiervoor moet een geadjungeerd (ook wel ‘duaal’) probleem opgelost worden, waarvan de oplossing als weegfunctie dient voor het modelleringsresidu. Tot op heden is de DWR methode niet toegepast op klassen van hiërarchische modellen waarin de

modellen van een verschillend wiskundig type zijn. Met verschillend type wordt in dit geval bedoeld dat de modelvergelijkingen verschillende randvoorwaarden nodig hebben. Dit kan worden veroorzaakt door de karakterisatie van de partiële differentiaalvergelijking (parabolisch, hyperbolisch of elliptisch) of de orde van de vergelijking. Wanneer het fijn en grof model verschillende randvoorwaarden nodig hebben, ontstaat er een modelresidu op de rand (een ‘randresidu’ genoemd) naast het modelresidu op het binnengebied. Daarom is de hoofdvraag van dit proefschrift of de DWR methode geschikt is voor het schatten van de modelleringsfout in klassen van hiërarchische modellen waarin de modellen van een verschillend type zijn.

Twee verschillende benaderingen zijn gevolgd: een lineaire differentiële benadering en een variationele benadering. De eerstgenoemde is geschikt voor lineaire (en gelineariseerde) problemen en is een ongecompliceerde benadering. De variationele benadering, waarin de modelvergelijkingen in een zwakke formulering worden beschouwd, is complexer maar stelt ons in staat om hoge-orde termen af te leiden in niet-lineaire problemen. Voor een succesvolle toepassing van de DWR methode is het essentieel gebleken om de randresiduen expliciet in de foutschatting op te nemen. Om dit te bereiken bij de variationele benadering, is het van essentieel belang gebleken om de randvoorwaarden zwak op te leggen.

Een voorbeeld van een klasse van hiërarchische modellen waarin een fijn en grof model van een verschillend type zijn, is een (niet-lineair) convectie-diffusie probleem. Hierin is de convectie-diffusie vergelijking het fijn model en de convectievergelijking het grof model. Het weglaten van de diffusie term in het grof model betekent dat de orde van de vergelijking verandert. Dit is een singulier storingsprobleem waarin de modelleringsfout niet naar nul hoeft te gaan wanneer de diffusiecoëfficiënt naar nul gaat. De DWR methode volgens de variationele benadering is succesvol toegepast op stationaire en instationaire lineaire convectie-diffusie problemen. Het instationaire probleem is opgelost met behulp van een Spectrale Elementen Methode.

Voor het niet-lineaire Burgersprobleem is een analyse gemaakt van de hoge-orde termen die voortkomen uit de niet-lineaire convectieterm en de niet-lineaire grootheid. Deze analyse laat zien dat er berekenbare hoge-orde randtermen bestaan die van significante grootte kunnen zijn en om die reden in de foutschatting opgenomen moeten worden. Om de doelgerichte modelleringsfoutschatting door middel van de DWR methode te bestuderen in het Burgersprobleem, zijn berekeningen uitgevoerd met behulp van de Eindige Volume Methode. Ondanks het feit dat hierbij oplossingsrestricties volgens de variationele aanpak worden overtreden, zoals in het geval van een schok, worden goede resultaten verkregen.



Zowel de fijn als de grof geadjungeerde oplossing kan gebruikt worden als weegfunctie in de DWR methode. Het gebruik van de grof geadjungeerde oplossing is essentieel voor de efficiëntie van de DWR methode, omdat het oplossen van het fijn geadjungeerde probleem even duur is in termen van rekentijd als het fijn model. Hierdoor is het adaptief modelleren onbruikbaar om rekentijd te verkorten wanneer het fijn geadjungeerde probleem gebruikt wordt. Gebruiken we het grof geadjungeerde probleem, dan wordt er echter wel een extra fout in de foutschatter geïntroduceerd. Zoals verwacht kan worden, laten de gevallen die bestudeerd zijn zien dat de kwaliteit van de foutschatter op basis van de grof geadjungeerde oplossing minder goed is dan die op basis van de fijn geadjungeerde oplossing. In alle gevallen verbetert de foutschatter wanneer de diffusiecoëfficiënt afneemt.

Tot slot is een voorstudie gemaakt hoe de DWR methode volgens de lineaire differentiële benadering toegepast kan worden op een 2-D stromingsprobleem beschreven door de Navier-Stokes vergelijkingen (het fijn model) en de Euler vergelijkingen (het grof model). Op basis van de gevallen die zijn bestudeerd, kan geconcludeerd worden dat de DWR methode geschikt is voor klassen van hiërarchische modellen waarin de modellen van een verschillend type zijn. Voor niet-lineaire problemen heeft de variationele benadering de voorkeur.



# Contents

<b>Summary</b>	<b>i</b>
<b>Samenvatting</b>	<b>v</b>
<b>1 Introduction</b>	<b>1</b>
1.1 Background of the research . . . . .	1
1.2 Focus of the research . . . . .	4
1.3 Outline of the thesis . . . . .	5
<b>I Theory</b>	<b>7</b>
<b>2 Linear differential approach</b>	<b>9</b>
2.1 The fine and coarse models . . . . .	10
2.2 The dual problems . . . . .	11
2.3 The error estimator . . . . .	14
2.4 Illustration: 1-D diffusion-reaction . . . . .	16
2.4.1 The model problem . . . . .	16
2.4.2 Finding the dual problem . . . . .	18
2.4.3 The error estimator . . . . .	21
2.5 Discrete example with adaptive modelling . . . . .	22
2.5.1 Adaptive modelling algorithm . . . . .	23
2.5.2 Discrete estimation and localisation of the error . . . . .	23
2.5.3 Global and local refinement criteria . . . . .	25
2.5.4 Numerical results . . . . .	26
2.6 Conclusions . . . . .	29
<b>3 Variational approach</b>	<b>31</b>
3.1 Preliminaries and comments . . . . .	32
3.2 The fine or sophisticated model . . . . .	32

3.3	The coarse models . . . . .	34
3.4	The error estimator . . . . .	34
3.5	Treatment of boundaries . . . . .	38
3.6	Illustration: 1-D diffusion-reaction . . . . .	39
3.6.1	Weak formulation of the hierarchical models . . . . .	40
3.6.2	The error estimator . . . . .	43
3.7	Conclusions . . . . .	46
<b>II Applications</b>		<b>49</b>
<b>4</b>	<b>Linear convection-diffusion</b>	<b>51</b>
4.1	Approach for convection-diffusion problems . . . . .	52
4.1.1	The fine model problems . . . . .	53
4.1.2	The coarse model . . . . .	55
4.1.3	The error estimator . . . . .	57
4.1.4	Coarse dual-weighted estimator . . . . .	58
4.2	Steady case 1: integral $Q(u)$ . . . . .	59
4.2.1	The primal problems . . . . .	59
4.2.2	The dual problems . . . . .	60
4.2.3	The error estimator . . . . .	61
4.3	Steady case 2: boundary derivative $Q(u)$ . . . . .	63
4.3.1	The dual problem . . . . .	64
4.3.2	The error estimator . . . . .	67
4.4	Steady case 3: point $Q(u)$ . . . . .	68
4.4.1	The dual problems . . . . .	69
4.4.2	The error estimator . . . . .	70
4.5	Unsteady discrete problem . . . . .	73
4.5.1	The dual solutions . . . . .	74
4.5.2	The error estimator . . . . .	74
4.5.3	Results . . . . .	76
4.6	Conclusions . . . . .	80
<b>5</b>	<b>Nonlinear Burgers</b>	<b>83</b>
5.1	Approach for Burgers problem . . . . .	83
5.1.1	The fine model problem . . . . .	84
5.1.2	The coarse model problem . . . . .	85
5.1.3	The error estimator . . . . .	86
5.2	Discrete problem . . . . .	91
5.2.1	The dual initial and boundary conditions . . . . .	91
5.2.2	Discrete approach . . . . .	92
5.3	Results . . . . .	94

---

5.3.1	Case 1 . . . . .	94
5.3.2	Case 2 . . . . .	101
5.4	Conclusions . . . . .	106
<b>6</b>	<b>An approach for steady 2-D flow problems</b>	<b>109</b>
6.1	The model equations . . . . .	110
6.1.1	The fine model: the Navier-Stokes equations . . . . .	110
6.1.2	The coarse model: the Euler equations . . . . .	111
6.2	Dual boundary operators . . . . .	112
6.2.1	Solid wall boundary operators . . . . .	117
6.2.2	Outflow boundary operators . . . . .	120
6.3	The error estimator . . . . .	122
6.3.1	Inner domain contribution . . . . .	123
6.3.2	Solid wall contribution . . . . .	123
6.3.3	Outflow boundary contribution . . . . .	124
6.4	Overview of the approach . . . . .	125
6.5	Conclusions and recommendations . . . . .	126
<b>7</b>	<b>Conclusions and recommendations</b>	<b>127</b>
7.1	Conclusions . . . . .	127
7.2	Recommendations . . . . .	130
	<b>References</b>	<b>132</b>
<b>A</b>	<b>Differentiation and linearisation of functionals</b>	<b>141</b>
<b>B</b>	<b>The Galerkin spectral element method</b>	<b>143</b>
<b>C</b>	<b>The finite volume method for the Burgers problem</b>	<b>147</b>
C.1	The discrete primal problem . . . . .	147
C.2	The discrete dual problem . . . . .	148
	<b>Dankwoord</b>	<b>153</b>
	<b>Curriculum Vitae</b>	<b>155</b>



# Chapter 1

## Introduction

### 1.1 Background of the research

Nowadays, computer simulations of real physical systems or processes play an indispensable role in science and engineering. For the simulation of a physical system or process a simulation *model* or mathematical *model* needs to be constructed. In this context the term *model* is defined following the AIAA definitions (Oberkampf [1]) as being: ‘a representation of a physical system or process intended to enhance our ability to understand, predict, or control its behaviour’. The ‘process of construction or modification of a model’ is referred to as *modelling* (Oberkampf [1]).

For many physical systems or processes, various models have been developed, each with its own level of sophistication, i.e., the degree to which the model is true to nature as it is observed. The collection of models describing the same physical system or process is called a *class of hierarchical models*. The hierarchy is determined by the level of sophistication of the model, with the most sophisticated model placed highest in the hierarchy, followed by the approximating models of decreasing sophistication. Considering two different models from the same class, the most sophisticated model is referred to as the ‘fine model’ and the other one as the ‘coarse model’. Often a coarse model is obtained by simplifying a sophisticated model.

As mentioned before, the process of construction or modification of a model is referred to as *modelling*. The error between a constructed or modified model and the reality is the *modelling error*. In computer simulations the term *modelling error* is also used to refer to the error between two models of different level of sophistication. When a model is implemented in a computer code, additional errors are introduced such as (possible) program-

ming and discretisation errors. This requires the *verification* of models, see for instance [2, 3], which is beyond the scope of this thesis.

The discrepancy between a model and real physics or between two models of different sophistication can only be determined when a model is applied to a specific problem. The 'process of determining the degree to which a model is an accurate representation of real physics from the perspective of the intended use of the model' (Oberkampf [1]) is called model *validation*. Since in computer simulations also other errors are introduced as explained earlier, the verification and validation of the model (as applied to a specific problem) often go hand in hand, see for instance [4, 5, 6, 7].

The relation between real physics, the class of hierarchical models and the computer code is illustrated in figure 1.1. It is based on the phases of modelling and simulation as identified and formulated by the Society for Computer Simulation (SCS) [8] in 1979 and adopted by the AIAA [1]. Much literature can be found on the definitions in modelling and simulation, many of this literature extend the semantics of modelling and simulation. A majority of these studies are aimed at certain fields of science and engineering, see for instance [2, 4, 9, 10]. For an extensive review of literature in the field of verification and validation, see [11]. The work presented in this thesis considers the *modelling error* of a coarse model with respect to a fine model.

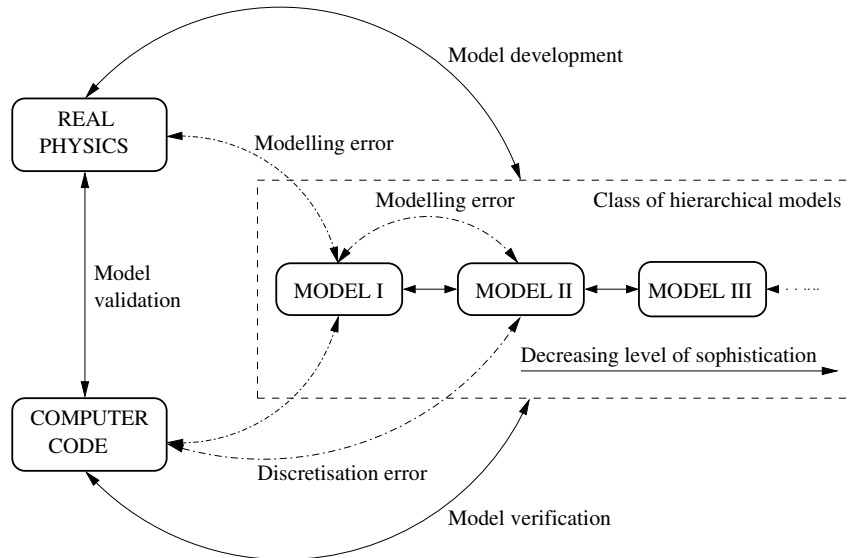


Figure 1.1: Phases of modelling and simulation



In many classes of hierarchical models the most sophisticated model is also the computationally most expensive model. An example of such a class is that consisting of, in ordering of decreasing sophistication: the Navier-Stokes equations, the approximating Euler equations and potential flow equations. A new trend in the field of computer simulations to reduce computational costs but to meet a certain required accuracy is *adaptive modelling*, see for instance [12, 13, 14, 15, 16]. Adaptive modelling means a coarse model(s) is (are) used to decrease computational time and the fine model is applied only when accuracy requires it. Accuracy can be studied in a local sense but also be in a global sense, for instance, in a global quantity of interest. In many engineering applications the goal of computer simulations is to compute a certain quantity of interest, e.g., the lift of an airfoil or the load on a structure. In that case the goal is to compute the quantity of interest within a certain accuracy whilst minimising computer resources, i.e., with as little use of the fine model as possible.

To drive an adaptive modelling process the *modelling error* needs to be estimated, see for instance [14, 17] about local modelling error estimation. When a specific quantity of interest is the goal of a computer simulation, the modelling error in that quantity of interest needs to be estimated. This is referred to as *goal-oriented modelling-error estimation* and is the field of research of the work presented in this thesis.

A general approach for deriving a goal-oriented error estimator in finite element approximations has been developed by Becker and Rannacher [18, 19] and is referred to as the Dual-Weighted Residual (DWR) method. Applications of the DWR method are given in [18, 19] for the goal-oriented estimation of discretisation errors, which is also the subject of [20, 21, 22, 23, 24, 25, 26].

The work of Becker and Rannacher [18, 19] has been extended by Oden and Prudhomme [21, 27] for goal-oriented modelling-error estimation in computational mechanics. So far, the DWR method has been applied to problems where the model complexity varies, for instance, due to different forms of constitutive relations or modified properties of the medium considered. In all these cases the hierarchical models are of the same mathematical character e.g., they are all elliptic partial differential equations. (See [28, 29, 30] for the characterisation of partial differential equations.) Examples are the modelling of heterogeneous materials [27, 31], structural mechanics [32] and molecular systems [15]. Also in work on flow(-type) problems [12, 13, 27, 33], the hierarchical models are all of the same mathematical type which means they require the same boundary conditions.

In the steady incompressible flow example by Oden and Prudhomme [27], the incompressible Navier-Stokes equations are approximated by the Stokes

equations in which the convective terms are neglected. In the adaptive modelling of free-surface flows by Perotto [33] all hierarchical models maintain the hyperbolic type and require the same boundary conditions. In the convection-diffusion problems considered by Braack and Ern [12, 13] the level of sophistication is determined by the diffusion model, by applying Fick's law as an approximation of a more accurate multicomponent diffusion model. In both cases, the problem is elliptic, such that the same boundary conditions apply to both models.

So far, no work has appeared on the application of the DWR method for the purpose of goal-oriented modelling-error estimation in a class of hierarchical models where the type of the model equation changes. This change in type can be due to a change in the characterisation (parabolic, hyperbolic or elliptic) or the order of the partial differential equation. A difference in type between the fine and the coarse model, is the case for classes describing singular perturbation problems [34, 35] where the coarse model is in fact the reduced problem. In this context, the reduced problem (also referred to as 'unperturbed' problem) is described by the model in which the term multiplied by the small perturbation parameter in the fine model is neglected. Examples of such classes are fluid flow models and convection-diffusion problems. In the class of fluid flow models, the solution of the Navier-Stokes equations is often approximated by solving the Euler equations in which viscosity and heat conduction are neglected. This means a change in type of the equation by omitting the highest order terms. This change is also the case for convection-diffusion problems when diffusion is neglected in the fine model to yield the coarse model. Therefore, the main issue of this thesis is the following question:

Is the Dual-Weighted Residual method suitable for goal-oriented modelling-error estimation in classes of hierarchical models where the model equations are of a different type?

## 1.2 Focus of the research

We focus our research on classes of hierarchical models in which models are of different type, since such classes play an important role in engineering. For instance the earlier mentioned Navier-Stokes and Euler equations in the class of fluid flow models. Another example is a convection-diffusion problem with the convection equation as approximating model of the convection-diffusion equation. These problems are known as singular perturbation problems. The work described in this thesis considers the application of the DWR method for goal-oriented modelling-error estimation in singular

perturbation problems. Singular perturbation problems differ from regular problems where the hierarchical models are of equal type, due to the possible difference in behaviour near boundaries for the fine and coarse model. Such a difference results in a modelling error or modelling residual on the boundary. In this thesis two approaches for dealing with modelling errors on a boundary, further referred to as boundary residuals, in the DWR method are presented. The first approach is derived for linear problems whereas the second approach is suitable for nonlinear problems.

Other approaches are also considered with varying degrees of success (e.g., the augmented functional approach and a direct discrete approach). In this thesis only the approaches with a proper foundation that have eventually led to a proper goal-oriented modelling-error estimator are described.

The DWR method to perform goal-oriented modelling-error estimation requires the computation of the modelling residual in the coarse model solution with respect to the fine model and the solution of a dual problem, also referred to as the adjoint problem. Another approach would be to derive and solve the equation for the modelling error itself and substitute the result in the quantity of interest. The advantage of the DWR method however, is that the dual problem provides information on the influence of the local modelling error on the (global) modelling error of the quantity of interest. This information is required when the goal of error estimation is to drive a local model adaptation algorithm.

It is important to emphasise that the work presented in this thesis concerns the application of the DWR method for particular situations that are relevant for fluid-flow related problems and does not strive for a general framework for goal-oriented modelling-error estimation in classes of hierarchical models that are of different type.

## 1.3 Outline of the thesis

The thesis is divided into two parts: part I considers the theory of dual-weighted residual modelling-error estimation including some simple examples and part II gives some applications of the DWR method to singular perturbation problems.

In part I, chapter 2, an estimator for the modelling error in a quantity of interest for linear problems is presented. This approach is referred to as the linear differential approach, since the problems are described by linear differential operators. In order to illustrate goal-oriented modelling-error estimation an example is given in which the approach is applied to a diffusion-reaction problem. To simplify the illustration, no boundary residuals are present yet.

For nonlinear problems, a possible approach is to linearise the considered hierarchical problems first, and then use the error estimator derived for linear problems. In that case however, we have no insight in the high-order contributions from the nonlinear operators. A variational approach is therefore followed in chapter 3 based on the work by Oden and Prudhomme [27]. In applying this approach to problems (written in a weak formulation) where hierarchical models are of different type, we show that it is essential to impose boundary conditions weakly in order to incorporate boundary residuals in the error estimator. An example is given based on the diffusion-reaction problem with different boundary conditions to illustrate the role played by the boundary residuals.

After the theory presented in part I, applications of the DWR method are given in part II beginning with the application to linear convection-diffusion problems in chapter 4. The convection-diffusion equation is considered as fine model and by omitting the diffusion operator, the coarse -reduced-model is obtained. Some steady analytical cases, as well as an unsteady discrete problem are studied. In chapter 5 the DWR method is applied to the nonlinear Burgers problem, which differs from linear convection-diffusion in the nonlinear convection term. An analysis is given of the high-order contributions in the error estimator from the nonlinear model operator, as well as a nonlinear quantity of interest. In chapter 6 a preliminary study is made of the approach for steady 2-D flow problems where the Navier-Stokes equations are considered as the fine model and the Euler equations as the coarse model. Finally conclusions and recommendations for further research are presented in chapter 7.

**Part I**  
**Theory**



## Chapter 2

# Linear differential approach

Two different approaches of the DWR method to perform goal-oriented modelling-error estimation are possible that both have their advantages and disadvantages. In this chapter the approach for linear(ised) models in terms of linear differential operators is described. The derivation of the modelling error in a quantity of interest is then relatively straightforward. In chapter 3, the variational approach is described which is considered suitable for nonlinear problems and gives some insight in high-order terms in the Dual-Weighted Residual method.

In the linear differential approach we consider problems with linear differential operators. Particular attention is paid to the derivation of the boundary operators for the dual problem. The linear differential approach can also be followed for a nonlinear problem when it is first linearised. This can be of particular interest for complex models such as the Euler and Navier-Stokes equations, since such models are sometimes solved in linearised form.

In section 2.1 the primal fine and coarse model equations are given and the derivation of the corresponding dual problems are discussed in section 2.2. The goal-oriented modelling-error estimator for linear problems is derived in section 2.3. A 1-D illustration of the linear differential approach is given in section 2.4 where the diffusion-reaction equation (representing the fine model) is approximated by the diffusion equation (representing the coarse model).

Finally, the application of the dual-weighted residual estimator in a model-adaptation algorithm is illustrated using the same diffusion-reaction

problem in section 2.5. For this purpose the problems are solved in a simple finite element setting.

## 2.1 The fine and coarse models

Suppose we are interested in evaluating the quantity of interest  $Q(u)$  from the solution  $u$  of the fine model on a domain  $\Omega$  with boundary  $\Gamma$ :

$$Lu = f \quad \text{in } \Omega, \quad (2.1a)$$

$$Bu = a \quad \text{on } \Gamma, \quad (2.1b)$$

where  $L$  and  $B$  are the linear differential operators governing the p.d.e. and the boundary conditions, respectively. Problem (2.1) is also referred to as the primal problem. The right-hand side term  $f$  is the source term and  $a$  is the boundary condition which both may be functions of  $\mathbf{x} \in \Omega \cap \Gamma$  and time  $t \in \mathbb{R}^+$ .

Now suppose that the fine model problem is computationally expensive to solve, such that an approximating model, or the coarse model, is required. This is given by:

$$L_0u_0 = f \quad \text{in } \Omega, \quad (2.2a)$$

$$B_0u_0 = a_0 \quad \text{on } \Gamma, \quad (2.2b)$$

assuming that both models have the same source term  $f$ . When the coarse model has a different source term  $f_0$ , the model equation  $L_0u_0 = f_0$  can be rewritten, such that a different coarse model arises with again the same source term  $f$ :

$$L_0u_0 - f_0 + f = f.$$

Call  $L_0u_0 - f_0 + f = \tilde{L}_0u_0$  the new coarse model. Therefore we only consider coarse models with the same source term  $f$  as the fine model equation.

When using the solution of the coarse problem (2.2) to evaluate the quantity of interest  $Q(u_0)$ , the modelling error in the quantity of interest is simply:

$$Q(u) - Q(u_0).$$

Estimation of this modelling error without solving the fine model (2.1) is now the goal.

As explained in the introduction, the approach to follow is to compute the modelling residual in the primal problem which is weighted by the solution of the dual problem. Therefore first the derivation of the dual problem is given.



## 2.2 The dual problems

Following Giles and Pierce [36], we consider the case in which the quantity of interest is an integral on the inner domain  $\Omega$  and boundary  $\Gamma$  with  $u$  the solution of (2.1):

$$Q(u) = (g, u)_\Omega + (h, Cu)_\Gamma, \quad (2.3)$$

with the inner product definitions:

$$(a, b)_\Omega = \int_\Omega ab \, d\Omega \quad \text{and} \quad (c, d)_\Gamma = \int_\Gamma cd \, d\Gamma. \quad (2.4)$$

The dual form (2.3) is given by the following theorem which is found in Giles and Pierce [36]:

**Theorem 1** *In case a dual problem of (2.1) exists, it has the following form:*

$$L^*p = g \quad \text{in } \Omega, \quad (2.5a)$$

$$B^*p = h \quad \text{on } \Gamma, \quad (2.5b)$$

where  $L^*$  is a linear p.d.e. which is adjoint to  $L$  and  $B^*$  is the boundary condition operator of the dual problem. The solution  $p$  of (2.5) is the adjoint variable or Lagrangian multiplier. The equivalent dual form of the quantity of interest (2.3) is then:

$$Q(u) = Q(p) = (p, f)_\Omega + (C^*p, a)_\Gamma. \quad (2.6)$$

The existence of the dual problem (2.5) and (2.6) can be proved by showing that the following primal-dual equivalence identity holds:

$$\begin{aligned} (p, f)_\Omega + (C^*p, a)_\Gamma &= (p, Lu)_\Omega + (C^*p, Bu)_\Gamma \\ &= (L^*p, u)_\Omega + (B^*p, Cu)_\Gamma \\ &= (g, u)_\Omega + (h, Cu)_\Gamma, \end{aligned} \quad (2.7)$$

The first and last steps are straightforward substitutions, but the intermediate step requires the proof that the identity:

$$(p, Lu)_\Omega + (C^*p, Bu)_\Gamma = (L^*p, u)_\Omega + (B^*p, Cu)_\Gamma, \quad (2.8)$$

has to hold for all  $u$  and  $p$ . Therefore integration by parts is performed of the inner product of  $p$  and  $Lu$  on  $\Omega$  which gives an identity of the form:

$$(p, Lu)_\Omega = (L^*p, u)_\Omega + (A_1p, A_2u)_\Gamma, \quad (2.9)$$

where  $A_1$  and  $A_2$  are differential operators on the boundary  $\Gamma$ . Comparing (2.9) with the identity (2.8) suggests that operators  $B^*$  and  $C^*$  exist such that:

$$(A_1 p, A_2 u)_\Gamma = (B^* p, Cu)_\Gamma - (C^* p, Bu)_\Gamma. \quad (2.10)$$

If for a particular problem the pair of operators  $B^*$  and  $C^*$  can be found from relation (2.10), the equivalence of the dual problem (2.5)–(2.6) and the primal problem (2.1)–(2.3) is proved. Therefore theorem 1 emphasises that equation (2.6) only exists when a dual problem exists. When the operators  $B^*$  and  $C^*$  can not be determined, the dual problem is ill-posed and no equivalent dual form of the quantity of interest (2.3) exists.

One of the great advantages of the dual (or adjoint) approach can be illustrated by the following. Consider the application of aerodynamic design optimisation for the quantity of interest  $Q(u) = (g, u)$ . Then  $Lu = f$  is the system of linearised flow equations with respect to a change in a design variable and the source term  $f$  represents the linearisation of the flow equations with respect to changes in a design variable. A change in the design variable means a change in  $f$ , and to evaluate  $Q(u)$  the system  $Lu = f$  needs to be re-evaluated. Once the dual problem  $L^*p = g$  is solved however, its solution  $p$  can be used to evaluate the quantity of interest  $Q(u) = (p, f)$  for every value of  $f$ . The advantage of the dual approach lies in the fact that the system  $Lu = f$  does not have to be re-evaluated for every change in design variable. Only one evaluation of the dual problem  $L^*p = g$  is enough. Much literature is available on aerodynamic design optimisation by the dual approach, see for instance [37, 38, 39, 40]. Furthermore, the dual solution  $p$  gives information on the local sensitivity of the quantity of interest for changes in the solution  $u$ . This aspect of the dual approach is applied in goal-oriented model-adaptation.

One way to find and prove the existence of the operators  $B^*$  and  $C^*$  is given by Giles and Pierce [36]. This method is, however, restricted to p.d.e.'s for which the boundary operators  $B$ ,  $C$ ,  $A_1$  and  $A_2$  involve only the values of  $u$  and  $p$  and any of their normal derivatives. In this case the vectors  $\mathbf{u}$  and  $\mathbf{p}$  are introduced which are composed of  $u$  and  $p$  together with the normal derivatives of the appropriate degree, e.g.:

$$\mathbf{u} = \left( u, \frac{\partial u}{\partial n} \right)^T, \quad \mathbf{p} = \left( p, \frac{\partial p}{\partial n} \right)^T.$$

Assuming the dual problem is well-posed, the boundary operators can then be rewritten as:

$$Bu \equiv \mathbf{B}\mathbf{u}, \quad Cu \equiv \mathbf{C}\mathbf{u}, \quad (2.11a)$$

$$B^*p \equiv \mathbf{B}^*\mathbf{p}, \quad C^*p \equiv \mathbf{C}^*\mathbf{p}, \quad (2.11b)$$

$$(A_1 p, A_2 u) \equiv \mathbf{p}^T \mathbf{A}\mathbf{u}, \quad (2.11c)$$

where  $\mathbf{B}$  and  $\mathbf{C}$  are rectangular matrices and  $\mathbf{A}$  is a square matrix. We need to find and prove the existence of the matrices  $\mathbf{B}^*$  and  $\mathbf{C}^*$ . An illustration is given for the diffusion-reaction equation in section 2.4.

With the matrix notation of the boundary operators from (2.11) the equivalence of relation (2.10) is written as:

$$\int_{\Gamma} \mathbf{p}^T \mathbf{A}\mathbf{u} - (\mathbf{B}^*\mathbf{p})^T \mathbf{C}\mathbf{u} + (\mathbf{C}^*\mathbf{p})^T \mathbf{B}\mathbf{u} ds = 0.$$

This is true when the integrand is zero which yields:

$$\mathbf{A} = (\mathbf{B}^*)^T \mathbf{C} - (\mathbf{C}^*)^T \mathbf{B}. \quad (2.12)$$

This can be reformulated by defining the matrices  $\mathbf{T}$  and  $\mathbf{T}^*$  as:

$$\mathbf{T} = \begin{bmatrix} \mathbf{B} \\ \mathbf{C} \end{bmatrix}, \quad \mathbf{T}^* = \begin{bmatrix} -\mathbf{C}^* \\ \mathbf{B}^* \end{bmatrix}, \quad (2.13)$$

This allows to write identity (2.12) as a product of matrices:

$$\mathbf{A} = (\mathbf{T}^*)^T \mathbf{T}, \quad (2.14)$$

from which the unknown  $\mathbf{T}$  needs to be solved. When  $\mathbf{T}$  is not singular, solving this system yields the dual boundary operators  $\mathbf{C}^*$  and  $\mathbf{B}^*$  such that the dual problem with appropriate boundary conditions can be derived together with the dual form of the quantity of interest (2.6).

The dual problem for the coarse model (2.2) is also derived. This is required for the goal-oriented modelling-error estimator, as will become clear in the next section. For the coarse model (2.2) we find in a similar fashion the dual problem and the corresponding boundary operators:

$$L_0^* p_0 = g \quad \text{in } \Omega, \quad (2.15a)$$

$$B_0^* p_0 = h \quad \text{on } \Gamma. \quad (2.15b)$$

The quantity of interest based on the coarse model is simply found by substituting the solution  $u_0$  into equation (2.3):

$$Q(u_0) \approx (g, u_0)_{\Omega} + (h, Cu_0)_{\Gamma}. \quad (2.16)$$

For completeness the quantity of interest in dual form based on the coarse problem is given:

$$Q(u_0) \approx (p_0, f)_\Omega + (C_0^* p_0, a_0)_\Gamma. \quad (2.17)$$

For goal-oriented modelling-error estimation the coarse dual solution  $p_0$  is of interest.

## 2.3 The error estimator

With the dual problem given, the (exact) modelling-error estimator for the linearised problem in terms of the inner domain and boundary operators is given in the following theorem:

**Theorem 2** *With  $u$  the solution of the linear fine model (2.1) and the corresponding dual solution  $p$  of (2.5) we have the exact modelling-error representation:*

$$\boxed{Q(u) - Q(u_0) = R(u_0, p) = (p, f - Lu_0)_\Omega + (C^* p, a - Bu_0)_\Gamma.} \quad (2.18)$$

where  $R$  denotes the residual estimator,  $f - Lu_0$  is the inner domain residual and  $a - Bu_0$  is the boundary residual.

**Proof** The proof of equation (2.18) is made by subtracting the general expressions for  $Q$  based on the fine model (2.3) and coarse model (2.16) and using (2.8):

$$\begin{aligned} Q(u) - Q(u_0) &= (g, u)_\Omega + (h, Cu)_\Gamma - (g, u_0)_\Omega - (h, Cu_0)_\Gamma \quad (2.19) \\ &= (g, u - u_0)_\Omega + (h, Cu - Cu_0)_\Gamma \\ &= (L^* p, u - u_0)_\Omega + (B^* p, C(u - u_0))_\Gamma \\ &= (p, L(u - u_0))_\Omega + (C^* p, B(u - u_0))_\Gamma \\ &= (p, f - Lu_0)_\Omega + (C^* p, a - Bu_0)_\Gamma. \end{aligned}$$

□

### The error estimator in practice

In the estimator (2.18) the fine dual solution  $p$  is used as a weighting function for the residuals. Solving the fine dual problem however, is equally expensive in the sense of computational time as solving the fine primal problem. To

reduce computational time the fine dual solution is replaced by the coarse dual solution. Therefore the fine dual solution  $p$  is split into a coarse model solution  $p_0$  and dual error  $\epsilon_0$ :

$$\begin{aligned} R(u_0, p) &= (p_0 + \epsilon_0, f - Lu_0)_\Omega + (C^*(p_0 + \epsilon_0), a - Bu_0)_\Gamma \quad (2.20) \\ &= (p_0, f - Lu_0)_\Omega + (C^*p_0, a - Bu_0)_\Gamma \\ &\quad + (\epsilon_0, f - Lu_0)_\Omega + (C^*\epsilon_0, a - Bu_0)_\Gamma, \end{aligned}$$

and after neglecting the contribution from  $\epsilon_0$  the coarse dual-weighted estimator is given by:

$$Q(u) - Q(u_0) \approx R(u_0, p_0) = (p_0, f - Lu_0)_\Omega + (C^*p_0, a - Bu_0)_\Gamma, \quad (2.21)$$

Concerning the influence of neglecting the dual error we assume that in the class of hierarchical models the primal error  $e_0 = u - u_0$  as well as the dual error  $\epsilon_0 = p - p_0$  are sufficiently small:  $e_0 \ll u_0$  and  $\epsilon_0 \ll p_0$ . This is essential for the derivation of coarse models: for the (often bounded) range of applicability of a coarse model the error with respect to the fine model is assumed to be sufficiently small where ‘sufficiently’ from an engineering point of view depends on the accuracy required.

When models are of a different type and require different boundary conditions however, situations might occur that  $e_0$  and  $\epsilon_0$  are indeed small on the inner domain but large on a boundary. For the inner domain we therefore assume:

$$\epsilon_0 \ll p_0 \quad \Rightarrow \quad (\epsilon_0, f - Lu_0)_\Omega \ll (p_0, f - Lu_0)_\Omega. \quad (2.22)$$

This can not be said for the boundary contributions in (2.18) when the fine and coarse dual equations show different behaviour on the boundaries. Furthermore it also depends on the form of the boundary operator  $C^*$ . When, for instance,  $\epsilon_0$  increases rapidly in a small region adjacent to the boundary due to boundary layer behaviour of  $p$ , and  $C^*$  is a gradient operator, the following does not hold:

$$C^*\epsilon_0 \ll C^*p_0 \quad \Rightarrow \quad (C^*\epsilon_0, f - Lu_0)_\Omega \ll (C^*p_0, f - Lu_0)_\Omega. \quad (2.23)$$

In that case using only the coarse dual solution  $p_0$  in the estimator as in equation (2.21) introduces a large error in the estimator and the reliability of the estimator is much lower than using the fine dual solution  $p$ . Only when the coarse and fine dual problem have the same type of boundary condition inequality (2.23) might hold. It might, therefore, be advisable to derive the boundary conditions for both the fine and coarse dual problem to study the behaviour of the dual problem at the boundary and the influence of  $(C^*\epsilon_0, a - Bu_0)_\Gamma$ .

**Correction by the estimator** When the estimator is based on the coarse dual model or, after adapting the model, a mix of the coarse and fine dual models, the estimator can still be too inaccurate to be used as a correction. The estimator used to drive the model adaptation algorithm is a single scalar value instead of an estimate in terms of rigorous upper and lower bounds. Therefore, using the estimator as correction on the computed quantity of interest is considered unreliable when the coarse dual-weighted estimator is used.

## 2.4 Illustration: 1-D diffusion-reaction

This section is based on the work presented in Cnossen [41]. The linear model problem on the domain  $\Omega = [0, 1]$  concerns the diffusion-reaction equation representing the fine model with the coarse model represented by diffusion equation.

First the details of the model problem are introduced in section 2.4.1 with the exact primal and dual solutions. The dual problems for the given fine and coarse models are derived in section 2.4.2. Then the modelling error in the quantity of interest is estimated in section 2.4.3 based on the estimator (2.18).

### 2.4.1 The model problem

The fine model represented by the 1-D diffusion-reaction equation on the unit interval domain  $\Omega = (0, 1)$  with Dirichlet boundary conditions on  $x = 0$  and  $x = 1$  is given by:

$$Lu := -u_{xx} + k^2u = 0, \quad x \in \Omega, \quad u(x) \in C^2(\Omega), \quad (2.24a)$$

$$Bu := u = \begin{cases} a^0 = 0, & x = 0, \\ a^1 = 1, & x = 1. \end{cases} \quad (2.24b)$$

with  $L$  the diffusion-reaction operator,  $B$  the Dirichlet boundary operator and  $k \in \mathbf{R}^+$  the reaction coefficient. The exact solution of (2.24) is:

$$u(x) = \frac{e^{kx} - e^{-kx}}{e^k - e^{-k}}. \quad (2.25)$$

Suppose now that fine problem (2.24) is approximated by the diffusion

equation with Dirichlet boundary conditions:

$$L_0 u_0 := -u_{0xx} = 0, \quad x \in \Omega, \quad u_0(x) \in C^2(\Omega), \quad (2.26a)$$

$$B_0 u_0 := u = \begin{cases} a^0 = 0, & x = 0, \\ a^1 = 1, & x = 1. \end{cases} \quad (2.26b)$$

with  $L_0$  the diffusion operator and  $B_0$  the boundary operator. The solution of (2.26) is given by:

$$u_0(x) = x. \quad (2.27)$$

The reaction coefficient  $k$  in (2.24) is used to simulate the difference between both models with the special case  $k = 0$  resulting in the coarse model. In figure 2.1(a) the solutions of both the coarse and fine model for  $k = 1, 2, 4$  are given, showing that the larger  $k$  the 'coarser' the approximation of the diffusion-reaction equation by the diffusion equation.

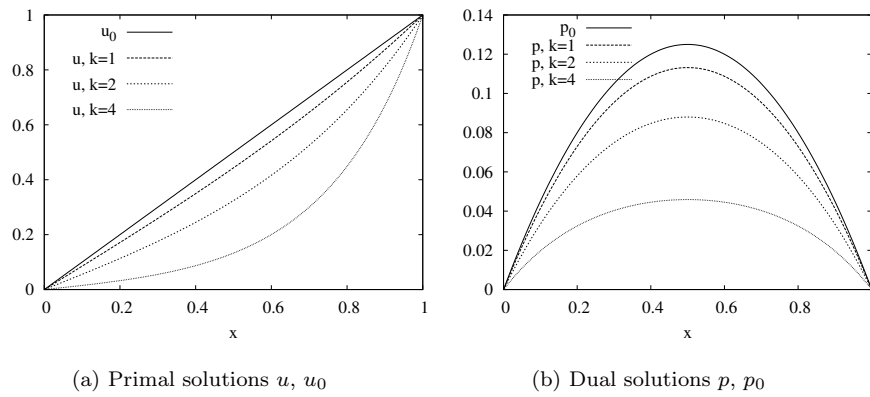


Figure 2.1: Primal and dual solutions for  $k = 1, 2, 4$ .

The quantity of interest  $Q$  considered is also linear and is chosen to be:

$$Q(u) = \int_{\Omega} u(x) dx. \quad (2.28)$$

The exact modelling error  $Q(u) - Q(u_0)$  is found by substituting the solutions of the fine and coarse model into (2.28) and subtracting the results:

$$Q(u) - Q(u_0) = \int_{\Omega} \left( \frac{e^{kx} - e^{-kx}}{e^k - e^{-k}} - x \right) dx = \frac{e^k + e^{-k} - 2}{k(e^k - e^{-k})} - \frac{1}{2}. \quad (2.29)$$

As expected, the modelling error  $Q(u) - Q(u_0)$  in (2.29) is zero for the limit of  $k \rightarrow 0$ .

### 2.4.2 Finding the dual problem

The dual problem of the fine problem (2.24) can be found by introducing the inner product (as defined in (2.4)) of the Lagrangian multiplier  $p$  and  $Lu$  and performing integration by parts as in equation (2.9):

$$(p, Lu) = \int_{\Omega} p(-u_{xx} + k^2 u) dx = \int_{\Omega} u(-p_{xx} + k^2 p) dx - pu_x|_0^1 + p_x u|_0^1. \quad (2.30)$$

We can directly find the dual equation  $L^*p = g$  from (2.30) and (2.28):

$$L^*p := -p_{xx} + k^2 p = 1, \quad x \in \Omega. \quad (2.31)$$

Knowing that the boundary terms of (2.30) have to satisfy relation (2.10) the dual boundary conditions can be derived from (2.30):

$$(B^*p, Cu)_{\Gamma} - (C^*p, Bu)_{\Gamma} = -pu_x|_0^1 + p_x u|_0^1. \quad (2.32)$$

Finding the dual boundary operators  $B^*$  and  $C^*$  is problematic, even for the current illustrative 1-D problem. The starting point is that operator  $B$  is known on both boundaries in (2.24) (Dirichlet boundary conditions). In relation (2.32) the last term  $p_x u|_0^1$  contains the Dirichlet boundary condition  $Bu := u$  for the primal problem and therefore it remains that:

$$C^*p := p_x. \quad (2.33)$$

Then, automatically the first term on the lefthandside of relation (2.32) coincides with the first term on the right-hand side:  $(B^*p, Cu)_{\Gamma} = -pu_x|_0^1$  which yields the dual boundary operator:

$$B^*p := -p. \quad (2.34)$$

Note also that a boundary operator belonging to the general quantity of interest (2.3) is found:  $Cu := u_x$ , although the quantity of interest (2.28) has no boundary contributions. With the general (linearised) form in (2.3) the value of  $h$  on both boundaries  $x = 0$  and  $x = 1$  can only be zero in this case, yielding the boundary values for the dual equation (2.5). To conclude, the complete dual problem for this diffusion-reaction problem is:

$$L^*p := -p_{xx} + k^2 p = 1, \quad x \in \Omega, \quad p(x) \in C^2(0, 1), \quad (2.35a)$$

$$B^*p := -p = \begin{cases} h^0 = 0, & x = 0, \\ h^1 = 0, & x = 1. \end{cases} \quad (2.35b)$$

Another approach is to follow Giles and Pierce [36] in proving the existence of the dual boundary operators  $B^*$  and  $C^*$ . This proof immediately



yields the operators when the dual problem is well-posed. This approach is more straightforward than the derivation of the dual boundary operators described above.

Following [36] identity (2.30) is written with the boundary terms in vector form from (2.11c):

$$(p, Lu) - (L^*p, u) = [\mathbf{p}^T \mathbf{A} \mathbf{u}]_0^1 \quad (2.36)$$

with

$$\mathbf{u} = \begin{pmatrix} u \\ u_x \end{pmatrix}, \quad \mathbf{p} = \begin{pmatrix} p \\ p_x \end{pmatrix}$$

and the matrix  $A$  which can be constructed using relation (2.32) as a result from integration by parts:

$$\mathbf{A} \equiv \begin{bmatrix} 0 & -1 \\ 1 & 0 \end{bmatrix}.$$

The primal boundary operators are written in terms of  $\mathbf{u}$  at both boundaries:

$$\mathbf{B} \mathbf{u} := u \Rightarrow \mathbf{B} \equiv (1 \ 0),$$

Furthermore we find from the remaining boundary term in identity (2.30) that  $Cu := u_x$ . The matrix  $\mathbf{C}$  is therefore given by:

$$\mathbf{C} \mathbf{u} := u \Rightarrow \mathbf{C} \equiv (0 \ 1).$$

For identity (2.36) to satisfy (2.8) one has to find  $\mathbf{B}^*$  and  $\mathbf{C}^*$  on each boundary  $\Gamma$  such that the following holds:

$$\mathbf{A} = \mathbf{B}^{*T} \mathbf{C} - \mathbf{C}^{*T} \mathbf{B}. \quad (2.37)$$

Since  $Bu$  and  $Cu$  are the same on both boundaries, also  $\mathbf{B}^*$  and  $\mathbf{C}^*$  are the same on  $x = 0$  and  $x = 1$ . By virtue of (2.13) and (2.14) equation (2.37) is solved by:

$$\begin{bmatrix} -\mathbf{C}^* \\ \mathbf{B}^* \end{bmatrix} = \left( \begin{bmatrix} \mathbf{B} \\ \mathbf{C} \end{bmatrix}^{-1} \right)^T \mathbf{A}^T = \begin{pmatrix} 0 & 1 \\ -1 & 0 \end{pmatrix}, \quad (2.38)$$

and hence  $B^*p = -p$  and  $C^*p = -p_x$  at both boundaries as found earlier in (2.34) and (2.33), respectively. With  $B^*p = h$  and  $h = 0$  on both boundaries, the boundary conditions for the dual problem become:

$$-p(0) = -p(1) = 0 \quad \Rightarrow \quad p(0) = p(1) = 0,$$

which is the same result as found earlier, given in (2.35).

The solution of the dual problem (2.35) is given by:

$$p(x) = \frac{1}{k^2} \left( \frac{(e^{-k} - 1)(e^{kx} - e^{-kx})}{e^k - e^{-k}} + 1 \right), \quad (2.39)$$

which is shown in figure 2.1(b) for  $k = 1, 2, 4$ .

For completeness, the quantity of interest is also computed by its dual equivalent (2.9), although it is not of importance in goal-oriented modelling error estimation. With  $f = 0$  and  $a$  from the primal problem (2.24) one finds:

$$Q = (C^* p, a)_{\partial\Omega} = -p_x u|_0^1 = -p_x(1) = \frac{e^k + e^{-k} - 2}{k(e^k - e^{-k})}, \quad (2.40)$$

which is equal to substitution of  $u$  in (2.28). Note that in the primal case the quantity of interest  $Q$  is an integral over the whole domain  $\Omega = (0, 1)$  and in the dual case  $Q$  depends solely on the derivative of the dual variable at the boundary  $x = 1$ .

For the coarse model equation we can follow the same procedure to define its corresponding dual problem, resulting in:

$$L_0^* p_0 := -p_{0,xx} = 1, \quad x \in \Omega, \quad p_0(x) \in C^2(0, 1), \quad (2.41a)$$

$$B_0^* p_0 := -p_0 = \begin{cases} h^0 = 0, & x = 0, \\ h^1 = 0, & x = 1, \end{cases} \quad (2.41b)$$

of which the solution is given by:

$$p_0(x) = -\frac{1}{2}x^2 + \frac{1}{2}x, \quad (2.42)$$

which is shown in figure 2.1(b) together with the fine dual solution for  $k = 1, 2, 4$ . This figure shows, not surprisingly, that the approximation of the fine model solution (2.39) by the coarse model solution (2.42) improves for a decreasing reaction coefficient  $k$ .

Based on the coarse dual solution (2.42) the quantity of interest  $Q$  can be approximated by its dual equivalent as in (2.40) noting that  $C_0^*$  is found to be the same as  $C^*$ :

$$Q = (C_0^* p_0, a)_{\partial\Omega} = -p_{0,x}(1) = \frac{1}{2}, \quad (2.43)$$

which is equal to substitution of the coarse model solution (2.27) in the quantity of interest (2.28).

### 2.4.3 The error estimator

The modelling-error estimator (2.20) for the diffusion-reaction problem using the fine dual solution and with the operator  $C^*$  given in (2.33), becomes:

$$\begin{aligned} R(u_0, p) &= (p, f - Lu_0)_\Omega + (C^*p, a - Bu_0)_\Gamma \\ &= (p, -Lu_0)_\Omega + (p_x, a^0 - Bu_0)_{x=0} + (p_x, a^1 - Bu_0)_{x=1}. \end{aligned} \quad (2.44)$$

To compute the model residuals on  $\Omega$  and  $\Gamma$  the fine model operators  $L$  and  $B$  as given in (2.24) are applied to the coarse model solution  $u_0(x) = x$  (see (2.27)). This yields together with the dual solution (2.39):

$$\begin{aligned} R(u_0, p) &= (p, -k^2 x)_\Omega + (p_x, a^0 - x)_{x=0} + (p_x, a^1 - x)_{x=1} \\ &= (p, -k^2 x)_\Omega = \int_0^1 \frac{1}{k^2} \left( \frac{(e^{-k} - 1)(e^{kx} - e^{-kx})}{e^k - e^{-k}} + 1 \right) (-k^2 x) dx \\ &= \frac{e^k + e^{-k} - 2}{k(e^k - e^{-k})} - \frac{1}{2}. \end{aligned} \quad (2.45)$$

As expected, for a linear problem with use of the fine dual solution, the result (2.45) is exact (see the real modelling error in (2.29)). There are no boundary contributions to the error estimator since the fine and coarse models have the same boundary conditions.

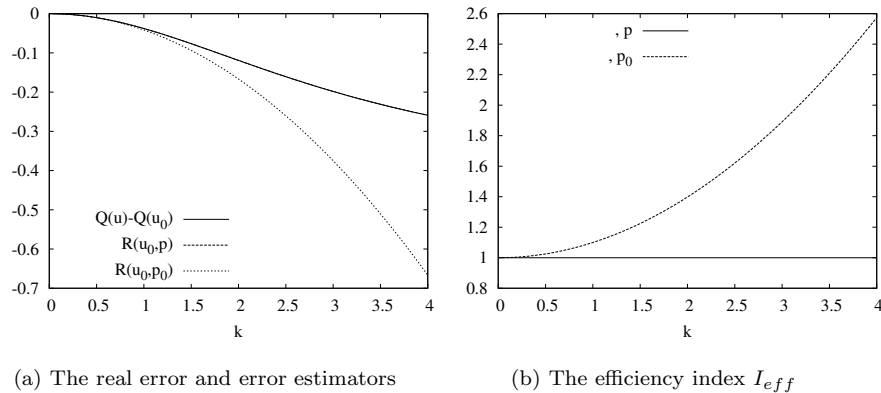
As mentioned before, when using the modelling-error estimator to drive a model-adaptation algorithm, the efficiency of the algorithm lies in the use of the coarse dual solution (2.42) in the estimator, see equation (2.21):

$$\begin{aligned} R(u_0, p_0) &= (p_0, f - Lu_0)_\Omega = (p_0, -k^2 x)_\Omega \\ &= \int_\Omega \left( -\frac{1}{2}x^2 + \frac{1}{2}x \right) (-k^2 x) dx = -\frac{1}{24}k^2. \end{aligned} \quad (2.46)$$

The real error and the error estimators (2.45) and (2.46) are shown for  $k = 0 \dots 4$  in figure 2.2(a). The figure shows that  $R(u_0, p_0)$  follows closely the real error (and the exact estimator  $R(u_0, p)$ ) for small  $k$ , but the over-estimation grows rapidly for  $k \gtrsim 2$ . This behaviour is emphasised by the efficiency index shown in figure 2.2(b). The efficiency index is common for indicating the quality of an error estimator, and is defined as the ratio of the error estimator and the real error:

$$I_{eff} = \frac{R(u_0, \cdot)}{Q(u) - Q(u_0)}, \quad (2.47)$$

where  $R(u_0, \cdot)$  can be either the fine dual-weighted estimator  $R(u_0, p)$  or the coarse dual-weighted estimator  $R(u_0, p_0)$ .



(a) The real error and error estimators

(b) The efficiency index  $I_{eff}$ Figure 2.2: The error estimators and efficiency index as function of  $k$ .

## 2.5 Discrete example with adaptive modelling

In this section, which is an extended version of the work presented in [42], the illustration for the linear differential approach in section 2.4 is computed by means of the finite element method (FEM). A local adaptation of the model is applied to improve the approximation of the coarse model. The problem is reformulated in a discrete way by a first-order finite element approximation. This causes a discretisation error in the primal and dual solutions which also affects the modelling-error estimator. Obtaining estimates of the discretisation error in the quantity of interest in case of adaptive modelling is however, beyond the scope of the present study. See [43, 44, 12, 13, 14] for (goal-oriented) estimation and minimisation of discretisation errors by mesh adaptation.

The case studied in this example is the same as in section 2.4 where the linear differential approach is illustrated for a diffusion-reaction problem. First the details of the applied adaptive modelling algorithm are given in section 2.5.1. Then the details on the computation of the discrete modelling-error estimator is given in section 2.5.2 followed by the refinement criteria in the adaptation algorithm in section 2.5.3. The results of the computations are given and discussed in the final section 2.5.4.

### 2.5.1 Adaptive modelling algorithm

The implemented adaptive modelling algorithm is based on the work of Oden and Vemaganti [31] on goal-oriented adaptive modelling of heterogeneous materials. Other similar algorithms can be found in [12, 33, 45]. The algorithm consists out of a global and a local loop and is summarised as follows:

```
do while  $|R(u_0, p_0)| > \underline{\text{global}}$  tolerance level
    • compute coarse model solutions  $u_0$  and  $p_0$ 
    • estimate the global modelling error  $R(u_0, p_0)$ 
    • localise modelling error estimate by  $e_Q^l$ 
    • if  $|e_Q^l| > \underline{\text{local}}$  tolerance level
        – refine model of element  $l$ 
```

In the global loop the coarse primal and dual solutions are computed and the global modelling-error is estimated. When the estimated error is outside a user-defined tolerance with respect to the quantity of interest (based on the coarse model solution)  $Q(u_0)$ , the local loop is entered. In the local loop the modelling error is localised and compared with a threshold value. In case the threshold is exceeded, the model type (i.e. the element ‘stiffness’ matrix<sup>1</sup>) of the relevant element is modified to represent the fine model equation.

In the following sections the computation of the discrete modelling-error estimator and localisation of the estimator are discussed, as well as the global and local refinement criteria used in the adaptation algorithm given above.

### 2.5.2 Discrete estimation and localisation of the error

In the discrete approach the modelling-error estimator (2.18) in the quantity of interest consists of contributions by the modelling error and the discretisation error:

$$Q(u) - Q(u_0) = R(u_0, p) = R(u_0^h, p^h) + R(u_0 - u_0^h, p - p^h), \quad (2.48)$$

where  $u_0^h$  and  $p^h$  are the discrete approximations (computed by any type of discretisation, e.g. a finite element or finite volume approach) of  $u_0$

---

<sup>1</sup>The term ‘stiffness’ is commonly used in the FEM to refer to the coefficient matrix for a single element since the FEM was first applied to structural analysis but it is used in other applications as well.

and  $p$ , respectively. The first term in equation (2.48),  $R(u_0^h, p^h)$ , is the computed modelling-error estimate and the second term is the discretisation error in the estimator. As can be seen in the adaptation algorithm in the previous section and for reasons described in the theory in section 2.3, the coarse dual-weighted estimator  $R(u_0, p_0)$  will be used in practice, so the real modelling-error in  $Q$  is estimated by:

$$Q(u) - Q(u_0) \approx R(u_0, p_0) = R(u_0^h, p_0^h) + R(\delta_u^h, \delta_p^h), \quad (2.49)$$

where  $\delta_u^h = u_0 - u_0^h$  and  $\delta_p^h = p_0 - p_0^h$  are the discretisation errors in the primal and dual approximations, respectively. The discretisation error can be computed by using the analytical solutions as computed in section 2.4. After the model is (locally) adapted however, the coarse solution  $u_0^h$  is computed by a mix of coarse and fine model elements. This also means that besides the coarse primal solution  $u_0^h$ , the coarse dual solution  $p_0^h$  improves after applying local adaptation of the model. Therefore the discretisation error can only be computed by constructing an analytical solution on the sub-domains where the fine and coarse models are used. This is however, beyond the scope of the research. The discretisation error is computed for the initial computation in the adaptive modelling algorithm when all the elements are of diffusion type.

The estimator in the case discussed in section 2.4 only has a contribution from the inner domain as can be seen in equation (2.46). With  $N_n$  the number of nodes in the finite element formulation the discrete implementation for the estimator becomes:

$$R(u_0^h, p_0^h) = \sum_{i=1}^{N_n} p_{0i}^h \sum_{j=1}^{N_n} (f_i^h - L_{i,j}^h u_{0j}^h), \quad (2.50)$$

where  $L_{i,j}^h$  is the discrete operator (i.e. the global stiffness matrix) of the fine model.

**Localisation of the estimator** For the adaptive modelling algorithm the modelling-error estimator needs to be localised to yield  $e_Q^l$  in each individual element (see the algorithm in section 2.5.1). The local error estimate  $e_Q^l$  is derived from the global estimator (2.50) by considering the individual contribution of each element to the global error estimator:

$$e_Q^l \approx R_i(u_{0i}^h, p_{0i}^h) = \frac{1}{n_l} \sum_{i=1}^{n_l} p_{0i}^h \sum_{j=1}^{N_n} (f_i - L_{i,j}^h u_{0j}^h) \quad (2.51)$$

where  $n_l$  is the number of nodes of the considered element  $l$  ( $n_l = 2$  for a first-order one-dimensional element).

### 2.5.3 Global and local refinement criteria

As given in the adaptation algorithm in section 2.5.1, the adaptation loop is entered when the estimator  $R(u_0^h, p_0^h)$  exceeds a tolerance level:

$$|R(u_0^h, p_0^h)| > \alpha_{tol} |Q(u_0^h)|.$$

The choice of  $\alpha_{tol}$  is determined by the required accuracy of the quantity of interest and is therefore a user-defined parameter. One should be aware however, that the required accuracy in this case is defined with respect to the quantity of interest based on the coarse model solution  $Q(u_0^h)$ , since the fine model-based quantity of interest  $Q(u^h)$  is not available. After adapting the model locally however, the quality of the approximation  $u_0^h$  improves (i.e. converges to the fine model solution  $u^h$  for increasing number of fine-model elements) and therefore the approximation of the quantity of interest  $Q(u_0^h)$  as well.

When the error in the global quantity of interest exceeds the tolerance level, the local refinement loop is entered. In this local refinement loop the individual contribution of each element to the global error estimator is considered. When the localised error exceeds a tolerance level, expressed as:

$$|e_Q^l| > \frac{1}{N_n} \beta_{tol} |R(u_0^h, p_0^h)|, \quad (2.52)$$

the element stiffness matrix of the considered element is modified to represent the fine model equation. The choice of  $\beta_{tol}$  is less simple and is more or less problem dependent. The following general requirements determine the bounds on  $\beta_{tol}$ :

- Minimisation of the number of adaptation loops. This determines the upper bound of  $\beta_{tol}$ .
- Minimisation of the size of the sub-domain(s) in which the fine model is applied. This determines the lower bound of  $\beta_{tol}$ .

Note that both aspects focus on limiting the computational time but determine different bounds on  $\beta_{tol}$ .

**Additional notes:** Braack and Ern [12] apply a slightly different adaptive modelling strategy from the one described in section 2.5.1. They describe a combined adaptive modelling and meshing strategy in which a balancing of the sources of error (mesh and model) is used to determine when the mesh and when the model is adapted. For the adaptation of the model the local

modelling error is compared with a tolerance level related to the  $L_1$ -norm of the error estimators:

$$|e_Q^l| > \frac{1}{N_n}TOL, \quad (2.53)$$

in which Braack and Ern choose  $TOL = 0.5\|e_Q\|_1$ . This strategy has been applied successfully to convection-diffusion-reaction problems. Braack and Ern [12] also mention that the strategy for refining the model depends strongly on the problem. The choice to multiply the  $L_1$ -norm of the estimated errors with 0.5 seems quite arbitrary though. One might compare this with the  $\beta_{tol}$  from the present refinement strategy. In fact, the refinement strategy based on the  $L_1$ -norm of the error is in practice equal to the present refinement strategy:

$$\|e_Q\|_1 = \sum_{i=1}^{N_n} |p_{0i}| \sum_{j=1}^{N_n} |f_i - L_{i,j}u_{0j}|, \quad (2.54)$$

which in this problem results in the absolute value of the global error estimate  $|Q(e_0)|$ , equation (2.50), used in the adaptation algorithm with the local refinement criteria of (2.52). When we choose  $\beta_{tol} = 0.5$  we indeed get the same results as for the computations using the  $L_1$ -norm based error tolerance level.

#### 2.5.4 Numerical results

In this section we present the results of the finite element approach with linear first-order elements. The adaptation algorithm as described in section 2.5.1 is implemented and the choice of the local adaptation threshold  $\beta_{tol}$  on the computations is investigated. Numerical tests are performed for  $\beta_{tol}=0.5, 1.0$  and  $1.5$  where  $\beta_{tol}=0.5$  corresponds to the error tolerance level according to [12]. The computations are performed with 10 elements,  $k = 2$  and a global error tolerance level of  $\alpha_{tol} = 0.05$ . The efficiency index  $I_{eff}$  of the estimator is defined as:

$$I_{eff} = \frac{R(u_0^h, p_0^h)}{Q(u^h) - Q(u_0^h)},$$

for which  $u^h$  is computed explicitly, which is an indication for the quality of the estimator. An efficiency index of  $I_{eff} = 1$  is the optimum. The discrete as well as initial analytical primal solutions for the three test-cases  $\beta_{tol}=0.5, 1.0$  and  $1.5$  are shown in figure 2.3. In the figures ‘run 0’ is the initial run before the adaptation algorithm is entered where all elements are of the



coarse model (diffusion) type. The figures show that the coarse solution approaches the fine model (analytical) solution, indicated by ‘ $u$ ,  $k = 2$ ’.

In table 2.1 the results from adaptation are given for the different values of  $\beta_{tol}$ . The ratio of fine-model elements over coarse-model elements is indicated by  $L/L_0$ . Furthermore the approximating quantity of interest  $Q(u_0^h)$ , the discrete error estimator  $R(u_0^h, p_0^h)$  and the discrete real error  $Q(u^h) - Q(u_0^h)$  are given. Comparing the results for different  $\beta_{tol}$  from table 2.1 shows that with  $\beta_{tol} = 0.5$  and  $1.0$  the prescribed accuracy is obtained after one adaptation step, but with  $\beta_{tol} = 0.5$  more elements have been adapted. Although this simple example does not illustrate the saving of computational time when adaptive modelling is applied, one can understand that in complex problems adapting 60 or 80% of the domain could mean a significant difference in computational time. Table 2.1 shows furthermore that computations with  $\beta_{tol} = 1.5$  require 2 adaptation steps to meet the required tolerance and therefore one can conclude that  $\beta_{tol} = 1.5$  is too high. In this particular example  $\beta_{tol} = 1.0$  gives optimal results in the sense of the requirements mentioned in section 2.5.3. The choice of  $\beta_{tol} = 0.5$  corresponds to the local refinement strategy by Braack and Ern [12], but in the diffusion-reaction problem discussed in this section it is not the optimal. Therefore no conclusions can be drawn on the optimal value for  $\beta_{tol}$  in other problems.

$\beta_{tol}$	run	$L/L_0$	$Q(u_0^h)$	$R(u_0^h, p_0^h)$	$Q(u^h) - Q(u_0^h)$	$I_{eff}$
-	0	0	0.5	-1.6500e-01	-1.1920e-01	1.38
0.5	1	.8	0.38481	-4.2573e-03	-4.0111e-03	1.06
1.0	1	.6	0.39404	-1.3039e-02	-1.2330e-02	1.06
1.5	1	.3	0.43038	-5.8524e-02	-4.9587e-02	1.18
	2	.6	0.39404	-1.3039e-02	-1.2330e-02	1.06

Table 2.1: Adaptation results for  $k = 2$ ,  $\alpha_{tol}=0.05$ ,  $\beta_{tol} = 0.5, 1$  and  $1.5$ .

**Quality of the modelling-error estimator** The efficiency index  $I_{eff}$  demonstrates the quality of the error estimator; in the ideal case it is equal to unity. Table 2.1 shows that the efficiency index is equal to 1.38 for the initial run with the coarse model. After locally adapting the model in several elements  $I_{eff}$  improves drastically. Table 2.1 shows that the more elements are adapted, the closer  $I_{eff}$  approaches unity. This improvement of the estimator is caused by the improvement of the coarse primal as well as the dual solution (i.e.  $u_0^h$  and  $p_0^h$  approach the fine model solutions  $u^h$  and  $p^h$ , respectively).

We see that the efficiency index for  $\beta_{tol} = 0.5$  and 1.0 in both cases is 1.06 although for  $\beta_{tol} = 0.5$  there are 80% of the elements modified to the fine model vs. 60% in case of  $\beta_{tol} = 1.0$ . This is due to the discretisation error: when applying 100 elements for  $\beta_{tol} = 1.0$ ,  $I_{eff}=1.04$  and 72% of the elements are adapted. The overestimation of the coarse dual-weighted estimator appears to grow with decreasing number of elements.

**Influence of discretisation error** The discretisation error in the modelling-error estimator  $R(\delta_u^h, \delta_p^h)$  is computed for the pre-adaptation solution by using the exact analytical solutions. (See section 2.4.1.) This is shown together with the computed modelling-error estimate for  $N = 10$  and  $N = 100$  in table 2.2. A comparison between the discretisation error  $R(\delta_u^h, \delta_p^h)$  and the estimator  $R(u_0^h, p_0^h)$  shows that the discretisation error is two orders of magnitude lower than the estimator in case of 10 elements and four orders of magnitude lower with 100 elements.

N	$R(\delta_u^h, \delta_p^h)$	$R(u_0^h, p_0^h)$
10	1.2685e-3	-1.6500e-01
100	1.2693e-5	-1.6665e-01

Table 2.2: Discretisation error in the estimator.

The discretisation error in the modelling-error estimator might indirectly influence the number of adaptation loops. Due to the discretisation error in the estimated modelling error, the adaptive modelling threshold may (or may not) just be exceeded. When it exceeds the adaptation threshold due to discretisation error whilst the ‘real’ modelling error (in the limit of infinitely small mesh-size) is below the adaptation threshold, a new computational expensive adaptation loop is entered. Therefore, it is preferable to combine model adaptation with mesh adaptation for global functionals as in [12].

Another advantage of combining adaptive modelling and meshing lies in their common goal to minimise computational time. Minimising the number of elements as well requires the decoupling of the model and discretisation error. It is then possible to balance adaption of the model and mesh in an optimal way to minimise computational time. The necessity for this balancing for flow problems can be illustrated by the following situation. If one solves the inviscid Euler equations and wants to determine the modelling error in a quantity of interest with respect to the Navier-Stokes equations, the residuals in viscous areas are strongly influenced by the mesh size through artificial diffusion. In that case, the ‘Euler cells’ are adapted to ‘Navier-Stokes cells’ whilst instead the mesh should be adapted to decrease the artificial diffusion. The model should be only modified in case the phys-

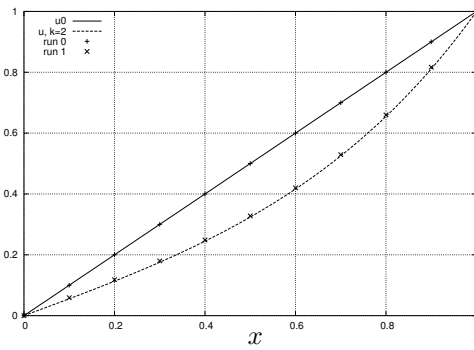
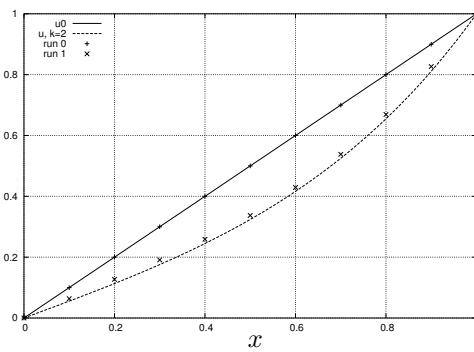
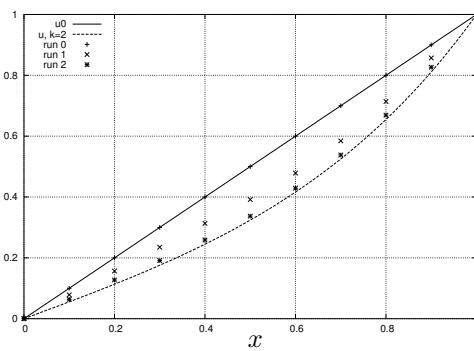
ical diffusion is large. Therefore the modelling error should be separated from the discretisation error.

## 2.6 Conclusions

In this chapter the linear differential approach is presented and illustrated analytically for a linear problem. Also a discrete example is given of an adaptive modelling process for a linear problem by means of a finite element approach.

The analytical illustration shows that the goal-oriented modelling-error estimator for a linear quantity of interest is exact when using the fine dual solution. When the coarse dual solution is used as weighting function a dual error is introduced. This results in an over-estimation of the real modelling error in the quantity of interest.

In the discrete example the modelling-error estimator is combined with an adaptive modelling algorithm. Numerical experiments show that the coarse model is locally (i.e. in a discrete element) refined to the fine model when the required accuracy for the quantity of interest is not achieved. The refined elements are those that are of most influence on the accuracy of the quantity of interest. After refinement and a new computation based on a mix of fine and coarse model elements, the modelling error in the quantity of interest decreases as can be expected.

(a) Primal solutions for  $\beta_{tol} = 0.5$ (b) Primal solutions for  $\beta_{tol} = 1.0$ (c) Primal solutions for  $\beta_{tol} = 1.5$ Figure 2.3: Primal solutions during adaptation for  $\beta_{tol}=0.5, 1.0$  and  $1.5$

## Chapter 3

# Variational approach

To perform goal-oriented modelling-error estimation for nonlinear problems a possible approach is to linearise the hierarchical models and then follow the linear differential approach described in chapter 2. However, linearising the model equations before deriving the modelling-error estimator, means that all information contained by high-order terms in the modelling-error estimator is lost. To incorporate these terms in the estimator, now the general variational approach to modelling-error estimation for nonlinear problems is presented here. The variational approach, in which the problems are considered in a weak formulation, is developed by J.T. Oden *et. al.* in [17, 27, 31, 46] on modelling-error estimation and adaptive methods for hierarchical modelling in computational mechanics. The DWR method in the variational approach was introduced by Becker and Rannacher in [18, 19] for the *a-posteriori* estimation of discretisation errors.

In applying the variational approach to problems with hierarchical models with different boundary conditions (due to a difference in the type of the equations), it is shown that it is essential to impose boundary conditions weakly. In this case the boundary operators are included in the model operator explicitly such that boundary residuals can be included in the error estimator explicitly.

Another advantage of the variational approach is the derivation of the dual problem and its boundary conditions. One can determine whether or not the dual problem is well-posed, as will be discussed later.

Firstly, some preliminaries and comments are given in section 3.1 required for a better understanding of the problem in variational form. Then, the fine model and the derivation of its dual problem are presented in section 3.2 after which the coarse problem is discussed in section 3.3. Addi-

tional comments are given on the treatment of boundary conditions in the variational form in section 3.5. This section is followed by an illustration of the variational approach by the diffusion-reaction problem. In this illustration, two aspects are discussed: the high-order term in the estimator in case of a nonlinear quantity of interest and the occurrence of a boundary residual in the estimator. The latter is caused by different boundary conditions for the fine and coarse model.

### 3.1 Preliminaries and comments

The general theory of goal-oriented modelling-error estimation as derived by Oden and Prudhomme [27] based on the Dual-Weighted Residual (DWR) method developed by Becker and Rannacher [18, 19], is based on two assumptions which must be stated before continuing:

- functionals are assumed to be differentiable up to sufficiently high order,
- the semi-linear and possibly nonlinear differentiable forms used are defined on a Banach space  $V$ .

This allows to represent nonlinear functions as Taylor or mean-value expansions in certain function spaces in terms of abstract derivatives and (well-defined) remainders which are described in more detail in the appendix A. In that case, differentiability of an abstract form means the existence of a limit of the Gâteaux derivative of that form (see appendix A).

### 3.2 The fine or sophisticated model

We want to find the solution of the *fine* (or sophisticated) model, i.e. find  $u \in V$  such that:

$$N(u, q) = F(q), \quad \forall q \in V,$$

where  $N(\cdot, \cdot) : V \times V \rightarrow \mathbb{R}$  is the fine model operator which is a bilinear or semi-linear form on  $V$ . The right-hand side  $F(\cdot)$  is a linear functional on  $V$ . It is noticed that all nonlinear terms are assumed to be included in  $N(\cdot, \cdot)$ . The quantity of interest  $Q(u)$  where  $Q : V \rightarrow \mathbb{R}$  is a possibly nonlinear differentiable functional. Such an evaluation can be formulated as solving the (trivial) constrained optimisation problem for  $u \in V$  (see Becker and Rannacher [19]):

Find  $u \in V$  such that:

$$Q(u) = \inf_{v \in M} Q(v), \quad (3.1)$$

where  $M = \{v \in V; N(v; q) = F(q), \forall q \in V\}$ .

The minimum  $u$  corresponds to the stationary point  $(u, p) \in V \times V$  of the Lagrangian (or modified functional):

$$\mathcal{L}(u, p) := Q(u) + F(p) - N(u, p), \quad (3.2)$$

with  $p$  the adjoint variable or Lagrangian multiplier. The dual problem is now derived by considering the Lagrangian in the stationary point  $(u, p)$ . For the stationary point  $(u, p)$  applies that small perturbations in  $u$  and  $p$  lead to insignificantly small perturbations in the Lagrangian  $\mathcal{L}(u, p)$ :

$$\mathcal{L}'((u, p); (v, q)) = 0, \quad \forall (v, q) \in V \times V. \quad (3.3)$$

Here  $v$  indicates the variation in the direction of  $u$  and  $q$  the variation in the direction of  $p$ . For a particular problem the derivative of the Lagrangian with respect to  $u$  and  $p$  can be found by using the Gâteaux derivative:

$$\mathcal{L}'((u, p); (v, q)) = \lim_{\varepsilon_1, \varepsilon_2 \rightarrow 0} \frac{1}{\varepsilon_{1,2}} [\mathcal{L}(u + \varepsilon_1 v, p + \varepsilon_2 q) - \mathcal{L}(u, p)] = 0, \quad (3.4)$$

when applying small perturbations  $\varepsilon_1 v$  and  $\varepsilon_2 q$  to  $u$  and  $p$ . For the Lagrangian (3.2) this yields:

$$\mathcal{L}'((u, p); (v, q)) = Q'(u; v) - N'(u; v, p) + F(q) - N(u, q), \quad (3.5)$$

where the semicolon indicates that  $Q$  might be nonlinear in  $u$ .

Since the Lagrangian derivative (3.5) has to be zero according to equation (3.3) the result is that we seek  $(u, p) \in V \times V$  such that:

$$N(u; q) = F(q), \quad \forall q \in V, \quad (3.6a)$$

$$N'(u; v, p) = Q'(u; v), \quad \forall v \in V. \quad (3.6b)$$

These equations are the primal and dual problem, respectively.

Since  $N(\cdot; \cdot)$  is linear in the second argument<sup>1</sup>, but possibly nonlinear in the first argument, we write  $N'(\cdot; \cdot, \cdot)$  to indicate its 'Gâteaux derivative' (see appendix A for details on Gâteaux derivatives of the operator  $N$ ). In a similar fashion higher order derivatives of  $N$  can be found such as  $N''(\cdot; \cdot, \cdot, \cdot)$  which is tri-linear in the arguments following the semicolon, see also appendix A. Since the output functional  $Q(\cdot)$  might be nonlinear as well it can be linearised by the Gâteaux derivatives for functionals given in (A.2), appendix A.

---

<sup>1</sup>Semi-linear forms such as  $N(\cdot; \cdot)$  are linear in all arguments that follow the semicolon.

### 3.3 The coarse models

Consider a coarse model with the subscript 0. The same procedure for deriving the dual problem for the fine model is followed for the coarse model. We seek  $(u_0, p_0) \in V_0 \times V_0$  from:

$$N_0(u_0; q) = F(q), \quad \forall q \in V_0, \quad (3.7a)$$

$$N'_0(u_0; v, p_0) = Q'(u_0; v), \quad \forall v \in V_0, \quad (3.7b)$$

with  $p_0$  the coarse-model adjoint variable. In case  $V_0 = V$ ,  $u_0$  corresponds to an approximation of  $u$ . This is a general assumption in adaptive modelling which is not *a-priori* valid anymore when hierarchical models are of a different type. First we assume that indeed  $V_0 = V$  and derive the residuals required for the DWR method.

### 3.4 The error estimator

When solving the coarse model instead of the fine model, the modelling error in the quantity of interest is defined as:

$$Q(u) - Q(u_0). \quad (3.8)$$

To find an estimate for this modelling error in the quantity of interest, we consider the degree to which the coarse model solution  $(u_0, p_0)$  fails to satisfy the fine problem (3.6a), which is characterised by the residuals:

$$R(u_0; q) = F(q) - N(u_0; q), \quad (3.9a)$$

$$\bar{R}(u_0, p_0; v) = Q'(u_0; v) - N'(u_0; v, p_0), \quad (3.9b)$$

which are the primal and dual residuals, respectively.

A relation between the modelling error in the quantity of interest  $Q(u) - Q(u_0)$  and the residuals (3.9) is given by THEOREM 1 in Oden and Prudhomme [27]:

**Theorem 3** *When  $(u_0, p_0)$  is an approximation of the solution  $(u, p)$  from the system (3.6) the following a posteriori error representation is found:*

$$Q(u) - Q(u_0) = R(u_0; p_0) + \frac{1}{2}(R(u_0; \epsilon_0) + \bar{R}(u_0, p_0; e_0)) + r(e_0, \epsilon_0), \quad (3.10)$$

with the primal and dual errors given by:

$$e_0 = u - u_0 \quad \text{and} \quad \epsilon_0 = p - p_0. \quad (3.11)$$



and the term  $r(e_0, \epsilon_0)$  containing integral remainders of order three:

$$r(e_0, \epsilon_0) = \frac{1}{2} \int_0^1 \{Q'''(u_0 + se_0; e_0, e_0, e_0) - 3N'''(u_0 + se_0; e_0, e_0, \epsilon_0) - N'''(u_0 + se_0; e_0, e_0, e_0, p_0 + s\epsilon_0)\}(s-1)s ds. \quad (3.12)$$

Note that  $r(e_0, \epsilon_0)$  is zero for linear problems together with a quadratic or linear quantity of interest.

Since this estimator representation is essential for the work in this thesis, we will give the proof of Theorem 1 for completeness.

**Proof** The goal is to express the modelling error in terms of a (computable) residual. Therefore the quantity of interest based on the fine as well as the coarse model should be expressed in terms of residuals for which we use (3.2):

$$Q(u) = \mathcal{L}(u, p) - (F(p) - N(u; p)) = \mathcal{L}(u, p), \quad (3.13a)$$

$$Q(u_0) = \mathcal{L}(u_0, p_0) - (F(p_0) - N(u_0; p_0)) = \mathcal{L}(u_0, p_0) - R(u_0; p_0), \quad (3.13b)$$

where we use the fact that  $(u, p)$  is an exact solution of the system (3.6). We now obtain:

$$Q(u) - Q(u_0) = R(u_0; p_0) + \mathcal{L}(u, p) - \mathcal{L}(u_0, p_0). \quad (3.14)$$

For the Lagrangian terms we can find an expression by using a particular Taylor expansion with integral remainders (see appendix A) which yields:

$$\begin{aligned} \mathcal{L}(u, p) - \mathcal{L}(u_0, p_0) &= \frac{1}{2} \mathcal{L}'((u_0, p_0); (e_0, \epsilon_0)) + \frac{1}{2} \mathcal{L}'((u, p); (e_0, \epsilon_0)) + \\ &\frac{1}{2} \int_0^1 \mathcal{L}'''((u_0, p_0) + s(e_0, \epsilon_0); (e_0, \epsilon_0), (e_0, \epsilon_0)(e_0, \epsilon_0))(s-1)s ds. \end{aligned} \quad (3.15)$$

Since  $(u, p)$  is a stationary point of  $\mathcal{L}$  resulting in equation (3.3) it follows that  $\mathcal{L}'((u, p); (e_0, \epsilon_0)) = 0$ . Here we assume that  $(e_0, \epsilon_0)$  are small as well and that  $e_0 \in V$  and  $\epsilon_0 \in V$ . The latter follows by virtue of (3.11) and the assumption  $V_0 = V$  (described in section 3.3). For  $\mathcal{L}'((u_0, p_0); (e_0, \epsilon_0))$  we can do the same but instead we will use (3.5) to incorporate the residuals:

$$\begin{aligned} \mathcal{L}'((u_0, p_0); (e_0, \epsilon_0)) &= \{Q'(u_0; v) - N'(u_0; v, p_0)\} + \{F(q) - N(u_0; q)\} \\ &= \bar{R}(u_0, p_0; v) + R(u_0; q). \end{aligned}$$

Finally, the tri-linear form of  $\mathcal{L}$  in the integral of (3.15) is also written in terms of derivatives of  $N$  and  $Q$ , of which the final result is:

$$\begin{aligned} \mathcal{L}'''((u_0, p_0) + s(e_0, \epsilon_0); (e_0, \epsilon_0), (e_0, \epsilon_0)(e_0, \epsilon_0))(s-1)s ds = \\ Q'''(u_0 + s e_0; e_0, e_0, e_0) - 3N''(u_0 + s e_0; e_0, e_0, \epsilon_0) - \\ N'''(u_0 + s e_0; e_0, e_0, e_0, p_0 + s \epsilon_0). \end{aligned} \quad (3.16)$$

This allows us to write for (3.15):

$$\mathcal{L}(u, p) - \mathcal{L}(u_0, p_0) = \frac{1}{2}R(u_0; \epsilon_0) + \frac{1}{2}\bar{R}(u_0, p_0; e_0) + r(e_0, \epsilon_0), \quad (3.17)$$

where  $r(e_0; \epsilon_0)$  is given by (3.12) and the proof of Theorem 3 is complete.  $\square$

To limit ourselves to a single residual evaluations, the dual residual  $\bar{R}(u_0, p_0; e_0)$  in (3.17) is expressed in terms of the primal residual  $R(u_0; \epsilon_0)$ , which is given in Lemma 1 in [27]:

**Lemma 1** *Given any approximation  $(u_0, p_0)$  of the solution  $(u, p)$  from the system (3.6), the equality*

$$\bar{R}(u_0, p_0; v) = R(u_0; \epsilon_0) + \Delta R, \quad (3.18)$$

holds where

$$\Delta R = \int_0^1 N''(u_0 + s e_0; e_0, e_0, p_0 + s \epsilon_0) ds - \int_0^1 Q''(u_0 + s e_0; e_0, e_0) ds. \quad (3.19)$$

**Proof** The dual residual can be rewritten as follows:

$$\begin{aligned} \bar{R}(u_0, p_0; v) &= Q'(u_0; v) - N'(u_0; v, p_0) \\ &= Q'(u_0; v) - Q'(u; v) + Q'(u; v) - N'(u_0; v, p_0) \\ &= -[Q'(u; v) - Q'(u_0; v)] + N'(u; v, p) - N'(u_0; v, p_0) \\ &= -[Q'(u; v) - Q'(u_0; v)] \\ &\quad + [N'(u; v, p) - N'(u_0; v, p)] + N'(u_0; v, \epsilon_0). \end{aligned}$$

Using the following (exact) Taylor expansion with integral remainder derived using appendix A:

$$\begin{aligned} Q'(u; v) - Q'(u_0; v) &= Q'(u_0 + e_0; v) - Q'(u_0; v) \\ &= \int_0^1 Q''(u_0 + s e_0; e_0, v) ds, \\ N'(u; v, p) - N'(u_0; v, p) &= N'(u_0 + e_0; v, p) - N'(u_0; v, p) \\ &= \int_0^1 N''(u_0 + s e_0; e_0, v, p) ds, \end{aligned}$$

we obtain:

$$\begin{aligned} \bar{R}(u_0, p_0; v) &= N'(u_0; v, \epsilon_0) - \int_0^1 Q''(u_0 + s e_0; e_0, v) ds \\ &\quad + \int_0^1 N''(u_0 + s e_0; e_0, v, p) ds. \end{aligned} \quad (3.20)$$

Furthermore the primal residual can be rewritten in terms of the first derivate  $N'(u_0; v, \epsilon_0)$  as appears in equation (3.20) which would complete the proof. Therefore we use that  $u$  is the solution of (3.6a) in order to replace  $F(q)$  by  $N(u; q)$  in the residual (3.9a):

$$\begin{aligned} R(u_0; q) &= F(q) - N(u_0; q) = N(u; q) - N(u_0; q) \\ &= N(u + e_0; q) - N(u_0; q), \forall q \in V, \end{aligned}$$

for which we can write using Taylor expansion (A.3b) from appendix A:

$$R(u_0; q) = N'(u_0; e_0, q) + \int_0^1 N''(u_0 + s e_0; e_0, e_0, q)(1 - s) ds. \quad (3.21)$$

Taking  $q = \epsilon_0$  in (3.21) and  $v = e_0$  in (3.20) gives the relation:

$$\begin{aligned} \bar{R}(u_0, p_0; e_0) &= R(u_0; \epsilon_0) - \int_0^1 Q''(u_0 + s e_0; e_0, e_0) ds + \\ &\quad \int_0^1 N''(u_0 + s e_0; e_0, e_0, p - (1 - s)\epsilon_0) ds, \end{aligned}$$

which completes the proof from Lemma 1 since  $p - (1 - s)\epsilon_0 = p_0 + s \epsilon_0$ .  $\square$

With Lemma 1 and Theorem 3 the goal-oriented modelling-error estimator can now be given in terms of the primal residual:

$$Q(u) - Q(u_0) = R(u_0; p_0) + R(u_0; \epsilon_0) + \frac{1}{2}\Delta R + r(e_0; \epsilon_0). \quad (3.22)$$

Since the residual  $R(u_0; \cdot)$  is linear in the second argument, equation (3.22) can be written as:

$$\boxed{Q(u) - Q(u_0) = R(u_0; p) + \frac{1}{2}\Delta R + r(e_0; \epsilon_0)}. \quad (3.23)$$

Observation of  $\Delta R$  and  $r(e_0; \epsilon_0)$  in equation (3.19) and (3.12), respectively, shows that for linear problems with a quantity of interest which is linear or quadratic in  $u$ , the estimator (3.23) reduces to the readily computable residual  $R(u_0, p)$  when the solutions  $u_0$  and  $p$  are known. For

nonlinear problems the estimator (3.23) requires the computation of the high-order terms  $\Delta R$  and  $r(e_0; \epsilon_0)$ . When the errors (or residuals)  $e_0$  and  $\epsilon_0$  are known to be small however, these terms may be neglected. Note that when the hierarchical models are of a different type however, this does not have to be the case. Therefore, similar to the linear differential approach in section 2.3, the primal residual  $e_0$  on the boundary has to be considered explicitly. This will be discussed in section 3.5.

### The error estimator in practice

As explained in section 2.3 for the linear differential approach, computations of the fine dual solution  $p$  is undesirable. This is due to the fact that solving the fine dual problem is equally expensive as solving the fine primal problem. Therefore, in practice, the coarse dual solution instead of the fine dual solution is used in the error estimator:

$$Q(u) - Q(u_0) \approx R(u_0; p_0) + \frac{1}{2}\Delta R + r(e_0; \epsilon_0). \quad (3.24)$$

Neglecting the dual error  $\epsilon_0$  can have a large effect on the quality of the estimator. This effect however, depends on the dual boundary conditions and is problem dependent. See section 2.3 for a discussion on possible effects when neglecting the dual error.

For nonlinear problems the high-order terms  $\Delta R$  and  $r(e_0, \epsilon_0)$  are nonzero. The error estimator (3.23) with the high-order terms  $\Delta R$  and  $r(e_0, \epsilon_0)$  requires the computation or estimation of these high-order terms. Since the primal and dual errors  $e_0$  and  $\epsilon_0$  are unknown on the inner-domain, high-order terms can not be computed on the inner-domain. An analysis of the high-order terms on boundaries is required to find whether computable high-order boundary terms are present. Possible high-order terms should be included in the estimator when they are of significant magnitude.

## 3.5 Treatment of boundaries

In the theory derived above we assume  $V_0 = V$ , which is not the case when hierarchical models are of a different type. An example of this is a convection-diffusion problem where the diffusion operator is omitted in the coarse model. One way to circumvent this issue is to impose boundary conditions weakly and imply additional restrictions to  $V_0$  such that  $V_0 \subset V$ . The problem concerning convection-diffusion is studied in chapter 4.

The case  $V_0 \neq V$  means that the assumption in the previous section that the high-order terms  $\Delta R$  and  $r(e_0; \epsilon_0)$  can be neglected when the errors  $e_0$  and  $\epsilon_0$  are known to be small, does not have to apply to such problems.

When model equations are of a different type, the errors can be large on the boundary. Consider, for instance, the solution  $u_0$  of the Euler equations for a particular problem as an approximation of the Navier-Stokes solution  $u$ . The required boundary conditions on a wall (slip versus no-slip) mean that the error  $e_0$  is large (order of  $u$ ) on the boundary! The same can be said for the error  $\epsilon_0$  of the corresponding dual problems. The errors  $e_0$  and  $\epsilon_0$  on the boundary are also mentioned as the boundary modelling residuals for the primal and dual problem. In the next sections we mean the error  $e_0$  on the boundary when we speak of the boundary residual.

By applying the DWR method to model problems where hierarchical models are of a different type, such as the convection-diffusion problem, we will study the influence of the boundary residuals on the modelling-error estimator and its dependence on a control-parameter such as the diffusion coefficient in convection-diffusion problems. Such a control parameter determines the degree in which the approximation  $(u_0, p_0)$  differs from the fine model solution  $(u, p)$ .

Weakly imposing boundary conditions in the weak formulation of the problems ensures the incorporation of boundary residual contributions in modelling-error estimates by the DWR method. By weak implementation of boundary conditions the boundaries are treated separately in the operator  $N(\cdot, \cdot)$  in (3.6a) where the value assigned to the boundary condition is substituted in the right-hand side  $F(q)$ . A consequence is that the right-hand side for the fine model (3.6a) and coarse model (3.7a) are different which is indicated by using the subscript 0 for the right-hand side as well:

$$N_0(u_0; q) = F_0(q), \quad \forall q \in V. \quad (3.25)$$

The residual in the estimator (3.23) as given in (3.9a) is now modified by adding  $N_0(u_0; p) - F_0(p) = 0$ , which yields:

$$Q(u) - Q(u_0) = F(p) - N(u_0; p) + N_0(u_0; p) - F_0(p) + \frac{1}{2} \Delta R + r(e_0; \epsilon_0). \quad (3.26)$$

Equation (3.26) allows us to split the contributions in the estimator into contributions from the inner domain and the boundaries. A comparison of equation (3.26) with the estimator (2.18) derived for linear problems shows that both approaches separate the error estimator in inner-domain and boundary contributions.

### 3.6 Illustration: 1-D diffusion-reaction

The variational approach is now applied to the diffusion-reaction problem described in section 2.4 for the linear approach but with different boundary conditions for the coarse model and a nonlinear quantity of interest.

This demonstrates the inclusion of boundary residuals in the modelling-error estimator and with this the importance of the weak implementation of boundary conditions in a variational approach. The weak formulation of the primal and dual equations of the diffusion-reaction problem is given in section 3.6.1 after which the modelling-error estimator is derived in section 3.6.2.

### 3.6.1 Weak formulation of the hierarchical models

The weak formulation of the fine model problem (2.24) with weakly imposed boundary conditions is obtained by integration by parts and yields: find  $u \in V$  such that

$$N(u, q) = F(q) \quad \forall q \in V, \quad (3.27)$$

where:

$$N(u, q) = \int_0^1 \left( \frac{\partial u}{\partial x} \frac{\partial q}{\partial x} + k^2 u q \right) dx - \frac{\partial u}{\partial x} q \Big|_0^1 + u(1) \frac{\partial q(1)}{\partial x} - u(0) \frac{\partial q(0)}{\partial x},$$

$$F(q) = a^1 \frac{\partial q(1)}{\partial x} - a^0 \frac{\partial q(0)}{\partial x},$$

with  $V = H^1(\Omega)$  and  $a^0 = 0$  and  $a^1 = 1$  the boundary conditions as in (2.24). The solution to this primal problem is given in (2.25).

The nonlinear quantity of interest is the ‘energy measure’ on  $x \in (0, 1)$ :

$$Q(u) = \int_0^1 \frac{u^2}{2} dx \Rightarrow Q'(u; v) = \int_0^1 uv dx, \quad (3.28)$$

which is linearised using (A.2). The dual equation is derived according to section 3.2:

$$N'(u; v, p) = Q'(u; v), \quad \forall v \in H^1(0, 1) \Rightarrow$$

$$\int_0^1 \left( \frac{\partial p}{\partial x} \frac{\partial v}{\partial x} + k^2 pv \right) dx + v \frac{\partial p}{\partial x} \Big|_0^1 - p \frac{\partial v}{\partial x} \Big|_0^1 = \int_0^1 uv dx. \quad (3.29)$$

Since (3.29) has to hold for all  $v$  the boundary conditions are found by:

$$-p \frac{\partial v}{\partial x} \Big|_0^1 = 0 \Leftrightarrow p(0) = p(1) = 0. \quad (3.30)$$

Suppose now the coarse model has a different boundary condition  $a_0^1 \neq a^1$  on  $x = 1$  which ‘improves’ the approximation, especially for larger values of  $k$ . What the exact value of the boundary condition  $a_0^1$  for the ‘optimal’ approximation should be, is not considered here and goes beyond the scope

of the illustration. Due to the difference in boundary conditions between the fine and the coarse model a boundary contribution appears in the modelling-error estimator. On  $x = 0$  the same values are assigned to the boundary condition for both models:  $a_0^0 = a^0$ . The coarse model (2.2a) in variational form is then written as:

$$\begin{aligned} N_0(u_0, q) &= F_0(q), \quad \forall q \in H^1(0, 1) \Rightarrow \\ &\int_0^1 \left( \frac{\partial u_0}{\partial x} \frac{\partial q}{\partial x} \right) dx - \frac{\partial u_0}{\partial x} q \Big|_0^1 + u_0(1) \frac{\partial q(1)}{\partial x} - u_0(0) \frac{\partial q(0)}{\partial x} \\ &= a_0^1 \frac{\partial q(1)}{\partial x} - a_0^0 \frac{\partial q(0)}{\partial x}. \end{aligned} \quad (3.31)$$

The solution to this problem with  $a_0^0 = 0$  and  $a_0^1 \in (0, 1)$  is given by:

$$u_0(x) = a_0^1 x. \quad (3.32)$$

The fine and coarse model solutions from (3.27) and (3.32), respectively, are given in figure 3.1(a). From this figure it is imaginable that the coarse model with  $a_0^1 = 0.5$  is a better approximation of the fine model with  $k = 4$  than the coarse model with  $a_0^1 = 1$  when the goal is to compute the given quantity of interest (3.28).

The dual problem of the coarse model (3.31) is given as well in order to compute both the fine and coarse dual-weighted estimator:

$$\begin{aligned} N_0'(u_0; v, p_0) &= Q'(u_0; v), \quad \forall v \in H^1(0, 1) \Rightarrow \\ &\int_0^1 \left( \frac{\partial p_0}{\partial x} \frac{\partial v}{\partial x} \right) dx + v \frac{\partial p_0}{\partial x} \Big|_0^1 - p_0 \frac{\partial v}{\partial x} \Big|_0^1 = \int_0^1 u_0 v dx. \end{aligned} \quad (3.33)$$

Equation (3.33) yields the same boundary conditions as found for the fine dual problem (3.30):

$$p_0(0) = p_0(1) = 0.$$

Note that the coarse model dual boundary conditions have not changed compared to (2.41b), although the boundary conditions of the primal problem have changed. This is due to the quantity of interest being an integral over the domain and not over the boundary.

Without giving the complete analytical solutions here, the fine and coarse dual solutions of (3.31) and (3.33), respectively, are given in figure (3.1(b)) for various  $k$  and  $a_0^1$ . The fine dual solution shows that the highest weight for the modelling residual moves to the right for increasing  $k$ . This behaviour is expected since the quantity of interest is quadratic in  $u$  and therefore a perturbation in  $u$  in the vicinity of  $x = 1$  has more

influence on the quantity of interest than a perturbation in the vicinity of  $x = 0$ . This trend for increasing  $k$  lacks in the coarse dual solution which is independent of  $k$ , although the coarse dual solution is also slightly ‘shifted’ to the right (compare with the solutions in figure 3.1(b)).

The derivation of the dual problems with their boundary conditions in the variational form as described above is more straightforward than in the linear differential approach as given in section 2.4.2. As will become clear in the application to linear convection-diffusion, not every quantity of interest leads to a well-posed coarse dual problem when terms are omitted in the coarse models. In that case, it is impossible to use the coarse dual solution in the error estimator. The variational form of the dual problem reveals whether or not the dual problem is well-posed more easily than in case of the linear differential approach.

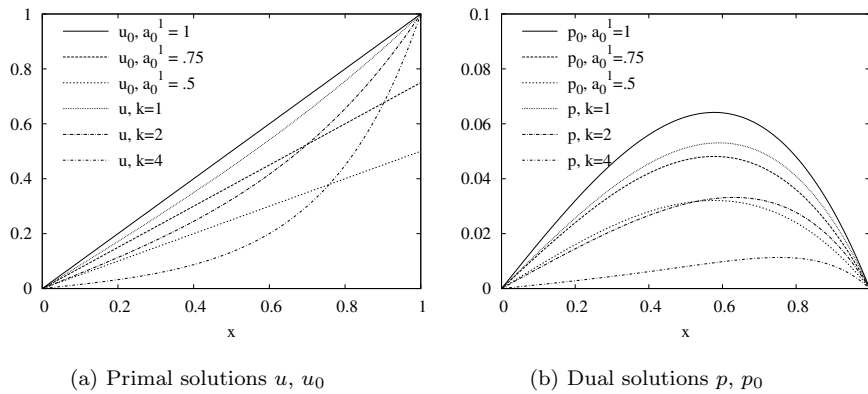


Figure 3.1: Primal and dual solutions for various  $k$  and  $a_0^1$ .



### 3.6.2 The error estimator

The modelling-error estimator is now derived according to the exact modelling-error representation by (3.26):

$$\begin{aligned}
Q(u) - Q(u_0) &= R(u_0; p) + \frac{1}{2}\Delta R + r(e_0, \epsilon_0) \tag{3.34} \\
&= F(p) - N(u_0; p) + N_0(u_0; p) - F_0(p) + \frac{1}{2}\Delta R + r(e_0, \epsilon_0) \\
&= a^1 \frac{\partial p(1)}{\partial x} - a^0 \frac{\partial p(0)}{\partial x} \\
&\quad - \left\{ \int_0^1 \left( \frac{\partial u_0}{\partial x} \frac{\partial p}{\partial x} + k^2 u_0 p \right) dx - \frac{\partial u_0}{\partial x} p|_0^1 + u_0(1) \frac{\partial p(1)}{\partial x} - u_0(0) \frac{\partial p(0)}{\partial x} \right\} \\
&\quad + \left\{ \int_0^1 \left( \frac{\partial u_0}{\partial x} \frac{\partial p}{\partial x} \right) dx - \frac{\partial u_0}{\partial x} p|_0^1 + u_0(1) \frac{\partial p(1)}{\partial x} + u_0(0) \frac{\partial p(0)}{\partial x} \right\} \\
&\quad - a_0^1 \frac{\partial p(1)}{\partial x} + a_0^0 \frac{\partial p(0)}{\partial x} + \frac{1}{2}\Delta R + r(e_0, \epsilon_0).
\end{aligned}$$

The expressions for the high-order terms  $\Delta R$  and  $r(e_0, \epsilon_0)$  can be found by (3.19) and (3.12), respectively. One finds that  $r(e_0, \epsilon_0) = 0$  and for  $\Delta R$ :

$$\Delta R = - \int_0^1 Q''(u_0 + se_0; e_0, e_0) ds = - \int_{\Omega} e_0^2 dx. \tag{3.35}$$

Equation (3.35) is not a computable term however, since  $e_0$  is not known on  $\Omega$ . Using  $a^0 = a_0^0 = 0$  and with cancellation of terms the modelling-error (3.34) reduces to:

$$Q(u) - Q(u_0) = - \int_0^1 (k^2 u_0 p) dx + (a^1 - a_0^1) \frac{\partial p(1)}{\partial x} + \frac{1}{2}\Delta R, \tag{3.36}$$

which is still exact. As mentioned in section 3.4, the high-order terms from the inner domain are neglected in practice (it requires the solution of the modelling-error equation). Also estimation of these contributions is generally not straightforward. Therefore the fine dual-weighted estimator is computed by  $R(u_0; p)$ :

$$R(u_0; p) = - \int_0^1 (k^2 u_0 p) dx + (a^1 - a_0^1) \frac{\partial p(1)}{\partial x}. \tag{3.37}$$

In figure 3.2 the estimator  $R(u_0; p)$  and the real error  $Q(u) - Q(u_0)$  are given by the upper two surfaces, respectively, for  $k = 0, \dots, 4$  and  $a_0^1 = 0.5, \dots, 1$ . The difference between the real error and the estimator (i.e. the upper two surfaces in figure 3.2) is the high-order term  $\frac{1}{2}\Delta R$  with  $\Delta R$  given in (3.35).

Using the coarse dual solution  $p_0$  from (3.33) to estimate the modelling error according to (3.24) gives:

$$R(u_0; p_0) = - \int_0^1 (k^2 u_0 p_0) dx + (a^1 - a_0^1) \frac{\partial p_0(1)}{\partial x}, \quad (3.38)$$

which is represented in figure 3.2 by the lower surface.

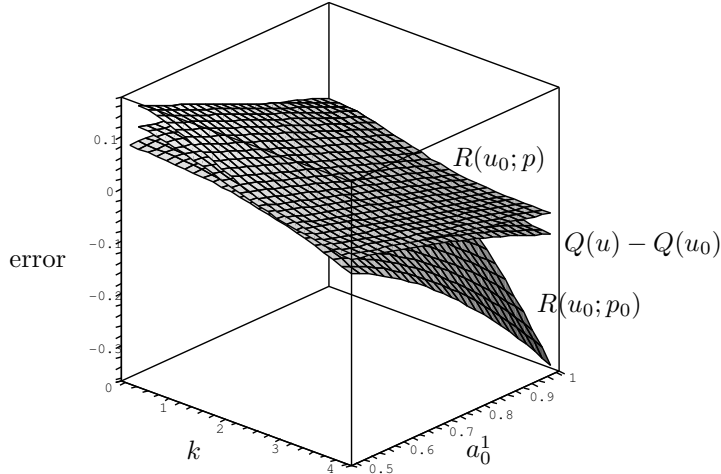


Figure 3.2: The real error and error estimators as function of  $k$  and  $a_0^1$ .

Since the reaction coefficient  $k$  does not appear in the coarse primal and dual problems (equations (3.31) and (3.33), respectively) the derivative  $\frac{\partial p_0}{\partial x}$  is also independent of  $k$ . As a consequence, the boundary contribution in (3.38) is also independent of  $k$  for  $a_0^1 \neq 0$ , even when the models converge for decreasing  $k$ , i.e.:

$$\lim_{k \rightarrow 0} N(u; q) = N_0(u_0; q). \quad (3.39)$$

This means that the boundary contribution in the error estimator remains while the inner-domain contribution approaches zero. The remaining boundary contribution for  $k \rightarrow 0$  can also be observed in figure 3.2.

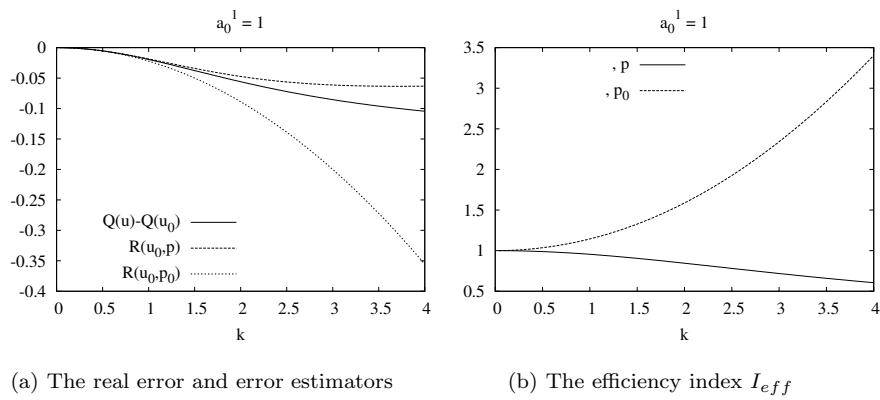


Figure 3.3: The error estimators and efficiency index as function of  $k$  for  $a_0^1 = 1$ .

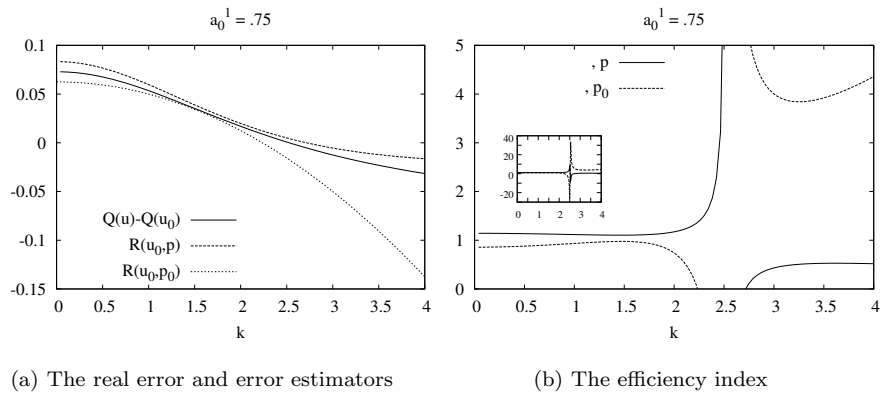


Figure 3.4: The error estimators and efficiency index as function of  $k$  for  $a_0^1 = .75$ .

Three slices of figure 3.2 for  $a_0^1 = .5$ ,  $.75$  and  $1$  are given in the figures 3.3–3.5 together with their corresponding efficiency index (defined by equation (2.47)). The efficiency index indicates the quality of the error estimator with respect to the real error. The case for  $a_0^1 = 1$  (which means no boundary residual at  $x = 1$ ) as shown in figure 3.3 is very similar to

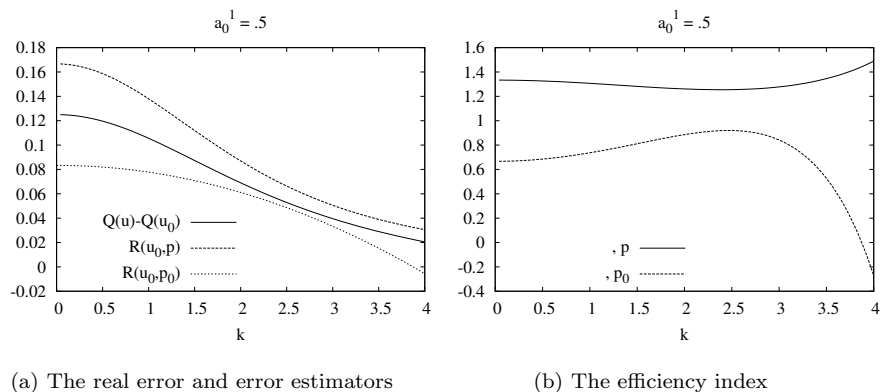


Figure 3.5: The error estimators and efficiency index as function of  $k$  for  $a_0^1 = .5$ .

the illustration in section 2.4 shown in figure 2.2, except for the quantity of interest (compare (2.28) and (3.28)). The fine dual-weighted estimator  $R(u_0, p)$  is no longer exact due to the high-order term (3.35). As suggested in section 3.6.1 based on the primal solutions shown in figure 3.1(a) the coarse model improves for increasing  $k$  when the boundary condition  $a_0^1$  decreases. This behaviour is confirmed by the figures 3.3–3.5: for decreasing  $a_0^1$  the best approximation of the error estimators moves to larger  $k$ . For  $a_0^1 = .75$  this is at  $k \approx 1,5$  and for  $a_0^1$  this point lies at  $k \approx 2.5$ . The singularity in the efficiency index in figure 3.4(b) is caused by the change in sign of the real error around  $k \approx 2.5$ .

### 3.7 Conclusions

In this chapter the variational approach is presented, which is suitable for nonlinear problems since it allows to incorporate high-order terms originating from nonlinear terms in the model equations. An analytical illustration of the application of the variational approach is given for a linear problem but with nonlinear quantity of interest. Due to this nonlinear quantity the fine-dual weighted modelling-error estimator is not exact as in the case for a linear quantity of interest.

In the illustrative problem the boundary conditions for the coarse and fine problem are different which results in a boundary residual. It is shown

that this boundary residual needs to be incorporated explicitly in the modelling-error estimator.



**Part II**

**Applications**





## Chapter 4

# Linear convection-diffusion

In the diffusion-reaction illustrations in the previous chapters the hierarchical models are of the same type. The difference between the fine and the coarse model is controlled by the reaction coefficient  $k$  and characterised by the convergence of the sophisticated model by the approximating model for the limit of vanishing  $k$ . For several classes of hierarchical models such as in fluid dynamics however, models are not of equal type and the aforementioned convergence of the fine model to the coarse model is not present. An example is the solution of the Navier-Stokes equations which for the limit of zero viscosity is not automatically equal to the solution of the Euler equations.

The solution of a convection-diffusion problem often approaches a discontinuous limit as  $\mu$  approaches zero. When  $\mu$  is small it is regarded a perturbation parameter and the situation is characterised as a singular perturbation problem. The solution of a singularly perturbed boundary value problem such as convection-diffusion is, *except for small layers*, very close to the solution of the reduced or approximating problem in which the diffusion term is omitted. Omitting the diffusion term in the convection-diffusion equation means that the mathematical type changes. In case of unsteady problems, the equations change type from parabolic to hyperbolic. The change of type of the equations, is in this case caused by a change in the order of the equations, since the highest-order term is omitted. For these problems special attention needs to be paid to the construction of the dual problems and the modelling-error estimator.

Numerous literature has appeared on error estimation in singular per-

turbation problems and it is still topic of ongoing research. The error estimation however, often considers the (local) estimation in approximations by asymptotic expansions [47], (time-) averaging techniques [48] or a-posteriori estimates in numerical approximations [49, 50, 51, 52]. No literature is available on goal-oriented modelling-error estimation in singular perturbation problems where the reduced problem is considered as the coarse model.

The application of the DWR method for goal-oriented modelling-error estimation in singular perturbation problems is not that straightforward as in regular perturbation problems such as the diffusion-reaction problem described in the section 2.4. As highlighted in the previous chapters, boundary residuals need to be taken into account explicitly, when boundary conditions for the sophisticated and approximating models are not the same. This is the case in singular perturbation problems and will be shown for the linear convection-diffusion problem in this chapter.

First the general approach to convection-diffusion problems is given in section 4.1. Then the application of the error-estimator is illustrated by steady 1-D problems. These problems are analysed in an analytical way in sections 4.2 and 4.4. It is shown that in these steady 1-D problems, the error-estimator has only contributions from the boundaries. This emphasises that it is important include the boundary residuals explicitly in the error-estimator. In the final section 4.5 an unsteady cases is studied using a spectral element approach.

## 4.1 Approach for convection-diffusion problems

The general approach to goal-oriented modelling-error estimation in convection-diffusion problems is based on the variational approach discussed in chapter 3. In the next chapter a nonlinear convection-diffusion problem is studied in the variational form. To make comparison between linear and nonlinear convection-diffusion easier, also the linear problem in this chapter is given in variational form. From the analysis in the variational formulation it becomes apparent what the mathematical drawbacks are, when applying the DWR method to a singular perturbation problem.

### 4.1.1 The fine model problems

Consider the convection-diffusion equation in  $(\mathbf{x}, t) \in \Omega \times (0, T)$  where  $\Omega$  is a domain in  $\mathbb{R}^d$  with boundary  $\Gamma$  and  $T \in \mathbb{R}^+$ :

$$\frac{\partial u}{\partial t} + \nabla \cdot (\mathbf{c} u) - \mu \nabla^2 u = 0, \quad \mathbf{x} \in \Omega, \quad t \in (0, T), \quad (4.1)$$

with  $\mathbf{c}$  the constant convective velocity and  $\mu > 0$  the constant scalar diffusion coefficient. The boundary  $\Gamma$  is divided into an inflow, outflow and noflow boundary,  $\Gamma^-$ ,  $\Gamma^+$  and  $\Gamma^0$ , respectively, which are defined by:

$$\begin{aligned} \Gamma^- &:= \{\mathbf{x} | \mathbf{x} \in \Gamma; \mathbf{c} \cdot \mathbf{n} < 0\}, \\ \Gamma^+ &:= \{\mathbf{x} | \mathbf{x} \in \Gamma; \mathbf{c} \cdot \mathbf{n} > 0\}, \\ \Gamma^0 &:= \{\mathbf{x} | \mathbf{x} \in \Gamma; \mathbf{c} \cdot \mathbf{n} = 0\}. \end{aligned} \quad (4.2)$$

Here,  $\mathbf{n}$  is the outward unit normal vector. Due to the parabolic character of equation (4.1), boundary conditions need to be imposed on all boundaries. We restrict ourselves to Dirichlet boundary conditions  $u(\mathbf{x}, t) = a(\mathbf{x}, t)$ ,  $\mathbf{x} \in \Gamma$ , which yield for the inflow, outflow and noflow boundaries, respectively:

$$\begin{aligned} u(\mathbf{x}, t) &= a^-(\mathbf{x}, t), \quad \mathbf{x} \in \Gamma^-, \quad t \in [0, T], \\ u(\mathbf{x}, t) &= a^+(\mathbf{x}, t), \quad \mathbf{x} \in \Gamma^+, \quad t \in [0, T], \\ u(\mathbf{x}, t) &= a^0(\mathbf{x}, t), \quad \mathbf{x} \in \Gamma^0, \quad t \in [0, T]. \end{aligned} \quad (4.3)$$

With the initial condition  $u(\mathbf{x}, 0) = \phi(\mathbf{x})$ , the initial boundary conditions can be found, e.g.:  $a^-(\mathbf{x}, 0) = \phi(\mathbf{x})$ ,  $\mathbf{x} \in \Gamma^-$ . The weak form of the problem is found by introducing a test function  $q$ , without imposing restrictions for  $q$  on the boundaries and at  $t = 0$ . Then, integration by parts is performed after which the boundary and initial conditions are imposed weakly. With  $u \in V$ , where  $V$  is the Sobolev space  $H^1(\Omega)$ , this yields: find  $u \in V$  such that

$$N(u; q) = F(q), \quad \forall q \in V, \quad (4.4)$$

with

$$\begin{aligned}
N(u; q) &= \int_0^T \int_{\Omega} \left( \frac{\partial u}{\partial t} q + q \nabla \cdot (\mathbf{c} u) + \mu \nabla u \nabla q \right) d\Omega dt \\
&\quad - \int_0^T \int_{\Gamma} \mu \frac{\partial u}{\partial n} q d\Gamma dt + \int_{\Omega} u(\mathbf{x}, 0) q(\mathbf{x}, 0) d\Omega \\
&\quad - \int_0^T \int_{\Gamma} \mu u \frac{\partial q}{\partial n} d\Gamma dt - \int_0^T \int_{\Gamma} \mathbf{c}_n u q d\Gamma dt, \tag{4.5a}
\end{aligned}$$

$$\begin{aligned}
F(q) &= \int_{\Omega} \phi(\mathbf{x}) q(\mathbf{x}, 0) d\Omega - \int_0^T \int_{\Gamma} \mu a \frac{\partial q}{\partial n} d\Gamma dt \\
&\quad - \int_0^T \int_{\Gamma} \mathbf{c}_n a q d\Gamma dt, \tag{4.5b}
\end{aligned}$$

where  $\frac{\partial}{\partial n} \equiv \mathbf{n} \cdot \nabla$  and  $\mathbf{c}_n \equiv \mathbf{c} \cdot \mathbf{n}$ . It is mentioned that the last integral of  $N(u; q)$  in (4.5a), is usually not included in the weak form. For a proper inclusion of boundary residuals in the goal-oriented error-estimator however, the terms are included. This will become clear shortly when the error estimator is derived.

Suppose one is interested in evaluating the functional  $Q(u)$  from the solution  $u$  of (4.4). Following the variational approach in chapter 3, such an evaluation can be formulated as solving the (trivial) constrained optimisation problem (3.1), yielding the primal and dual equations:

$$N(u; q) = F(q), \quad \forall q \in V, \tag{4.6a}$$

$$N'(u; v, p) = Q'(u; v), \quad \forall v \in V. \tag{4.6b}$$

The dual operator  $N'(u; v, p)$  for the convection-diffusion problem with  $p$  the dual solution, is derived from  $N(u, q)$  as given in (4.4) using the limit form (A.1) from appendix A. This yields:

$$\begin{aligned}
N'(u; v, p) &= \int_0^T \int_{\Omega} \left( -v \frac{\partial p}{\partial t} - v(\mathbf{c} \cdot \nabla p) + \mu \nabla p \nabla v \right) d\Omega dt - \int_0^T \int_{\Gamma} \mu v \frac{\partial p}{\partial n} d\Gamma dt \\
&\quad + \int_{\Omega} v(\mathbf{x}, T) p(\mathbf{x}, T) d\Omega - \int_0^T \int_{\Gamma} \mu p \frac{\partial v}{\partial n} d\Gamma dt. \tag{4.7}
\end{aligned}$$

In equation (4.7) the convective boundary terms and the initial condition have cancelled. The operator  $N'(u; v, p)$  in (4.7) shows that the characteristic direction of the dual problem is exactly opposite of the primal characteristic direction with the dual initial condition given on  $t = T$ . This means that an outflow boundary for the primal problem, is an inflow boundary

for the dual problem. The dual problem is solved backward in time. Since equation (4.6b) has to hold for all  $v \in V$  the dual boundary conditions and the dual initial condition can be derived for each specific quantity of interest that leads to a well-posed dual problem. This is illustrated by the problems studied later in this chapter.

### 4.1.2 The coarse model

The coarse model problem is the convection equation which is also referred to as the *unperturbed* or *reduced* problem, since  $\mu$  is zero (see for instance [52, 35]). The coarse model is then given in strong form by:

$$\frac{\partial u_0}{\partial t} + \nabla \cdot (\mathbf{c} u_0) = 0, \quad \mathbf{x} \in \Omega, \quad t \in (0, T), \quad (4.8)$$

with the same initial condition as the fine model problem:  $u_0(\mathbf{x}, 0) = \phi(\mathbf{x})$ . Boundary conditions for the coarse model are only required on the inflow boundary  $\Gamma^-$ . The approximating model in weak form is then given by: find  $u_0 \in V_0$  such that

$$N_0(u_0; q) = F_0(q), \quad \forall q \in V_0, \quad (4.9)$$

where

$$\begin{aligned} N_0(u_0; q) = & \int_0^T \int_{\Omega} \frac{\partial u_0}{\partial t} q + q \nabla \cdot (\mathbf{c} u_0) d\Omega dt + \int_{\Omega} u_0(\mathbf{x}, 0) q(\mathbf{x}, 0) d\Omega \\ & - \int_0^T \int_{\Gamma^-} \mathbf{c}_n u_0 q d\Gamma dt, \end{aligned} \quad (4.10a)$$

$$F_0(q) = \int_{\Omega} \phi(\mathbf{x}) q(\mathbf{x}, 0) d\Omega - \int_0^T \int_{\Gamma^-} \mathbf{c}_n a^- q d\Gamma dt, \quad (4.10b)$$

with  $\mathbf{c}_n \equiv \mathbf{c} \cdot \mathbf{n}$ . Note that  $F_0(q) \neq F(q)$  because the boundary and initial conditions are imposed weakly, see also section 3.5. When the hierarchical models are of equal type, we would have  $F_0(q) = F(q)$ . Before continuing with the dual problem, some remarks are given on the solution spaces  $V$  and  $V_0$ .

**Remarks on solution spaces** Considering only sufficiently smooth solutions of equation (4.9) allows to consider  $V_0 = V$  and therefore  $u_0 \in V$ . This is essential for the variational approach in deriving the error estimator, as described in chapter 3 and Oden and Prudhomme [27]. This restricts

the possible solutions of (4.9) drastically. The work presented in this thesis however, concerns the application of the DWR method for particular situations that are relevant for fluid-flow related problems. We do not strive for a general framework for goal-oriented modelling-error estimation in classes of hierarchical models in which models are of a different type. In such classes one can have  $u \in V$  and  $u_0 \in V_0$  with  $V_0 \neq V$  which requires a new and thorough mathematical basis in order to apply dual-weighted residual error estimation. This is however, a research on its own and therefore not considered in this thesis.

Apart from ensuring the inclusion of boundary residuals in the modelling-error estimator, another important reason to impose boundary conditions weakly is the following. When Dirichlet boundary conditions are imposed strongly, the solution space for the convection-diffusion problem in (4.6a) and for the convection problem in (4.9) are not identical since additional restrictions are required. This is shown by considering the convection equation with strongly imposed homogeneous Dirichlet boundary conditions: find  $u_0 \in V_0$  such that

$$N_0(u_0; w) = F(w), \quad \forall w \in V_0, \quad (4.11)$$

where

$$\begin{aligned} N_0(u_0; w) &= \int_0^T \int_{\Omega} u_{0t} w + w \nabla \cdot (\mathbf{c} u_0) d\Omega dt, \\ F(w) &= 0, \end{aligned}$$

with  $V_0 = \{u_0, w \in H^1(\Omega); u_0, w = 0 \text{ on } \Gamma^-\}^1$ . By imposing the boundary conditions weakly as in (4.9) no restrictions on the test-function are required such that  $V_0 = \{u_0 \in H^1(\Omega)\}$  and therefore the test-function  $w$  for the convection equation can be chosen from  $V$ , the test space of the convection-diffusion problem.

Continuing the equations with weakly imposed boundary conditions and considering only sufficiently smooth solutions, the coarse dual problem is given by (see (3.7)):

$$N'_0(u_0; v, p_0) = Q'(u_0; v), \quad \forall v \in V, \quad (4.12)$$

with  $p_0$  the coarse dual solution. The coarse dual model operator  $N'_0(u_0; v, p_0)$  is derived from  $N_0(u_0; q)$ , given in (4.10a). Using the relations (A.1) from

---

<sup>1</sup>In case of non-homogeneous Dirichlet boundary conditions, the problem can be made homogeneous by so called ‘lifting’, see for instance [53].

appendix A and performing integration by parts to transfer derivatives from the  $v$  to  $p_0$ , yields:

$$\begin{aligned} N'_0(u_0; v, p_0) = & \int_0^T \int_{\Omega} -v \frac{\partial p_0}{\partial t} - v(\mathbf{c} \cdot \nabla p_0) d\Omega dt + \int_{\Omega} v(\mathbf{x}, T) p_0(\mathbf{x}, T) d\Omega \\ & + \int_0^T \int_{\Gamma^+} \mathbf{c}_n v p_0 d\Gamma dt. \end{aligned} \quad (4.13)$$

Since equation (4.12) has to hold for all  $v \in V$ , the dual boundary conditions and initial condition can be derived for each specific quantity of interest that leads to a well-posed dual problem.

### 4.1.3 The error estimator

In deriving the goal-oriented modelling-error estimator to estimate  $Q(u) - Q(u_0)$ , the approach described in section 3.4 is followed. The general error estimator is based on the exact error representation given in equation (3.22):

$$Q(u) - Q(u_0) = R(u_0; p_0) + R(u_0; \epsilon_0) + \frac{1}{2} \Delta R + r(e_0; \epsilon_0),$$

with  $\Delta R$  and  $r(e_0; \epsilon_0)$  the high-order terms given in (3.19) and (3.12), respectively. For linear problems such as the convection-diffusion problem, these high-order terms depend only on the quantity of interest  $Q(u)$  (equivalent to the linear diffusion-reaction problem, discussed in section 3.6). With  $Q(u)$  linear in  $u$ , both terms  $\Delta R$  and  $r(e_0; \epsilon_0)$  are zero and we have the exact a-posteriori error representation:

$$Q(u) - Q(u_0) = R(u_0; p_0) + R(u_0; \epsilon_0) = R(u_0; p). \quad (4.14)$$

With the residual defined in (3.9a) and adding  $N_0(u_0; p) - F_0(p) = 0$  following section 3.5, yields.

$$R(u_0; p) = F(p) - N(u_0; p) + N_0(u_0; p) - F_0(p), \quad (4.15)$$

This form allows to split the contributions in the estimator into a contribution from the inner domain  $\Omega$  and from the boundary  $\Gamma$ . For the goal-oriented modelling-error estimator for the convection-diffusion problem, we

then find:

$$\begin{aligned}
Q(u) - Q(u_0) &= R(u_0; p) = N_0(u_0; p) - N(u_0; p) - (F_0(p) - F(p)) \\
&= - \int_0^T \int_{\Omega} \mu \nabla u_0 \nabla p \, d\Omega dt + \int_0^T \int_{\Gamma} \mu \frac{\partial u_0}{\partial n} p \, d\Gamma dt \\
&\quad - \int_0^T \int_{\Gamma} \mu (a - u_0) \frac{\partial p}{\partial n} \, d\Gamma dt \\
&\quad + \int_0^T \int_{\Gamma^{+,0}} \mathbf{c}_n (a^{+,0} - u_0) p \, d\Gamma dt, \tag{4.16}
\end{aligned}$$

where contributions from the boundaries are separated in ‘convective’ (involving  $\mathbf{c}$ ) and ‘diffusive’ contributions (involving  $\mu$ ). Note that the convective contribution is limited to outflow and noflow boundaries. This is caused by the fact that the applied boundary conditions in the fine model (4.4), involve all boundaries. The coarse model (4.9) however, only involves the inflow boundary. Subtracting the model operators as done in (4.16), means ‘subtracting’ the boundaries:  $\Gamma - \Gamma^- = \Gamma^{+,0}$ . This result is obvious, since on an inflow boundary both the fine and coarse model have the same boundary condition. Therefore the residual  $a - u_0$  is zero on an inflow boundary and, as a result, it does not contribute to the modelling error. This applies to the diffusive contribution as well and therefore the inflow boundary  $\Gamma^-$  can also be left out of (4.16), which yields:

$$\int_0^T \int_{\Gamma} \mu (a - u_0) \frac{\partial p}{\partial n} \, d\Gamma dt = \int_0^T \int_{\Gamma^{+,0}} \mu (a^{+,0} - u_0) \frac{\partial p}{\partial n} \, d\Gamma dt. \tag{4.17}$$

Thus, the error estimator has no contributions from an inflow boundary.

#### 4.1.4 Coarse dual-weighted estimator

For reasons of efficiency, when applying the error estimator in adaptive modelling, the coarse dual solution  $p_0$  should be used to compute the estimator:

$$Q(u) - Q(u_0) \approx R(u_0; p_0). \tag{4.18}$$

This is explained in sections 2.3 and 2.4.3. (See also [12, 27, 32].) For the linear convection-diffusion problem described above, where  $p_0$  is the solution



of (4.12), we have:

$$\begin{aligned}
R(u_0; p_0) &= - \int_0^T \int_{\Omega} \mu \nabla u_0 \nabla p_0 \, d\Omega dt + \int_0^T \int_{\Gamma} \mu \frac{\partial u_0}{\partial n} p_0 \, d\Gamma dt \\
&\quad - \int_0^T \int_{\Gamma^{+,0}} \mu (a^{+,0} - u_0) \frac{\partial p_0}{\partial n} \, d\Gamma dt \\
&\quad + \int_0^T \int_{\Gamma^{+,0}} \mathbf{c}_n (a^{+,0} - u_0) p_0 \, d\Gamma dt. \tag{4.19}
\end{aligned}$$

In the following sections, both analytical and numerical examples are given in which the fine dual and coarse dual-weighted estimators are computed and compared. Integral as well as point quantities of interest are studied.

## 4.2 Steady case 1: integral $Q(u)$

In this section, the goal-oriented modelling-error estimator is studied for an integral quantity of interest evaluated from the solution of the steady 1-D convection-diffusion equation. First the primal problems (both fine and coarse) are given, from which the dual problems are derived.

### 4.2.1 The primal problems

The integral quantity of interest, given by:

$$Q(u) = \int_{\Omega} u \, dx, \tag{4.20}$$

is evaluated from the solution of the steady, linear 1-D convection-diffusion equation<sup>2</sup> on  $\Omega = (0, 1)$ , with the boundary conditions  $a^0 = 0$  and  $a^1 = 1$ :

$$\begin{aligned}
N(u; q) = F(q) &\Rightarrow \\
&\int_{\Omega} (c u_x q + \mu u_x q_x) dx - \mu u_x q|_0^1 + \mu u(0) q_x(0) - \mu u(1) q_x(1) + \\
&c u(0) q(0) - c u(1) q(1) = \mu a^0 q_x(0) + c a^0 q(0) \mu a^1 q_x(1) - c a^1 q(1). \tag{4.21}
\end{aligned}$$

A positive convective velocity  $c > 0$  is considered. The solution of equations (4.21) is given by:

$$u(x) = \frac{e^{c/\mu} - e^{cx/\mu}}{e^{c/\mu} - 1}. \tag{4.22}$$

---

<sup>2</sup>The equations are not made ‘dimensionless’ by introducing the Péclet number  $\text{Pe} = \frac{cL}{\mu}$  since for the approximating model the convective velocity must be identical to that of the sophisticated model. Only then a meaningful approximation is obtained which leaves only the diffusion coefficient to be varied.

For  $c = 1$  and three values of  $\mu$ , the fine model solution is given in figure 4.1(a). The quantity of interest is then given by:

$$Q(u) = \int_{\Omega} u \, dx = \frac{1 + e^{c/\mu}(c/\mu - 1)}{c/\mu(e^{c/\mu} - 1)}. \quad (4.23)$$

Now, we want to evaluate the quantity of interest based on the coarse model in which the diffusion is omitted:

$$N_0(u_0; q) = F_0(q) \Rightarrow \int_{\Omega} c u_{0,x} q \, dx + c u_0(0)q(0) = c a^0 q(0), \quad c > 0. \quad (4.24)$$

The solution of this problem depends solely on the boundary conditions:

$$u_0(x) = a^0 = 1. \quad (4.25)$$

This yields for the quantity of interest  $Q(u_0) = a^0$  and for the real error in  $Q(u_0)$ :

$$Q(u) - Q(u_0) = \frac{1 + e^{c/\mu}(c/\mu - 1)}{c/\mu(e^{c/\mu} - 1)} - 1 = \frac{-e^{-c/\mu}}{e^{-c/\mu} - 1} - \frac{\mu}{c}. \quad (4.26)$$

On the inner domain, the limit of the fine model solution for vanishing diffusion  $\mu \rightarrow 0$ , is equal to the coarse model solution:

$$\lim_{\mu \rightarrow 0} u(x) = u_0(x), \quad \forall x \in (0, 1).$$

On the boundary, however, this is not the case:

$$\lim_{\mu \rightarrow 0} u(1) \neq u_0(1),$$

emphasising we are dealing with a singular perturbation problem.

### 4.2.2 The dual problems

In order to estimate the modelling error in the quantity of interest by the DWR method, we first derive the dual problems. The fine dual problem in weak form is given by:

$$N'(v; p) = Q(u; v) \Rightarrow \int_{\Omega} (-c v p_x + \mu v_x p_x) \, dx - \mu v p_x|_0^1 - \mu v_x(1)p(1) + \mu v_x(0)p(0) = \int_{\Omega} v \, dx. \quad (4.27)$$

Since equation (4.27) has to hold for all  $v$ , the boundary conditions are:  $p(0) = p(1) = 0$ . The fine dual solution is then:

$$p(x) = \frac{e^{-cx/\mu} - 1}{e^{-c/\mu} - 1} - \frac{x}{c}, \quad (4.28)$$

which is shown in figure 4.1(b) for three values of  $\mu$ .

For the coarse dual problem we have:

$$N'_0(v, p_0) = Q(v) \Rightarrow \int_{\Omega} -c v p_{0,x} dx + c v(1) p_0(1) = \int_{\Omega} v dx. \quad (4.29)$$

Since (4.29) has to hold for all  $v$ , the boundary condition is found to be  $p_0(1) = 0$ . The coarse dual solution is then given by  $p_0(x) = (1 - x)/c$ . This solution is shown together with the solution of the fine dual problem for  $c = 1$  and three values of  $\mu$  in figure 4.1(b). Figure 4.1(b) shows that

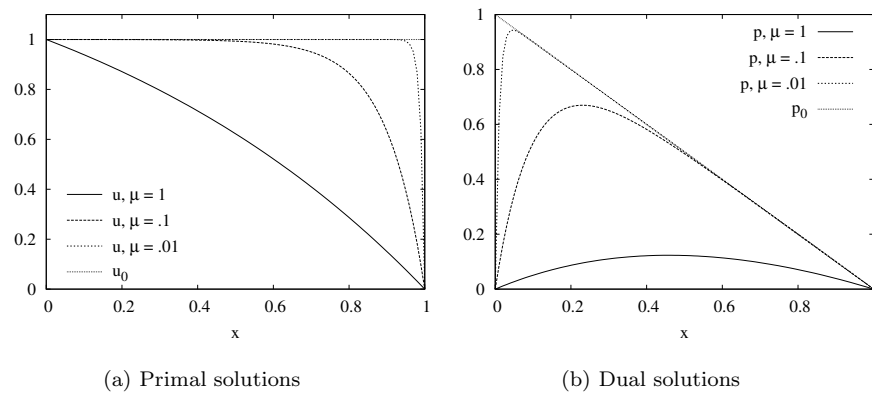


Figure 4.1: Primal and dual solutions for  $\mu = 1, 0.1$  and  $0.01$ .

the dual problem is also a singular perturbation problem. The fine dual solution approaches the coarse dual solution on  $(0, 1)$  for  $\mu \rightarrow 0$ , but on the dual outflow boundary a residual remains:  $\lim_{\mu \rightarrow 0} p(0) \neq p_0(0)$ .

### 4.2.3 The error estimator

The fine dual-weighted residual estimator, can now be evaluated according to equation (4.16) for the steady case. The boundary residuals derived from

the given boundary conditions and the computed coarse model solution are:

$$\begin{aligned} a^0 - u_0(0) &= 0, \\ a^1 - u_0(1) &= -1. \end{aligned}$$

Using the dual boundary conditions found from (4.27), the fine dual-weighted estimator yields:

$$\begin{aligned} R(u_0; p) &= N_0(u_0; p) - N(u_0; p) - (F_0(p) - F(p)) \\ &= - \int_{\Omega} \mu u_{0x} p_x dx + \mu u_{0x} p|_0^1 \\ &\quad - \mu(a^1 - u_0(1))p_x(1) - c(a^1 - u_0(1))p(1) \\ &= -\mu(a^1 - u_0(1))p_x(1) = \frac{-e^{-c/\mu}}{e^{-c/\mu} - 1} - \frac{\mu}{c}, \end{aligned} \quad (4.30)$$

which is exact (compare with the exact error  $Q(u) - Q(u_0)$  in (4.23)). Note that the error estimator in equation (4.30) only has a contribution from the boundary residual.

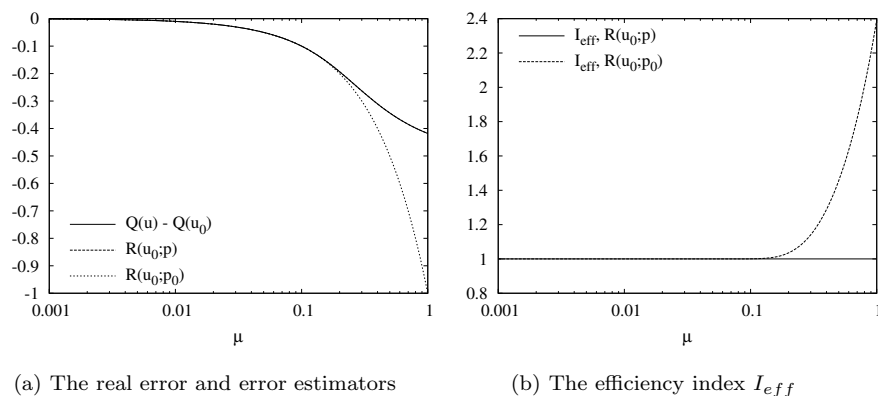
Similarly, we find for the coarse dual-weighted estimator:

$$\begin{aligned} R(u_0; p_0) &= N_0(u_0; p_0) - N(u_0; p_0) - (F_0(p_0) - F(p_0)) \\ &= -\mu(a^1 - u_0(1))p_{0x}(1) = -\frac{\mu}{c}. \end{aligned} \quad (4.31)$$

Also the coarse dual-weighted estimator (4.31) has a contribution exclusively from the boundary. The estimators  $R(u_0; p)$  and  $R(u_0; p_0)$  and the real error  $Q(u) - Q(u_0)$ , are shown in figure 4.2 for  $c = 1$  together with the efficiency index (defined in equation (2.47)). Note that the fine dual-weighted estimator  $R(u_0; p)$  is exact and therefore coincides with the real error  $Q(u) - Q(u_0)$ . For  $\mu \gtrsim 0.3$ , the exact error is over-estimated by the coarse dual-weighted estimator  $R(u_0; p_0)$ . For small  $\mu$  the coarse dual-weighted estimator (4.31) approaches the fine dual-weighted estimator (4.30). Both estimators are of order  $O(\mu)$ :

$$R(u_0; p_0) = -\frac{\mu}{c} \equiv \lim_{\mu \rightarrow 0} R(u_0; p), \quad (4.32)$$

which is due to the derivative of  $p(x)$  at  $x = 1$  that approaches the derivative of the coarse dual solution:  $\lim_{\mu \rightarrow 0} p_x(1) = p_{0x}(1)$ , see also figure 4.1(b). Although this is not the case at the other boundary  $x = 0$ , this has no consequence, because it is an inflow boundary. In section 4.1.3 it is explained that inflow boundaries have no contribution to the error estimator.



(a) The real error and error estimators

(b) The efficiency index  $I_{eff}$ Figure 4.2: The error estimators and efficiency index as function of  $\mu$  for  $c = 1$ .

### 4.3 Steady case 2: boundary derivative $Q(u)$

In this section, a point quantity of interest is discussed. Some of the limitations of the DWR method will become clear when the coarse dual solution is applied, despite only 1-D steady and linear problems are considered.

Again, the same fine model (4.21) and coarse model (4.24) as in section 4.2 are considered. The solutions of these models are shown in figure 4.1(a). The quantity of interest considered now, concerns the solution derivative at  $x = 1$ :

$$Q(u) = \mu u_x(1). \quad (4.33)$$

Since the fine model solution has a boundary layer at  $x = 1$ , the quantity of interest  $Q(u) = \mu u_x(1)$  can be seen as a ‘stress’ term. Through differentiation of (4.22), we find:

$$Q(u) = \mu u_x(1) = \frac{c}{e^{-c/\mu} - 1}. \quad (4.34)$$

The coarse model solution (4.25) is constant at  $\Omega$  and has no boundary layer, as expected from the ‘unperturbed’ or ‘reduced’ problem. The quantity of interest based on the approximating solution is zero:

$$Q(u_0) = \mu u_{0x}(1) = 0.$$

This situation can be compared with the evaluation of the shear stress at a wall in fluid dynamics. The shear stress based on the Euler equations

is zero, contrary to the shear stress in the Navier-Stokes solution ('slip' vs 'no-slip').

In the following sections, the dual problems are derived and the goal-oriented modelling-error estimator is evaluated based on both the fine and coarse dual solution  $R(u_0, p)$  and  $R(u_0, p_0)$ , respectively.

### 4.3.1 The dual problem

The fine dual problem can be derived similar to the procedure described in section 4.1.1, but for the steady case and with a different quantity of interest:

$$\int_{\Omega} (-c v p_x + \mu v_x p_x) dx - \mu v p_x|_0^1 - \mu v_x(1)p(1) + \mu v_x(0)p(0) = \mu v_x(1). \quad (4.35)$$

Since (4.35) must hold for all  $v$ , we find as boundary conditions  $p(0) = 0$  and  $p(1) = -1$ . The solution to this dual problem for arbitrary  $c$  and  $\mu$  is:

$$p(x) = \frac{1 - e^{-cx/\mu}}{e^{-c/\mu} - 1}, \quad (4.36)$$

which is shown in figure 4.3 for  $c = 1$  and three values of  $\mu$ .

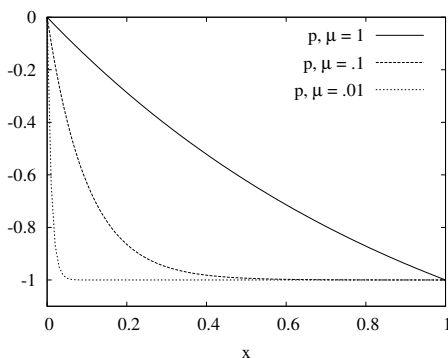


Figure 4.3: Fine-model dual solutions for  $c = 1$  and  $\mu = 1, 0.1$  and  $0.01$ .

The coarse dual problem in weak form is given by:

$$N'_0(p_0; v) = Q(v) \Rightarrow \int_{\Omega} -c v p_{0,x} dx + c v(1)p_0(1) = \mu v_x(1). \quad (4.37)$$

From equation (4.37) it is clear that this problem is ill-posed for  $\mu > 0$ . Only for the trivial case with  $-c p_{0,x} = 0$ ,  $p_0(1) = 0$  and  $\mu = 0$ , this is a well-posed

problem, but useless for our purpose. A more physical explanation is the following: the dual problem should give the sensitivity of the quantity of interest  $Q$  for perturbations in the primal solution. However, the quantity of interest is of a form that can not be represented by the coarse problem: we want to evaluate a diffusive functional  $Q$  by use of a model that lacks the presence of a diffusion.

Since we want to utilise the coarse dual solution in the modelling-error estimator for reasons of efficiency (as mentioned earlier in chapters 2 and 3), we do not want to use the fine-model dual solution. At least not in the whole domain. In the discrete approach one possible way to use the fine model solution but to save computational time, is by solving the fine dual problem on a coarse mesh to save computational time. This might give rise to stability problems in solving the dual problem numerically, since the fine dual solution might have boundary layers as well (as in the previous case shown in figure 4.1(b)). Therefore another approach is studied to construct an approximating solution for the coarse dual problem (4.37). The sensitivity information provided by the fine dual solution, can then also be used to decide where the fine dual problem should be used and where the coarse dual problem can be applied.

#### Approximation by increasing the domain by size $\epsilon$

A solution can be constructed by increasing the domain with a small parameter  $0 < \epsilon \ll 1$ . The quantity of interest is rewritten as a distribution on the increased domain, and integration by parts is performed. This yields:

$$v_x(1) = \int_0^{1+\epsilon} v_x(x)\delta(x-1) dx = - \int_0^{1+\epsilon} v(x)\delta_x(x-1) dx, \quad (4.38)$$

where  $\delta(x-1)$  is a Dirac delta function in  $x = 1$ . The coarse dual problem (4.37) on  $x \in (0, 1 + \epsilon)$  becomes now:

$$\int_0^{1+\epsilon} -c v p_{0,x} dx + c v(1+\epsilon)p_0(1+\epsilon) = -\mu \int_0^{1+\epsilon} v(x)\delta_x(x-1) dx. \quad (4.39)$$

To let this equation hold for all  $v$ , the boundary condition is  $p_0(1+\epsilon) = 0$ . The quantity of interest ends up as right-hand side for the dual equation, from which the solution follows:

$$\int_0^{1+\epsilon} p_{0,x} dx = \int_0^{1+\epsilon} \frac{\mu}{c} \delta_x(x-1) dx \quad \Rightarrow \quad p_0(x) = \frac{\mu}{c} \delta(x-1). \quad (4.40)$$

The solution on the original domain  $x \in (0, 1)$  is found by taking the limit  $\epsilon \rightarrow 0$ , which yields the same solution for  $p_0(x)$  as given in (4.40). The

derivative of the dual solution appearing in the model-error estimator however, only exists in distributed sense as given in (4.40). Since the derivative of the dual solution at the boundary  $x = 1$  is required, the above described approach to construct the dual solution (4.40) is not of much help.

### Approximation by domain decomposition

To obtain an alternative dual problem instead of the ill-posed coarse-model dual problem (4.37), we can apply the fine model dual problem in a small region, close to the boundary where the quantity of interest is defined. This approach is not the same as the method to construct an asymptotic expansion to approximate the solution of singular perturbation problems involving boundary layer behaviour. In the latter case, a region of size  $\delta(\mu)$  near the point where the boundary layer arises, is ‘rescaled’ or ‘stretched’, see for instance [35]. Our objective is however, not to construct an approximating solution of the fine dual equation, including its boundary layer by an asymptotic expansion. Our objective is to construct an approximating dual problem based on the fine and coarse dual problem, in order to have a well-posed approximating dual solution with as little use of the fine model for reasons of efficiency.

For this purpose, the domain is split into two non-overlapping sub-domains  $\Omega^c$  and  $\Omega^f$  ( $\Omega = \Omega^c + \Omega^f$ ,  $\Omega^c \cap \Omega^f = \emptyset$ ) with interface  $\mathcal{I} = \partial\Omega^c \cap \partial\Omega^f$ . On  $\Omega^c$ , the coarse dual model is applied and on  $\Omega^f$  the fine dual model. Minimising computational time, means that the size of  $\Omega^f$  should be as small as possible, for instance  $\epsilon$ . In the present case, this means that  $\Omega^c = (0, 1 - \epsilon)$  and  $\Omega^f = (1 - \epsilon, 1)$  with the interface  $\mathcal{I} = 1 - \epsilon$ . The solutions on both domains  $\Omega^c$  and  $\Omega^f$  are referred to as  $p^c$  and  $p^f$  respectively.

$C^0$ -continuity of the solution is required on the interface, which is enforced by adding an interface condition for the complete system (derived by performing two times integration by parts):

$$\int_{\Omega_1} -cvp_x^c dx + cv(p_R^c - p^c(\mathcal{I})) + \int_{\Omega_2} (-cvp_x^f + \mu v_x p_x^f) dx + cv(p_L^f - p^f(\mathcal{I})) + \mu v_x(p_L^f - p^f(\mathcal{I})) + \mu v_x(p^f(1)_R - p^f(1)) = 0. \quad (4.41)$$

The term  $p_L^f$  is the value from the left of the interface, coming from the solution on  $\Omega^c$ . The term  $p_R^c$  is the value from the right of the interface, coming from the solution on  $\Omega^f$ . The  $C^0$ -continuity on the interface demands that the terms  $p_L^f - p^f(\mathcal{I})$  and  $p_R^c - p^c(\mathcal{I})$  are zero. In equation (4.41),  $p^f(1)_R$  is the boundary condition determined by the quantity of interest as in equation (4.35), i.e.  $p^f(1)_R = -1$  and can be written at the right-hand side.



A problem is now that the fine problem on  $\Omega^f$  needs the value from the left and the coarse problem on  $\Omega^c$  needs information from the right to be solved, but for either side it cannot be determined. Therefore no solution can be constructed yet for equation (4.41). An additional condition is needed, for which we take  $C^1$ -continuity. This is achieved by rewriting equation (4.41) by using integration by parts such that the second derivative of  $p$  appears in the fine dual equation:

$$\begin{aligned} \int_{\Omega_1} -cvp_x^c dx + cv(p_R^c - p^c(\mathcal{I})) + \int_{\Omega_2} (-cvp_x^f - \mu v p_{xx}^f) dx \\ + \mu v((p_L^f)_x - p_x(\mathcal{I})) + cv(p_L^f - p^f(\mathcal{I})) \\ + \mu v_x(p_L^f - p^f(\mathcal{I})) - \mu v_x p^f(1) = \mu v_x(1). \end{aligned} \quad (4.42)$$

Now, the fine model solution on  $\Omega^f$  uses the derivative from the coarse model solution on  $\Omega^c$  and the problem is well-posed. The overall solution  $\tilde{p} = p^c \cap p^f$  is found to be:

$$\tilde{p} = -c, \quad x \in \Omega. \quad (4.43)$$

This is equal to the limit of the fine dual solution (4.36) on  $x = (0, 1)$ , for vanishing  $\mu$ . Therefore the approximation solution (4.43) is considered a useful coarse dual solution. Note that solution (4.43) is independent of the size of  $\Omega^f$ .

### 4.3.2 The error estimator

The modelling-error estimator based on the fine dual solution is found through evaluation of the estimator in equation (4.16) for the steady case:

$$\begin{aligned} R(u_0; p) &= N_0(u_0; p) - N(u_0; p) - (F_0(p) - F(p)) \\ &= - \int_{\Omega} \mu u_{0x} p_x dx + \mu u_{0x} p|_0^1 - \mu(a^1 - u_0(1))p_x(1) \\ &\quad - c(a^1 - u_0(1))p(1) \\ &= \frac{c}{e^{-c/\mu} - 1}. \end{aligned} \quad (4.44)$$

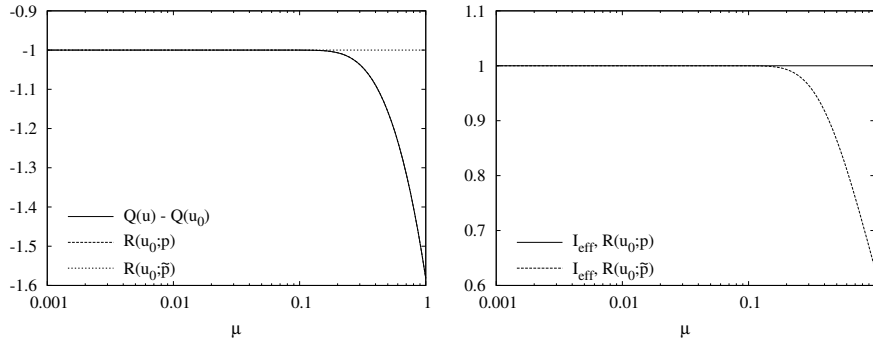
This estimator is exact (compare (4.44) with  $Q(u)$  in (4.34), remembering that  $Q(u_0) = 0$ ). Note that for the limit of vanishing  $\mu$  the estimator (4.44) approaches the negative convective velocity:  $\lim_{\mu \rightarrow 0} R(u_0; p) = -c$ . The estimator and the efficiency index are shown in figure 4.4. Note that the estimator is exact, therefore it coincides with the real error  $Q(u) - Q(u_0)$ .

### The error estimator based on the approximating dual solution

The error estimator based on the approximating dual solution  $\tilde{p}(x) = -c$  from equation (4.42), is found by:

$$\begin{aligned}
 R(u_0; \tilde{p}) &= N_0(u_0; \tilde{p}) - N(u_0; \tilde{p}) - (F_0(\tilde{p}) - F(\tilde{p})) \\
 &= - \int_{\Omega} \mu u_{0x} \tilde{p}_x dx + \mu u_{0x} \tilde{p}|_0^1 - \mu(a^1 - u_0(1)) \tilde{p}_x(1) \\
 &\quad - c(a^1 - u_0(1)) \tilde{p}(1) \\
 &= -c(-1) \tilde{p}(1) = -c.
 \end{aligned} \tag{4.45}$$

This is equal to the limit of the fine dual-weighted estimator (4.44) for vanishing  $\mu$ , which demonstrates that a reliable coarse dual-weighted estimator is obtained. This is confirmed by figure 4.4 which shows the estimator and the efficiency index.



(a) The real error and error estimators

(b) The efficiency index  $I_{eff}$

Figure 4.4: The error estimators and efficiency index as function of  $\mu$  for  $c = 1$ .

## 4.4 Steady case 3: point $Q(u)$

When one is interested in the solution in a point  $\xi \in \Omega$ :

$$Q(u) = u(\xi), \tag{4.46}$$

the DWR method can be of use again to estimate the modelling error when utilising the coarse model to approximate the quantity of interest by  $Q(u_0)$

(when  $\xi \in \Gamma$ ,  $u$  is known and approximation by  $u_0$  is superfluous). We will illustrate the use of the DWR method below for the case  $\xi = \frac{1}{2}$ .

We consider again the fine and coarse primal problems as defined in equations (4.21) and (4.24), respectively. The solutions of these fine and coarse problems are given in (4.22) and (4.25), respectively, and shown in figure 4.1(a). From these solutions, the real error  $Q(u(\xi)) - Q(u_0(\xi))$  can be computed which yields for  $\xi = 1/2$ :

$$Q(u(1/2)) - Q(u_0(1/2)) = \frac{-e^{c/2\mu} + 1}{e^{c/\mu} - 1}. \quad (4.47)$$

As in the previously studied case, the fine dual-weighted estimator  $R(u_0; p)$  is also derived to compare this with the coarse dual-weighted estimator  $R(u_0; p_0)$ .

#### 4.4.1 The dual problems

The fine dual problem for this example is given by:

$$\begin{aligned} N(p; v) = Q(u; v) \Rightarrow \\ \int_{\Omega} -c v p_x + \mu v_x p_x dx + \mu v p_x|_{\Gamma} - \mu v_x(1)p(1) + \mu v_x(0)p(0) = \\ \int_{\Omega} v(x)\delta(x - \xi)dx, \quad \forall v \in H^1, \quad \xi \in \Omega, \quad (4.48) \end{aligned}$$

where the quantity of interest is written in integral form, using the Dirac delta function  $\delta$ :

$$v(\xi) = \int_{\Omega} v(x)\delta(x - \xi)dx.$$

Since the problem (4.48) has to hold for all  $v$ , the boundary conditions are  $p(0) = p(1) = 0$ . Integrating the dual equation yields a Heaviside function in the right-hand side. This allows to separate the equation into two ODE's on  $x = (0, \xi)$  and  $x = (\xi, 1)$ , which are solved using the boundary conditions  $p(0) = p(1) = 0$  and the fact that  $p(x)$  should be continuous in  $x = \xi$ . The solution (without given the complete derivation) is given by:

$$\begin{aligned} p(x) = \frac{1}{c} \mathbf{H}(x - 1/2) e^{(c(1-2x)/2\mu)} - \frac{1}{c} \mathbf{H}(x - 1/2) \\ + \frac{e^{-cx/\mu}(1 - e^{-c/2\mu})}{c(e^{-c/\mu} - 1)} + \frac{e^{-c/2\mu} - 1}{c(e^{-c/\mu} - 1)}, \quad (4.49) \end{aligned}$$

and is shown in figure 4.5 for three values of  $\mu$  and convective velocity  $c = 1$ .

For the coarse dual problem in weak form we have:

$$N_0(p_0; v) = Q(v) \Rightarrow \int_{\Omega} -c v p_{0x} dx + c v(1) p_0(1) = \int_{\Omega} v(x) \delta(x - \xi) dx, \quad \forall v \in H^1, \quad \xi \in \Omega, \quad (4.50)$$

which has to hold for all  $v$  by virtue of which the boundary condition is  $p_0(1) = 0$ . The solution  $p_0(x)$  is a Heaviside function:

$$p_0(x) = -\frac{1}{c}(\mathbf{H}(x - 1/2) + 1), \quad (4.51)$$

and is shown in figure 4.5, together with the fine dual solution.

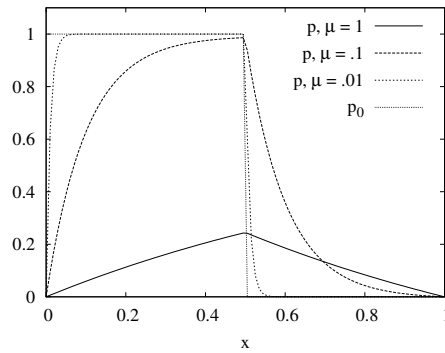


Figure 4.5: Fine and coarse dual solutions for  $\xi = 1/2$ ,  $c = 1$ , and  $\mu = 1$ , 0.1 and 0.01.

#### 4.4.2 The error estimator

With the dual solution available, the modelling-error estimator can be calculated. With  $u_{0x} = 0$  (since  $u_0(x) = 1$ ) and  $p(0) = p(1) = 0$ , the estimator becomes:

$$\begin{aligned} R(u_0; p) &= N_0(u_0; p) - N(u_0; p) - (F_0(p) - F(p)) \\ &= - \int_{\Omega} \mu u_{0x} p_x dx + \mu u_{0x} p|_0^1 - \mu(a^1 - u_0(1)) p_x(1) \\ &\quad - c(a^1 - u_0(1)) p(1) \\ &= -\mu(a^1 - u_0(1)) p_x(1). \end{aligned} \quad (4.52)$$

Note that in this case the estimator only has a contribution from the boundary, although the quantity of interest is defined in a point in the domain. Evaluating the derivative at  $x = 1$  and substituting in (4.52), we obtain:

$$R(u_0; p) = -\mu(0 - 1)p_x(1) = \frac{-e^{c/2\mu} + 1}{e^{c/\mu} - 1}, \quad (4.53)$$

which is equal to the exact error (4.47).

From figure 4.5 and from equation (4.51), it is clear that the derivative of  $p_0(x)$ , given by  $p_{0x}(x) = -\delta(x - 1/2)$ , is zero at  $x = 1$ . With  $u_{0x}(x) = 0$ ,  $p_0(1) = 0$  and  $a^0 \equiv u_0(0)$ , also the coarse dual-weighted estimator  $R(u_0, p_0)$  is zero:

$$\begin{aligned} R(u_0; p_0) &= N_0(u_0; p_0) - N(u_0; p_0) - (F_0(p_0) - F(p_0)) \\ &= - \int_{\Omega} \mu u_{0x} p_{0x} dx + \mu u_{0x} p_0|_0^1 - \mu(a^1 - u_0(1))p_{0x}(1) \\ &\quad - c(a^1 - u_0(1))p_0(1) \\ &= -\mu(a^1 - u_0(1))p_{0x}(1) = -\mu(0 - 1)0 = 0. \end{aligned} \quad (4.54)$$

The error estimators (4.52) and (4.54) are shown in figure 4.6 together with the exact error. Although the error is small, and for  $\mu \lesssim .1$  approxi-

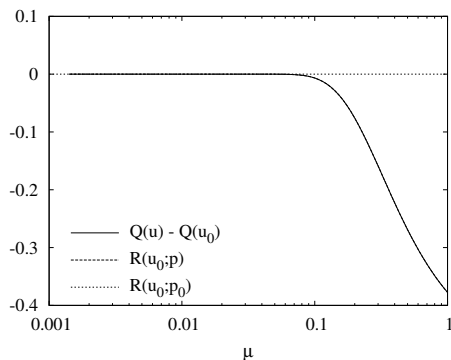


Figure 4.6: Real error and estimators based on fine and coarse dual solution ( $c = 1$ ).

mately zero, the coarse dual-weighted residual estimator  $R(u_0; p_0)$  is useless as error estimator for this case. This is easily explained from a 'physical' point of view enforced by the fine and coarse dual solutions as shown in figure 4.5. The coarse model only incorporates convection which means that

with  $c > 0$  the coarse model solution  $u_0$  in a point  $\xi \in \Omega$  only 'feels' information from the left. (For the unsteady case the characteristics  $dx/dt = c$  travel from left to right.) Or in other words: there is no process involved in the coarse model, that is able to transport disturbances in the solution occurring at  $x > \xi$  through the domain to  $x = \xi$ . This is exactly what the coarse dual solution  $p_0$  shows (see figure 4.5): at  $x \leq 1/2$  the dual solution is one and at  $x > 1/2$  it is zero.

For the fine dual problem this is different, since the diffusive part of the fine model (4.1) is able to transport perturbations 'upstream' i.e. in the opposite direction of the convection. The higher  $\mu$ , the stronger this phenomenon is; this is exactly what the dual solution  $p$  in figure 4.5 is showing. For the very diffusive case with  $\mu = 1$ , the dual solution is almost symmetric around  $x = \xi$ . This means that perturbations in  $u$  at equal distances left or right from  $x = \xi$ , have approximately the same influence on  $u(\xi)$  and therefore on  $Q(u(\xi))$ . Figure 4.5 also shows a decreasing sensitivity of  $u(\xi)$  for the solution at the right side of  $\xi$ , but an increasing sensitivity for the solution at the left of  $\xi$ . In fact, the fine dual solution  $p$  tends to  $p_0$  for small  $\mu$  on the inner domain:

$$\begin{aligned} \lim_{\mu \rightarrow 0} p(x) &= \lim_{\mu \rightarrow \infty} \left( \frac{1}{c} \mathbf{H}(x - 1/2) e^{(c(1-2x)/2\mu)} - \frac{1}{c} \mathbf{H}(x - 1/2) + \right. \\ &\quad \left. + \frac{e^{-cx/\mu}(1 - e^{-c/2\mu})}{c(e^{-c/\mu} - 1)} + \frac{e^{-c/2\mu} - 1}{c(e^{-c/\mu} - 1)} \right) \\ &= 0 - \frac{1}{c} \mathbf{H}(x - 1/2) + 0 + \frac{1}{c} = -\frac{1}{c} (\mathbf{H}(x - 1/2) + 1) = p_0(x). \end{aligned} \quad (4.55)$$

On the left boundary a singular perturbation remains, with  $p(0) = 0$  and  $p_0(0) = 1$ .

**Remark on fine dual solution** As can be seen in figure 4.5, the maximum of  $p(x)$  decreases with increasing  $\mu$ . This might look strange at first glance, but it is explained easily. The fine model solution (4.22) has the following limit for increasing  $\mu$ :

$$\lim_{\mu \rightarrow \infty} u(x) = \lim_{\mu \rightarrow \infty} \frac{e^{c/\mu} - e^{cx/\mu}}{e^{c/\mu} - 1} = 1 - x, \quad x \in \Omega. \quad (4.56)$$

This limit solution is independent from  $\mu$  (and  $c$  as well). So the more diffusive the fine model is, the more it tends to a constant solution. Therefore it will be less sensitive for perturbations anywhere in the domain. For completeness, we also illustrate this by the limit for increasing  $\mu$  of the fine-model dual solution:

$$\begin{aligned}
\lim_{\mu \rightarrow \infty} p(x) &= \lim_{\mu \rightarrow \infty} \left( \frac{1}{c} \text{H}(x - 1/2) e^{(c(1-2x)/2\mu)} - \frac{1}{c} \text{H}(x - 1/2) \right. \\
&\quad \left. + \frac{e^{-cx/\mu}(1 - e^{-c/2\mu})}{c(e^{-c/\mu} - 1)} + \frac{e^{-c/2\mu} - 1}{c(e^{-c/\mu} - 1)} \right) \\
&= \frac{1}{c} \text{H}(x - 1/2) - \frac{1}{c} \text{H}(x - 1/2) - \frac{1}{2c} + \frac{1}{2c} = 0. \tag{4.57}
\end{aligned}$$

## 4.5 Unsteady discrete problem

In this section, results are given for the unsteady convection-diffusion problem on  $(x, t) \in \Omega \times (0, T)$  with  $\Omega = (0, 1)$  and  $T = 0.5$ . The quantity of interest is the solution integral on the final time  $T$ , as given by:

$$Q(u) = \int_{\Omega} u(x, T) dx, \tag{4.58}$$

for which the fine dual-weighted estimator should be exact. The fine and coarse model dual equation for the quantity of interest (4.58), are derived in section 4.1.1 and 4.1.2, respectively. Computations are performed with a Galerkin spectral element method ([54, 55, 56, 57]). The initial solution is given by:

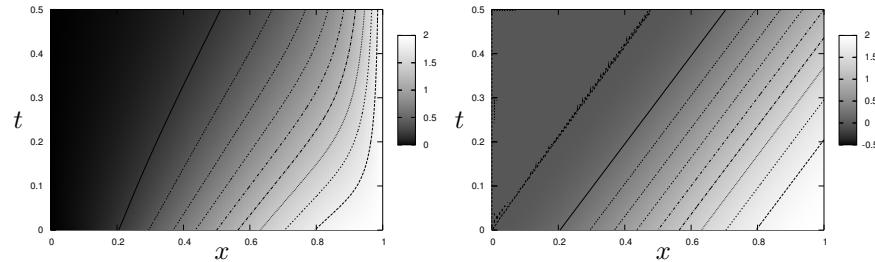
$$\phi(x) = 1 - \cos \pi x, \quad x \in [0, 1]. \tag{4.59}$$

In the examples, a fixed convective velocity  $c = 1$  is used. The boundary conditions  $u(0, t) = a^1$  and  $u(1, t) = a^0$  for the fine model (4.1), are derived from the initial condition:  $a^0 = \phi(0) = 0$  and  $a^1 = \phi(1) = 2$ . The boundary condition for the approximating model (4.8) with  $c > 0$ , is  $u_0(0) = \phi(0) = 0$ . The estimators  $R(u_0, p)$  and  $R(u_0, p_0)$  are evaluated for different values of the diffusion coefficient  $\mu$ .

In appendix B, some essential basics of the Galerkin spectral element model are given, necessary for the understanding of the numerical solutions and the derivation of the error estimator. For more details on the Galerkin spectral element method, the reader is referred to, e.g., [54, 55, 56]. Since the Galerkin method is unstable for convection (dominated) problems, a SUPG stabilisation [58] in space-time is applied with a stabilisation parameter  $\tau = \Delta x^2$ .

For the given initial condition (4.59), the solutions of the fine and coarse primal models (4.1) and (4.8), respectively, are shown in figure 4.7. These solutions are computed on a uniform mesh with 128 elements of second order in space and time. The diffusion coefficient used for the solution in Figure 4.7(a) is  $\mu = .1$ . The boundary layer near the boundary  $x = 1$ ,

becomes thicker/thinner with increasing/decreasing  $\mu$ . As can be seen in figure 4.7, the solution of the approximating convection problem (4.8) clearly lacks the presence of a boundary layer. The scales of both images differ somewhat, since small overshoots exist in the convection solution. Due to the applied SUPG the overshoots are non-increasing in time (see [58]).



(a) Fine model solution,  $\mu = 0.1$ .

(b) Coarse model solution.

Figure 4.7: Solutions of the fine and coarse model,  $N_{el} = 128$ ,  $P = 2$ ,  $Q = 2$ .

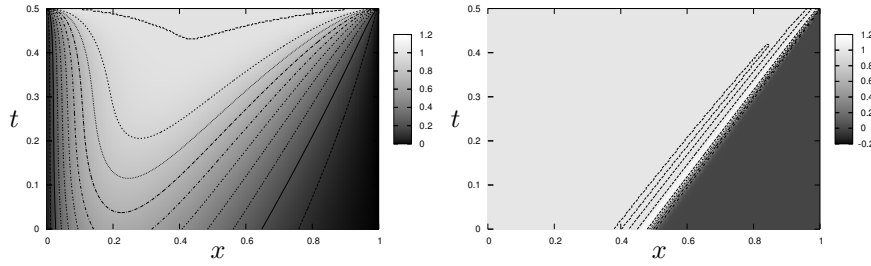
#### 4.5.1 The dual solutions

The fine and coarse dual solutions on  $(x, t) \in (0, 1) \times (0, 0.5)$ , are shown in figure 4.8 for 128 elements and  $P = Q = 2$  (second order in space and time). Note that the dual problem is solved backward in time with initial condition  $p(x, T) = 1$ ,  $x \in (0, 1)$ . In the fine dual solution in figure 4.8(a), a boundary layer is visible near the dual outflow boundary  $x = 0$ . The discontinuity introduced at  $x = 1$  is smeared out by the diffusion. The coarse dual solution in figure 4.8(b), clearly lacks diffusion (apart from artificial diffusion from the SUPG) and the discontinuity is transported unchanged into the domain. The scales from both plots in figure 4.8 differ slightly, due to the overshoots in the coarse dual solution. These overshoots are stable in time due to the SUPG stabilisation ([58]).

#### 4.5.2 The error estimator

The goal-oriented modelling-error estimator for a convection-diffusion problem is given by equation (4.16). Applied to the present unsteady 1-D prob-



(a) Fine dual solution,  $\mu = 0.1$ .

(b) Coarse dual solution.

Figure 4.8: Fine and coarse dual solutions,  $N_{el} = 128$ ,  $P = 2$ ,  $Q = 2$ .

lem and using the derived homogeneous dual boundary conditions  $p(0, t) = p(1, t) = 0$ , the estimator (4.16) becomes:

$$R(u_0; p) = - \int_0^T \int_{\Omega} \mu u_{0,x} p_x dx dt - \int_0^T \mu (a^1(t) - u_0(1, t)) p_x(1, t) dt. \quad (4.60)$$

The error estimator (4.60) is approximated in a discrete way using numerical integration and differentiation for the spectral element approach, as given by equations (B.3) and (B.5) in the appendix B. With  $e$  indicating the element on time-level  $k$ , the estimator in a discrete form is given by:

$$R(u_0^h; p^h) = -\mu \sum_{k=1}^n \sum_{e=1}^{N_{el}} (\mathbf{D}_x \vec{u}_0^h)^T|_e^k \mathbf{W}^k (\mathbf{D}_x \vec{p}^h)|_e^k - \mu \sum_{k=1}^n \sum_{q=1}^{Q+1} w_q (\vec{u}_R - \vec{u}_0^h(\xi_{P+1}, \eta_q)|_{N_{el}^k}) \vec{p}_x^h(\xi_{P+1}, \eta_q)|_{N_{el}^k} \frac{\partial y}{\partial \eta}|_{N_{el}^k}. \quad (4.61)$$

In equation (4.61),  $\vec{u}_R$  is a vector with the boundary condition  $a^1$  in the GLL-roots at  $\Omega_{N_{el}^k}(\xi_{P+1}, \eta_q)$  and  $\frac{\partial y}{\partial \eta}$  is the determinant. Furthermore,  $\vec{p}_x^h(\xi_{P+1}, \eta_q)|_{N_{el}^k}$  is the vector with the derivative of the dual solution, evaluated at the GLL-points on the right boundary  $(\xi_{P+1}, \eta)$  of element  $\Omega_{N_{el}}$  at time-level  $k$ . For computations which are first-order accurate in time, the GLL-points are on both right corners of the space-time element  $\Omega_{N_{el}}$ , or in local coordinates:  $(1, -1)$  and  $(1, 1)$ . The derivative  $\vec{p}_x^h(\xi_{P+1}, \eta_q)|_{N_{el}^k}$

is computed on element  $\Omega_{N_{el}^k}$  at the corresponding time-level  $k$  by:

$$\vec{p}_x^h(\xi_{P+1}, \eta_q)|_{N_{el}} = \frac{\partial p^h}{\partial \xi}(\xi_{P+1}, \eta_q)|_{N_{el}} \frac{\partial \xi}{\partial x}|_{N_{el}}, \quad (4.62)$$

where  $i = q(P+1)$  and  $1 < j < (Q+1)(P+1)$ .

### 4.5.3 Results

The results are presented for  $\mu = 10^{-2}$  to 1 by the numerical approximation of the real error  $Q(u^h) - Q(u_0^h)$ , the estimated errors  $R(u_0^h, p^h)$  and  $R(u_0^h, p_0^h)$ . The inner domain and boundary contributions to the estimator, as given in equation (4.61), are also given. The quantity of interest is computed using the integration by Gaussian quadrature as in equation (B.2):

$$\begin{aligned} Q(u^h) &= \sum_{e=1}^{N_{el}} \int_{-1}^1 u^h(\xi, \eta_{Q+1})|_e d\xi \frac{\partial x}{\partial \xi} \\ &\approx \sum_{e=1}^{N_{el}} \sum_{p=1}^{P+1} w_p u^h(\xi_p, \eta_{Q+1})|_e \frac{\partial x}{\partial \xi}|_{N_{el}}. \end{aligned} \quad (4.63)$$

The efficiency index is used to indicate the quality of the estimator and is computed for the discrete approximations by:

$$I_{eff} = \frac{R(u_0^h; p^h)}{Q(u^h) - Q(u_0^h)}. \quad (4.64)$$

The homogeneous boundary conditions  $p(0, t) = p(1, t) = 0$ , together with the dual initial condition  $p(x, T) = 1, \forall x \in (0, 1)$ , means that a discontinuity is introduced at the boundaries. For the convection-diffusion problem we experience numerical difficulties. Discontinuities do not exist in the solution space of problems with a diffusion operator (this is in fact a non-physical situation). It is however, important to have a good approximation of the boundary values, since the error estimator requires the derivative of the dual solution at the boundary  $x = 1$  (see equation (4.60)). Increasing the order  $P$  of the elements does not improve the resolution of the solution. To maintain the situation that we have an infinite boundary derivative  $p_x^h(1, T)$ , but to make the initial condition more smooth (or in other words: more ‘diffusion’ friendly), the values of the initial condition are modified on the elements neighbouring the boundaries, by a numerical ‘boundary fix’. Instead of the value  $p^h(\xi_p, T) = 1$  ( $p = 1 \dots P$ ), the values in the Gauss-Lobatto points are computed according to a circle with its centre in  $\vec{\xi} = (-1, \eta)$ . This is

illustrated in figure 4.9 for the right boundary element of order  $P = 4$  in space. Due to this modification of the dual initial condition at the boundary elements, the derivatives  $p_x(0, T)$  and  $p_x(1, T)$  at the boundaries are infinite. Furthermore, the oscillations of the polynomials are reduced since the jump from the boundary point to the neighbouring point of the element is eliminated.

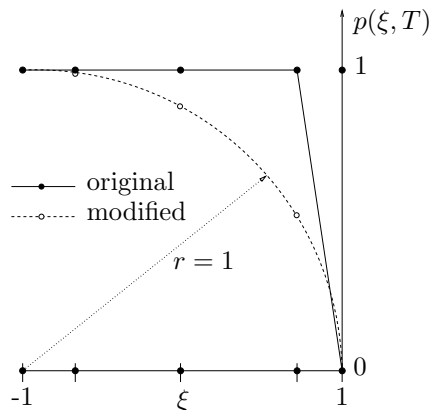


Figure 4.9: Original and modified dual initial condition at GLL-points of boundary element,  $P = 4$ .

The approximation of the real error  $Q(u^h) - Q(u_0^h)$  and the estimated errors by  $R(u_0^h; p^h)$  and  $R(u_0^h; p_0^h)$ , are shown in Figure 4.10 for  $N_{el} = 128$  elements and  $P = Q = 2$ . Also the absolute value of the individual contributions to the estimator from the inner domain and the boundaries are shown in Figure 4.10. Figure 4.10(a) shows that the boundary has a significant contribution in the estimator. The coarse dual-weighted estimator  $R(u_0^h; p_0^h)$  for  $\mu = 1$  is heavily over-estimated. This over-estimation can be expected though, since in the steady analytical case the real error is over-estimated as well for large  $\mu$ , see figure 4.2.

The efficiency index is given in figure 4.11 with  $h$ -refinement and in figure 4.12 for  $P$ -refinement, for both fine and coarse dual-weighted estimators. Since  $R(u_0; p)$  is exact for linear problems with a linear quantity of interest, the numerical approximation  $R(u_0^h; p^h)$  should be close to unity, see figure 4.11(a). Only for  $\mu = 1$  there is a slight deviation which decreases to unity for increasing order  $P$  and  $Q$ .

It is found that the coarse dual-weighted estimator  $R(u_0^h; p_0^h)$  is a good approximation of the real error for  $\mu \leq .1$ , see figures 4.11(b) and 4.12(b). For  $\mu = 1$ , the error is highly over-estimated by the coarse dual-weighted

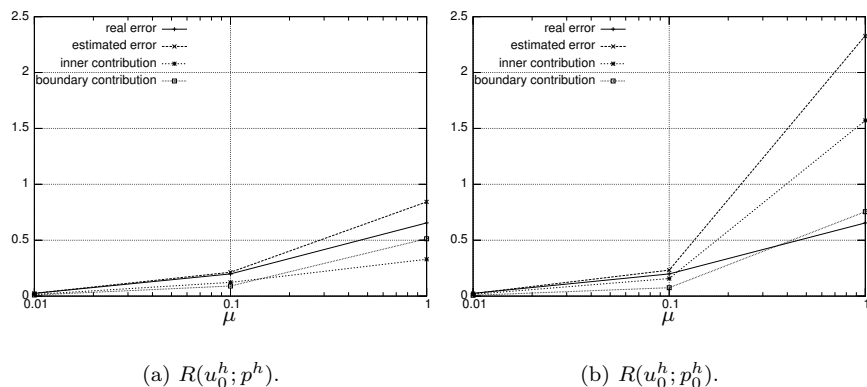


Figure 4.10: Real and estimated errors,  $N_{el} = 128$ ,  $P = Q = 2$ .

estimator  $R(u_0^h, p_0^h)$ , although the over-estimation decreases for increasing order  $P$  and  $Q$ , see figure 4.12(b). The trend of over-estimation of the coarse dual-weighted estimator for increasing  $\mu$ , is also found in the steady example in section 4.2 for a comparable quantity of interest  $Q(u) = \int_{\Omega} u dx$ , see figure 4.2.

Figure 4.11 shows furthermore, that the coarse dual-weighted estimator depends less on the element size  $h$  than the fine dual-weighted estimator. This is explained by the absence of boundary layers in the coarse dual solution. The accuracy of the solution is not influenced by a good or bad resolution of boundary layers. As mentioned before, the efficiency of the DWR method requires the use of the coarse dual solution. In this example, the coarse dual-weighted estimator is found to be a useful and reliable estimator, since:

- it gives a good approximation for  $\mu \lesssim 1$ ,
- it shows a low mesh dependence,
- it over-estimates the real error.

The latter makes the coarse dual-weighted estimator more useful as driving criterion in an adaptation algorithm than under-estimation of the real error. Under-estimation might cause the adaptation process to stop too early, due to which the required accuracy of the quantity of interest might not be achieved.

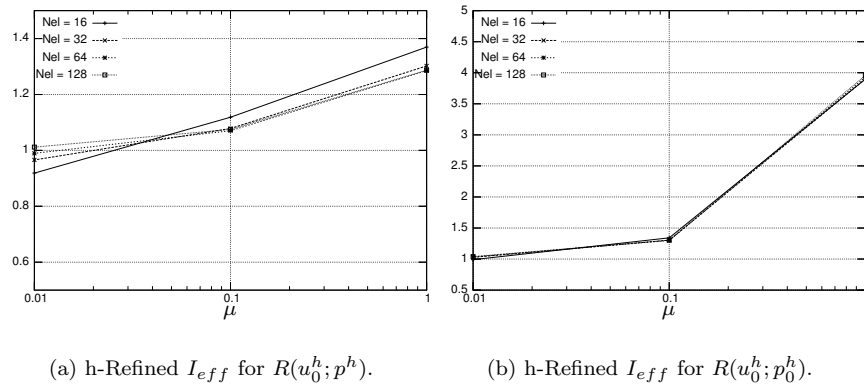


Figure 4.11: h-Refinement for efficiency index of  $R(u_0; p)$  and  $R(u_0; p_0)$ ,  $P = Q = 2$ .

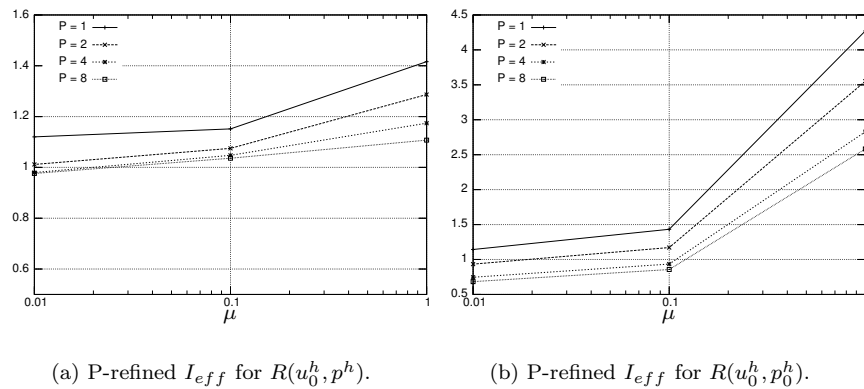


Figure 4.12: P-Refinement for efficiency index of  $R(u_0; p)$  and  $R(u_0; p_0)$ ,  $N = 128$ .

**Comments on the results** As mentioned before, the Gaussian quadrature used for numerical integration is an accurate method to compute integrals with a smooth integrand. In the dual problem however, discontinuities are introduced at the boundaries. In the fine dual problem the diffusion smears out the discontinuity, although in the first few iterations small instabilities occur. These instabilities affect an accurate computation of the

derivative of the dual solution and, consequently, also the accuracy of the error estimator.

In case of the coarse-model dual problem, also a discontinuity is introduced into the problem at the dual inflow boundary. Due to the artificial diffusion caused by the SUPG used for stabilisation of the convection problem however, also in the coarse dual problem the discontinuity is smeared out. The solution is more or less smooth again and Gaussian quadrature can be applied for numerical integration.

Applying the DWR method in unsteady problems is fairly expensive, since the dual problem needs to be solved on the whole space-time domain. In an adaptive modelling procedure, this would imply that after evaluating the quantity of interest based on the coarse model solution, the dual problem has to be solved back in time to  $t = 0$ . This drawback of the DWR method in unsteady problems is also mentioned by Perotto [33], considering adaptive modelling for free-surface flows.

## 4.6 Conclusions

An approach is presented for the use of the DWR method for goal-oriented modelling-error estimation in convection-diffusion problems, where the diffusion term is omitted in the approximating or reduced model. Omitting the diffusion term means that the mathematical type of the model equation changes. Due to the change in mathematical type of the problem the required boundary conditions change and, consequently, boundary residuals may arise between the fine and coarse model solutions.

### Importance of boundary residual inclusion

The goal-oriented modelling-error estimator is derived according to the variational approach, described in chapter 3. By imposing the boundary conditions weakly in the problem formulation, an estimator is obtained for  $Q(u) - Q(u_0)$  that includes both inner domain and boundary contributions. The boundary residual in the modelling-error estimator has a significant contribution, as shown by the steady (analytical) cases in which the boundary contribution is the only contribution.

The boundary residual in the diffusive boundary contribution is weighted by the derivative of the dual solution on the boundary. In numerical problems, this requires an accurate approximation of the derivative of the dual solution at the boundary. For the fine dual problem this is complicated in case the dual boundary conditions are zero while the dual initial condition is not: this introduces a discontinuity at the boundary. A numerical ‘fix’ of

the dual initial condition in the applied spectral element method is applied, which improves the approximation of derivatives of the dual solution.

### Applying the coarse dual solution

Inherent to the efficiency of the DWR method is the use of the coarse dual solution as weighting function in the residual estimator. Especially in linear problems where solving the fine dual problem requires equal numerical effort as the fine primal problem (in nonlinear problems the linearised fine dual problem is free of Newton-type linearisations). An advantage of the use of the coarse instead of the fine dual solution, is that in neither the primal nor the dual problem physical diffusion is present. In that case, no mesh refinement is required to capture possible boundary layers. For the given cases, the coarse dual-weighted estimator is a good approximation of the fine dual-weighted estimator and also of the real error. Numerical computations show that the coarse-dual based estimator is less mesh dependent than the fine dual-weighted estimator.

In all cases studied (steady and unsteady), the coarse dual-weighted estimator  $R(u_0; p_0)$  approaches the fine dual weighted estimator  $R(u_0; p)$  for vanishing diffusion coefficient  $\mu$ . However, since the type of the model equation changes when diffusion is omitted, not every quantity of interest leads to a well-posed coarse dual problem. This is the case in the example with a solution derivative at a boundary as quantity of interest.

### Approach for ill-posed coarse dual problem

From the studied steady cases with different quantities of interest, the solution derivative at the boundary results in an ill-posed coarse dual problem. A domain decomposition approach is presented in which the fine dual problem is applied in a small region adjacent to the boundary where the quantity of interest is defined. In the rest of the domain, the coarse dual problem is applied. For complex and computing intensive problems, the size of the fine model region should be chosen as small as possible from an efficiency point of view. The larger the region is chosen, the closer the problem is to the fine dual problem and the more accurate the error estimator is. This is proved for the given case.

### Additional comment on unsteady problems

As illustrated in the discrete unsteady case computed using a Galerkin Spectral Element Method, the application of the DWR method in unsteady problems is fairly expensive. This is because the dual problem needs to be

solved backward in time to the initial time  $t = 0$ . In an adaptive modelling procedure this requires the solution of the primal and dual problem, each time on the whole space-time domain.

In the given discrete unsteady example, a discontinuity is introduced at the boundary in the dual problem. This is caused by the difference in the initial and the boundary condition. In the derivation of the DWR method by the variational approach for convection-diffusion problems, it is mentioned that only sufficiently smooth solutions should be considered to maintain the validity of the DWR method. Although this is the case for the primal problems, this is not the case anymore for the dual problem, due to the difference in initial condition and boundary condition. Results however, show that the estimator does not suffer from this ‘violation’. The fine dual problem only suffers from the discontinuity initially, since diffusion smears out the discontinuity for  $t < T$ .



## Chapter 5

# Nonlinear Burgers

Goal-oriented modelling-error estimation for the nonlinear Burgers problem is the topic of this chapter. Here, the viscous Burgers equation is the fine model and the inviscid Burgers equation is the coarse (or reduced) model. As was shown in chapter 3, high-order contributions  $e_0$  and  $\epsilon_0$  (the primal and dual errors), arise in the modelling-error estimator from a nonlinear model operator and a nonlinear quantity of interest. These high-order terms are given for a general problem by  $\Delta R$  and  $r(e_0, \epsilon_0)$  in equations (3.19) and (3.12), respectively. We want to derive and study these high-order terms for the Burgers problem. For the linear diffusion-reaction problem with a nonlinear quantity of interest, it was shown that only a high-order contribution is found in the error estimator, that originates from the quantity of interest on the inner domain. In the nonlinear Burgers problem, on the other hand, also high-order contributions arise from the nonlinear model operator. The coefficient that multiplies the viscous term is referred to as diffusion coefficient to emphasise the similarity with the linear convection-diffusion problem, discussed in the previous chapter.

First the approach to derive the dual problems and the goal-oriented modelling-error estimator for the Burgers problem is studied in section 5.1. Attention is paid to linearisation of the dual problem and the high-order terms in the error estimator. Then a discrete example is given in section 5.2 using a finite volume approach.

### 5.1 Approach for Burgers problem

The difference between the Burgers problem and the linear convection-diffusion problem, discussed in the previous chapter, is the nonlinear con-

vection term. The fine model problem, i.e. the viscous Burgers equation, together with the dual problem are given in section 5.1.1 in weak form. The same is done for the coarse model problem in section 5.1.2. The error estimator is derived in section 5.1.3, where the high-order terms in the error estimator are studied as well.

### 5.1.1 The fine model problem

We want to evaluate the quantity of interest  $Q(u)$  from the solution of the 1-D parabolic viscous Burgers equation on  $\Omega \times (0, T)$  with  $\Omega = (0, 1)$ ,  $T \in \mathbb{R}^+$  and boundary  $\Gamma = \{x = 0, x = 1\}$ :

$$u_t + \left(\frac{1}{2}u^2\right)_x - \mu u_{xx} = 0, \quad x \in \Omega, \quad t \in (0, T), \quad (5.1)$$

with  $\mu$  is the diffusion coefficient. The initial condition is  $u(x, 0) = \phi(x)$  and time-invariant boundary conditions are given by  $u(x, t) = a(x)$ ,  $x \in \Gamma$ . For the two boundaries  $x = 0$  and  $x = 1$  we identify:

$$a(x) = \begin{cases} a^0, & x = 0, \\ a^1, & x = 1, \end{cases} \quad (5.2)$$

which are found from the initial condition:  $a^0 = \phi(0)$  and  $a^1 = \phi(1)$ . The weak form of the fine model problem where the initial and boundary conditions are imposed weakly, is obtained by multiplying equation (5.1) by a suitable testfunction  $q$  (without imposing restrictions for  $q$  on the boundaries and  $t = 0$ ). This yields: find  $u \in U$  such that

$$N(u; q) = F(q), \quad \forall q \in V, \quad (5.3)$$

with  $U$  and  $V$  suitable Banach spaces<sup>1</sup> and  $N(u; q)$  and  $F(q)$  given by:

$$\begin{aligned} N(u; q) &= \int_0^T \int_{\Omega} u_t q + \left(\frac{1}{2}u^2\right)_x q + \mu u_x q_x \, dx dt - \int_0^T \mu u_x n q|_{\Gamma} dt \quad (5.4a) \\ &+ \int_{\Omega} u(x, 0) q(x, 0) dx - \int_0^T \frac{1}{2} u^2 n q|_{\Gamma} dt - \int_0^T \mu u q_x n \, dt, \end{aligned}$$

$$F(q) = \int_{\Omega} \phi(x) q(x, 0) dx - \int_0^T \frac{1}{2} a^2 n q|_{\Gamma} dt - \int_0^T \mu a q_x n \, dt, \quad (5.4b)$$

where  $n$  is the outward unit normal on the boundary, in this 1-D case  $n = +1$  on  $x = 1$  and  $n = -1$  on  $x = 0$ . The inclusion of the convective terms at the

<sup>1</sup>We will not go into the details of the solution space here anymore, see section 4.1.2 for a short discussion on this topic.

boundaries in equation (5.4a) is superfluous in the standard weak form of the problem, but it is used in the derivation of the goal-oriented modelling-error estimator, similar to the approach for the linear convection-diffusion problem in chapter 4.

Following the theory in chapter 3, the dual problem is then given by:

$$N'(u; v, p) = Q'(u; v), \quad (5.5)$$

with  $p$  the fine dual solution. The operator  $N'(u; v, p)$  is derived using (A.1a) and performing integration by parts to transfer derivatives to  $p$ :

$$\begin{aligned} N'(u; v, p) = & \int_0^T \int_{\Omega} (-vp_t - uvp_x + \mu v_x p_x) dx dt - \int_0^T \mu v p_x|_{\Gamma} dt \\ & + \int_{\Omega} v(x, T) p(x, T) dx - \int_0^T \mu v_x p|_{\Gamma} dt, \quad (5.6) \end{aligned}$$

The initial and boundary conditions for the dual problem arise from the fact that equation (5.5) holds for all  $v$ . The convective term  $-u v p_x$  in the dual operator (5.6), shows that the fine model solution  $u$  is required as coefficient for the convective term. Since the whole idea of (goal-oriented) modelling-error estimation is based on the absence of the fine-model solution  $u$ , one can apply the coarse model solution  $u_0$  as coefficient for the convective term when using the fine dual solution for the error estimator. Solving the linear dual problem is cheaper than the nonlinear primal problem that requires Newton-type linearisations, see also Perotto [33].

### 5.1.2 The coarse model problem

The coarse or approximating model is the inviscid Burgers equation, which found by omitting the diffusion term in (5.1):

$$u_{0t} + \left(\frac{1}{2}u_0^2\right)_x = 0, \quad x \in (0, 1), \quad t \in (0, T). \quad (5.7)$$

The same initial condition as the fine model problem is used:  $u_0(x, 0) = \phi(x)$ . For the hyperbolic problem (5.7), a boundary condition is only required on the inflow boundary  $\Gamma^-$ . The inflow boundary  $\Gamma^-$  is the boundary where characteristics are incoming. In weak form, the coarse model is given by: find  $u_0 \in U$  such that

$$N_0(u_0; q) = F(q), \quad \forall q \in V, \quad (5.8)$$

with  $N_0(u_0; q)$  and  $F(q)$  given by:

$$N_0(u_0; q) = \int_0^T \int_{\Omega} u_{0t} q + \left(\frac{1}{2}u_0^2\right)_x q \, dx \, dt + \int_{\Omega} u_0(x, 0)q(x, 0) \, dx \quad (5.9a)$$

$$- \int_0^T \frac{1}{2}u_0^2 n q|_{\Gamma^-} \, dt,$$

$$F_0(q) = \int_{\Omega} \phi(x)q(x, 0) \, dx - \int_0^T \frac{1}{2}a(x)^2 n q|_{\Gamma^-} \, dt. \quad (5.9b)$$

Here,  $a(x)$  in  $F_0(q)$  is determined by (5.2), depending on which boundary is the inflow boundary. The corresponding dual problem is given by:

$$N'_0(u_0; v, p_0) = Q'(u_0; v), \quad (5.10)$$

with  $p_0$  the coarse dual solution. The coarse dual operator  $N'_0(u_0; v, p_0)$  is derived similar to the fine dual operator in (5.6) and yields:

$$N'_0(u_0; v, p_0) = \int_0^T \int_{\Omega} v(-p_{0t} - u_0 p_{0x}) \, dx \, dt - \int_{\Omega} v(x, T)p_0(x, T) \, dx$$

$$+ \int_0^T u_0 n v p_0|_{\Gamma^+} \, dt, \quad (5.11)$$

where  $\Gamma^+$  is the outflow boundary for the primal problem. Boundary and initial conditions are found from the fact that (5.10) must hold for all  $v$  and depend on the quantity of interest considered.

### 5.1.3 The error estimator

For linear convection-diffusion problems in chapter 4 (see also [59]), we showed that imposing the boundary conditions weakly is essential when the model equations are of a different type. Doing so, ensures that boundary residuals are incorporated in the goal-oriented modelling-error estimator. The same approach is applied here to the Burgers problem.

The general form of the estimator is given by (3.23) and repeated here:

$$Q(u) - Q(u_0) = R(u_0; p) + \frac{1}{2}\Delta R + r(e_0, \epsilon_0),$$

with the high-order terms  $\Delta R$  and  $r(e_0, \epsilon_0)$  defined by (3.19) and (3.12), respectively. First the weighted residual term  $R(u_0; p)$  for the Burgers equation is given, followed by an analysis of the high-order terms.

### Weighted residual contribution

With the fine model operators given in (5.4a) and (5.4b) and the coarse model operators in (5.9a) and (5.9b), the weighted residual is found to be:

$$\begin{aligned}
R(u_0; p) &= N_0(u_0; p) - N(u_0; p) - (F_0(p) - F(p)) \\
&= - \int_0^T \int_{\Omega} \mu u_{0,x} p_x dx dt + \int_0^T \mu u_{0,x} n p|_{\Gamma} dt \\
&\quad - \int_0^T \mu (a - u_0) p_x n|_{\Gamma} dt \\
&\quad + \int_0^T \frac{1}{2} (a^2 - u_0^2) n p|_{\Gamma} dt, \tag{5.12}
\end{aligned}$$

where  $a(x)$  is determined by (5.2).

To compare the weighted residual (5.12) with the estimator (4.16) for the linear convection-diffusion problem the convective boundary contribution is rewritten as:

$$\int_0^T \frac{1}{2} (a^2 - u_0^2) n p|_{\Gamma} dt = \int_0^T \frac{(a + u_0)}{2} (a - u_0) n p|_{\Gamma} dt. \tag{5.13}$$

Comparison between equation (5.13) and (4.16), shows that the boundary residual  $a - u_0$  at the outflow boundary is multiplied by the average outflow velocity from the fine and coarse model. For the linear convection-diffusion problem, we found that the boundary residual is multiplied by the (constant) convective velocity  $c$ , see equation (4.16).

### High-order terms

To discuss the high-order terms  $\Delta R$  and  $r(e_0, \epsilon_0)$  for the Burgers equations, the definitions (3.19) and (3.12) are repeated:

$$\Delta R = \int_0^1 N''(u_0 + se_0; e_0, e_0, p_0 + s\epsilon_0) ds - \int_0^1 Q''(u_0 + se_0; e_0, e_0) ds,$$

and

$$\begin{aligned}
r(e_0, \epsilon_0) &= \frac{1}{2} \int_0^1 \{ Q'''(u_0 + se_0; e_0, e_0, e_0) - 3N'''(u_0 + se_0; e_0, e_0, \epsilon_0) \\
&\quad - N'''(u_0 + se_0; e_0, e_0, e_0, p_0 + s\epsilon_0) \} (s - 1) s ds.
\end{aligned}$$

Since both terms depend on the quantity of interest (contrary to  $R(u_0; p)$ ), we consider a specific case of  $Q(u)$ . For  $Q(u)$  linear in  $u$ , both integrals in

$\Delta R$  and  $r(e_0, \epsilon_0)$  that involve  $Q''$  and  $Q'''$ , respectively, are zero. Therefore the high-order terms are analysed for the nonlinear energy measure on the final time  $T$ , as used in the discrete cases studied in section 5.2:

$$Q(u) = \int_{\Omega} \frac{1}{2} u(x, T)^2 dx.$$

For the Burgers problem with the dual operator  $N'$  given in (5.4a), the high-order terms are derived using the derivatives from appendix A and yield:

$$\begin{aligned} \Delta R = & - \int_0^T \int_{\Omega} \frac{\partial(e_0^2)}{\partial x} (p_0 + \frac{1}{2}\epsilon_0) dx dt + \int_0^T e_0^2 (p_0 + \frac{1}{2}\epsilon_0) n|_{\Gamma} dt \\ & - \int_{\Omega} e_0^2(x, T) dx, \end{aligned} \quad (5.14)$$

and

$$r(e_0, \epsilon_0) = \frac{1}{4} \left\{ - \int_0^T \int_{\Omega} \frac{\partial(e_0^2)}{\partial x} \epsilon_0 dx dt + \int_0^T e_0^2 \epsilon_0 n|_{\Gamma} dt \right\}. \quad (5.15)$$

Based on these forms some important conclusions can be drawn concerning the high-order terms in the error estimator (3.23) applied to the nonlinear Burgers problem. First the boundary contributions are discussed; these terms are important in the application of the DWR-method to (linear and nonlinear) convection-diffusion problems.

**Boundary contributions** As mentioned in section 4.1.1 for the linear convection-diffusion problem, a primal inflow/outflow boundary is an outflow/inflow boundary for the dual problem. This is also the case for the Burgers problem. Since on an inflow boundary (primal as well as dual) the boundary conditions for the fine and coarse model are equal, the residual is zero. This means that on each boundary either  $e_0$  or  $\epsilon_0$  is zero and therefore  $\Delta R$  and  $r(e_0, \epsilon_0)$  reduce to:

$$\begin{aligned} \Delta R = & - \int_0^T \int_{\Omega} \frac{\partial(e_0^2)}{\partial x} (p_0 + \frac{1}{2}\epsilon_0) dx dt + \int_0^T e_0^2 p_0 n|_{\Gamma} dt \\ & - \int_{\Omega} e_0^2(x, T) dx, \end{aligned} \quad (5.16)$$

and

$$r(e_0, \epsilon_0) = -\frac{1}{4} \int_0^T \int_{\Omega} \frac{\partial(e_0^2)}{\partial x} \epsilon_0 dx dt. \quad (5.17)$$

The boundary integral in  $\Delta R$  in (5.16) is however, a computable term and should be included in the error-estimator. This term cannot be neglected, which is shown by comparing it with the convective boundary integral in (5.12). In case  $e_0 \geq 0$ , the high-order boundary integral from  $\Delta R$  involving  $e_0^2$  is at least of the same magnitude as the convective contribution  $\int_0^T \frac{1}{2}(a^2 - u_0^2) n p|_{\Gamma^+} dt$ . This is proven below.

Assume  $e_0 = a - u_0 \geq 0$  and consider the term  $\frac{1}{2}(a^2 - u_0^2)$  as it appears in the convective boundary integral. Then the following inequality holds:

$$e_0 \geq 0 \Rightarrow \frac{1}{2}(a^2 - u_0^2) \equiv \frac{1}{2}(a - u_0)(a + u_0) \leq (a - u_0)^2 \equiv e_0^2, \quad (5.18)$$

and therefore:

$$\int_0^T \frac{1}{2}(a^2 - u_0^2) n p_0|_{\Gamma^+} dt \leq \int_0^T e_0^2 p_0 n|_{\Gamma^+} dt. \quad (5.19)$$

And since  $p = p_0$  on a dual inflow boundary  $\Gamma^+$ , we furthermore have:

$$\int_0^T \frac{1}{2}(a^2 - u_0^2) n p|_{\Gamma^+} dt \leq \int_0^T e_0^2 p_0 n|_{\Gamma^+} dt. \quad (5.20)$$

Equation (5.20) shows that in case of  $e_0 \geq 0$ , the high-order term is of at least the same magnitude as the convective contribution.

**Inner domain contribution** When the solutions  $u$  and  $u_0$  are sufficiently smooth in singular perturbation problems like the present Burgers problem, the errors  $e_0$  and  $\epsilon_0$  are assumed to be small on the domain  $\Omega$ . Then the integrals on  $\Omega$  in  $\Delta R$  and  $r(e_0, \epsilon_0)$  are small and it is allowed to neglect them. When shocks occur in the solution however, this is not the case.

Due to smearing of the shock in the viscous solution, there is a point in the shock where  $u = u_0$  and thus  $e_0 = 0$ . In close vicinity of the shock, however, the error can be of the same order as  $u_0$ :  $|e_0| \sim O(u_0)$  and thus  $e_0^2 \sim O(u_0^2)$ . For an internal viscous layer, e.g. a shock in a viscous solution, we can formulate the following limit:

$$\lim_{\mu \rightarrow 0} u(x, t) = u_0(x, t) \Rightarrow \lim_{\mu \rightarrow 0} e_0(x, t) = 0, \quad (5.21)$$

and no singularity remains. For the high-order term remaining from the quantity of interest, we then have:

$$\lim_{\mu \rightarrow 0} \int_{\Omega} e_0^2(x, T) dx = 0. \quad (5.22)$$

The derivative  $\partial e_0^2/\partial x$ , as appears in both  $\Delta R$  and  $r(e_0, \epsilon_0)$ , is large in close vicinity of the shock and discontinuous across the shock. However, since we have the limit of  $e_0 = 0$  for vanishing  $\mu$ , as given in (5.21), also the derivative will vanish. This means that the domain integrals in  $\Delta R$  and  $r(e_0, \epsilon_0)$  as given in (5.16) and (5.17), respectively, will vanish as well. In section 5.2 a case with a shock is studied.

Following the above given analysis of the high-order terms and including only computable terms, the error-estimator is written as:

$$Q(u) - Q(u_0) \approx R(u_0; p) + \int_0^T e_0^2 p_0 n|_{\Gamma^+} dt, \quad (5.23)$$

with  $R(u_0; p)$  given by (5.12). Computable in this context, means that the fine model solution  $u(x, t)$  is not available, only its approximation  $u_0(x, t)$  and the dual solution  $p$  or  $p_0$ .

### Applying the coarse dual solution

The error-estimator involving only the coarse dual solution, is found by substituting  $p = p_0 + \epsilon_0$  in the estimator and neglecting the dual error  $\epsilon_0$ . As described in section 2.3 about the error estimator in linear differential form however, the dual error  $\epsilon_0$  can not be neglected *a-priori*. Consider the error estimator (5.12) and remind that on a primal/dual inflow boundary the primal/dual error (i.e. the residual) is zero, since the fine and coarse problems have the same boundary conditions. The convective contributions in (5.12) therefore, remain the same when using  $p_0$  instead of  $p$ . Such an analysis can not be held for the diffusive boundary term:

$$\begin{aligned} & \int_0^T \mu(a - u_0(x, t)) (p_0 + \epsilon_0)_x(x, t)|_{\Gamma} dt = \\ & \int_0^T \mu(a - u_0(x, t)) p_{0x}(x, t)|_{\Gamma} dt + \int_0^T \mu(a - u_0(x, t)) \epsilon_{0x}(x, t)|_{\Gamma} dt. \end{aligned} \quad (5.24)$$

Only when both  $p_0$  and  $p$  are known, conclusions can be drawn about the effect on the reliability of the estimator when neglecting the dual error contribution. Ideally, one has on boundary  $\Gamma$ :

$$\epsilon_{0x}(\Gamma, t) \ll p_{0x}(\Gamma, t), \quad (5.25)$$

but no *a-priori* conclusion can be drawn whether or not this is the case. It needs to be evaluated for each individual problem.



## 5.2 Discrete problem

In this section, the Burgers problem is studied for two cases on  $(x, t) \in \Omega \times (0, T)$  with  $\Omega = (0, 1)$  and  $T = .5$ . The cases are defined by two different initial conditions, based on which the required boundary conditions for the primal problem are found:

$$\text{case 1: } \phi(x) = 1 - \cos \pi x, \Rightarrow a^0 = 0, a^1 = 2, \quad (5.26a)$$

$$\text{case 2: } \phi(x) = \cos \pi x, \Rightarrow a^0 = -1, a^1 = 1. \quad (5.26b)$$

Case 1 results in a boundary layer near  $x = 1$  and case 2 yields a stationary shock at  $x = .5$ . As mentioned before, the outflow boundary for the primal problem becomes an inflow boundary for the dual problem, due to the reversal of characteristic direction for the dual problem (see also the linear convection-diffusion problem in chapter 4). For the nonlinear Burgers problem, the characteristic direction is  $dx/dt = u$  for the fine model and  $dx/dt = u_0$  for the coarse model.

The quantity of interest considered in this chapter, is the energy measure at time  $T$ :

$$Q(u) = \int_{\Omega} \frac{1}{2} u(x, T)^2 dx \Rightarrow Q'(u; v) = \int_{\Omega} u(x, T) v(x, T) dx, \quad (5.27)$$

for which an analysis of high-order terms in the estimator is made in section 5.1.3. For the quantity of interest based on the coarse model solution  $u_0$ , substitute  $u_0$  for  $u$  in (5.27).

### 5.2.1 The dual initial and boundary conditions

With the linearised quantity of interest (5.27) and the initial conditions for both cases given in (5.26), the dual initial and boundary conditions can be derived from (5.3) and (5.8). The initial and boundary conditions for the dual problem of case 1 are given by:

$$p(0, t) = p(1, t) = 0, \quad (5.28a)$$

$$p_0(1, t) = 0, \quad (5.28b)$$

$$p(x, T)/p_0(x, T) = u(x, T)/u_0(x, T), \quad (5.28c)$$

and result in a discontinuity at the dual inflow boundary  $x = 1$  at  $t = T$ .

The initial and boundary conditions for the dual problem of case 2 are given by:

$$p(0, t) = p(1, t) = 0, \quad (5.29a)$$

$$p(x, T)/p_0(x, T) = u(x, T)/u_0(x, T), \quad (5.29b)$$

Note that the coarse dual problem has no boundary conditions, since the dual characteristics are outgoing (opposite to the incoming primal characteristics). Case 2 has no boundary residuals (due to incoming primal characteristics on both boundaries), but the shock in the coarse primal solution  $u_0$  violates the solution restriction that only sufficiently smooth solutions should be considered. See also section 4.1.2, paragraph ‘Remarks on solution spaces’.

The dual problem requires the fine model solution as coefficient for the convective term and the fine model solution  $u(0, T)$  as dual initial condition. As mentioned before, goal-oriented modelling-error estimation is based on the fact that in practice the fine model solution is not at hand. Therefore the fine dual solution is also computed using the coarse model solution  $u_0$  as coefficient for the convective term and the initial condition. The resulting dual solution is indicated by  $p^{u_0}$ .

The fact that the primal solution is required as coefficient for the convective term in the dual problem, requires memory storage of the primal solution at all time levels. For the present 1-D problem the required memory storage is not yet a problem, but for more complex and larger problems the memory storage becomes an important issue, see also Perotto [33]. A possible remedy is the so called check-pointing technique suggested in Griewank [60]. In the present problem no special attention is paid to the problem of memory storage.

### 5.2.2 Discrete approach

To solve the problem numerically, the primal and the dual Burgers equations are discretised by means of a cell-centred finite volume method on a non-uniform mesh. The latter allows to refine the mesh in a boundary layer when necessary for a proper resolution of the boundary layer. The convective term is discretised explicitly in time and the Engquist-Osher scheme [61] is used to evaluate the flux through a cell-face. This Engquist-Osher scheme is linearised for the dual problem as is shown in appendix C.

High-order accuracy in space is achieved by employing the so-called  $\kappa$ -scheme, introduced in [62] where we apply  $\kappa = 1/3$ . To prevent spurious oscillations in the solution due to the high-order discretisation, a flux limiter tailored for  $\kappa = 1/3$ , the so-called Koren limiter [63], is applied. The diffusion term is spatially discretised by a second-order scheme and in time it is discretised implicitly for stability reasons, see appendix C for details.

The details of the applied finite volume approach and the linearisation of the flux scheme are discussed in appendix C. For more details on the finite volume method the reader is referred to, e.g., [64, 65, 66, 67].

Special attention is paid to the discrete form of the goal-oriented modelling error estimator, as derived for the Burgers problem in section 5.1.3.

### The discrete goal-oriented modelling-error estimator

For the integration in time as well as in space, the trapezoidal rule is applied, which is third-order accurate. With  $N$  the number of time steps and  $J$  the number of cells, the discrete form of the weighted residual estimator (5.12) with inclusion of the high-order boundary term as in (5.23), is given by:

$$\begin{aligned}
Q(u) - Q(u_0) &\approx R(u_0; p) + \int_0^T e_0^2(x, t) p_0(x, t) |_{\Gamma^+} dt \\
&\approx -\mu \sum_{\bar{k}=0}^N \Delta t \left\{ \sum_{i=1}^J (u_{0,x}^h p_x^h h)_i \right\}^{\bar{k}} \\
&\quad - \mu \sum_{\bar{k}=0}^N \Delta t \left\{ (a - u_0^h) p_x^h n \right\}^{\bar{k}} |_{\Gamma^+} \\
&\quad + \sum_{\bar{k}=0}^N \Delta t \left\{ 1/2 (a^2 - u_0^{h^2}) p_x^h n \right\}^{\bar{k}} |_{\Gamma^+} \\
&\quad + \sum_{\bar{k}=0}^N \Delta t \left\{ (a - u_0^h)^2 p_0^h n \right\}^{\bar{k}} |_{\Gamma^+}. \tag{5.30}
\end{aligned}$$

Here  $\bar{k}$  denotes the time average over one time step of the discrete vector between curly brackets:

$$\{ \cdot \}^{\bar{k}} = \frac{\Delta t}{2} ((\cdot)^k + (\cdot)^{k+1}),$$

with  $k$  the time level and  $k = 0$  the initial time level  $t = 0$ . As mentioned before,  $n$  is the outward unit normal on the boundary, in this 1-D case  $n = +1$  on  $x = 1$  and  $n = -1$  on  $x = 0$ . Derivatives on the inner domain are computed by the following expression:

$$\sum_{i=1}^J (u_{0,x}^h p_x^h h)_i = \sum_{i=1}^J \frac{((u_0)_{i+1} - (u_0)_{i-1})}{h_- + h_+} \frac{(p_{i+1} - p_{i-1})}{h_- + h_+} h_i, \tag{5.31}$$

with  $h_-$  and  $h_+$  as in (C.7). This expression is of second-order accuracy in case of a uniform mesh ( $h$  is constant). Derivatives of the dual solution on the boundary, as they appear in the diffusive contribution in the

error estimator, are computed by a first-order difference. The reason for using first-order instead high-order differences on the boundary, is because of (possible) discontinuities introduced initially on the boundaries. In case of a discontinuity the derivative is approximated more accurately by a first-order difference.

## 5.3 Results

In this section, the results for case 1 and case 2 are given with an analysis of the individual contributions in the error estimator. The quality of the estimator is indicated by the efficiency index. For case 1 an analysis is given of the high-order inner-domain contributions. For case 2 some numerical aspects of the dual solution in case of a shock are discussed.

### 5.3.1 Case 1

The mesh used for the computations, is based on a uniform mesh of 64 cells with a refinement in the boundary layer that depends on the value of  $\mu$ , i.e. the boundary layer thickness. A transition layer is used for a smooth transition between the boundary layer and the uniform mesh. The total number of cells differs for each value of  $\mu$ . Both viscous and inviscid Burgers solutions are computed on the same mesh with refinement in the boundary layer. This is done to prevent the discretisation error from interfering with the results. The time step is equal (and constant) for both viscous and inviscid solutions.

The primal solutions of the viscous and inviscid Burgers equation for case 1 are shown in figure 5.1. This figure shows the difference between the models (5.1) and (5.7), by the boundary layer in the vicinity of the boundary  $x = 1$ . This is emphasised by figure 5.2, which shows the solutions at the final time  $u(x, T)$  and  $u_0(x, T)$ .

The fine and coarse dual solutions are shown in figure 5.3, where the scales for both solutions are equal for an easy comparison. As mentioned in section 5.1.2, the fine dual problem requires the fine model solution  $u$  as coefficient for the convective term. For case 1, the dual initial condition also depends on the fine model solution, see (5.28). Since the fine model solution is not available in practice however, the fine dual solution is also computed based on the coarse model solution  $u_0$ . The resulting dual solution, indicated by  $p^{u_0}$ , is shown in figure 5.4.

Note that the difference between the initial conditions  $p(x, T) = u(x, T)$  and  $p^{u_0}(x, T) = u_0(x, T)$ , is large close to the outflow boundary, see also figure 5.2 which shows  $u(x, T)$  and  $u_0(x, T)$ . The dual boundary condition

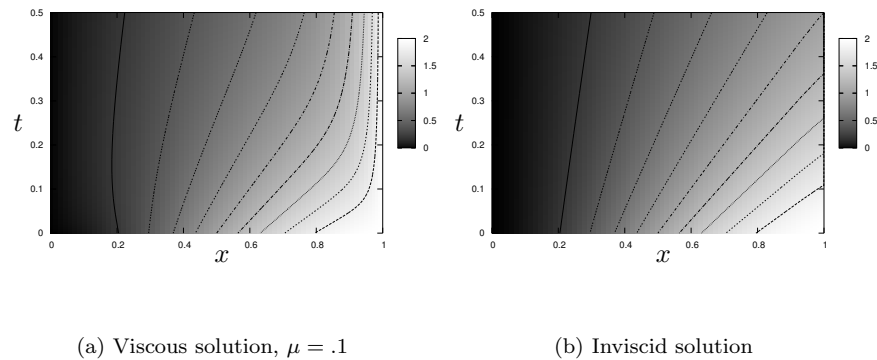


Figure 5.1: Primal solution of the inviscid and viscous Burgers equation.

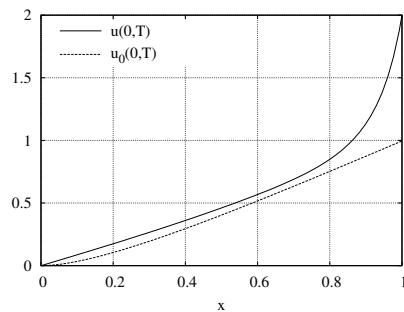
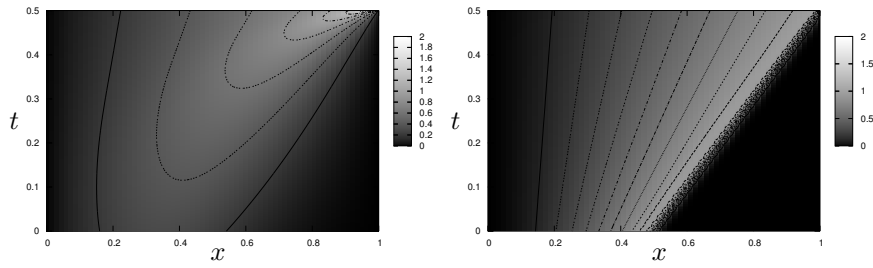


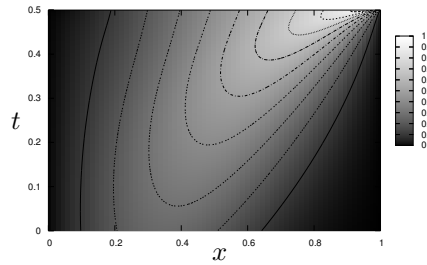
Figure 5.2: Final solutions  $u(x, T)$  and  $u_0(x, T)$ .

on  $x = 1$  however, is zero for both the fine and coarse dual problem, as given in (5.28). This is also shown in figure 5.3. The derivative of the dual solution appears in the error estimator. Therefore, care must be taken by using the coarse dual solution in the estimator, as mentioned in section 2.3 and at the end of section 5.1.3. In these sections it is stated that the boundary conditions for both the fine and coarse dual problem should be evaluated, in order to comment on the effect of neglecting the dual error. At  $t = T$ , both the fine and coarse dual solution have a discontinuity on  $x = 1$ , which means that the derivative is infinite. The derivative of the coarse dual solution is zero for  $t < T$ , since the discontinuity is transported

(a) Fine dual solution,  $\mu = .1$ .

(b) Coarse dual solution

Figure 5.3: Dual solutions of the fine and coarse model.

Figure 5.4: Fine dual solution  $p^{u_0}$  (based on  $u_0$ ) for  $\mu = .1$ 

into the domain, see figure 5.3(b). The initial discontinuity in the fine dual solution is also transported into the domain, but it is smeared by the diffusion. For decreasing  $t$  however, also the derivative of the fine dual solution decreases and becomes zero eventually, see figure 5.3(a). Therefore the effect of using the coarse instead of the fine dual solution has no dramatic effect on the estimator, although inequality (5.25) is not satisfied initially. In the following section the fine and coarse dual-weighted error estimators are studied in detail.

### The error estimator

In figure 5.5 the real error and the estimated modelling-error, computed by (5.30), are shown together with the efficiency index, defined by (2.47). The mesh that is used, is based on a uniform mesh with 64 cells. It is refined near  $x = 1$ , when it is required for a proper resolution of the boundary layer. Since the fine and coarse dual inflow boundary conditions  $p(1, t)$  and  $p_0(1, t)$  are zero, the contribution from the high-order term in the estimator (5.23) is zero as well. The estimated modelling error in figure 5.5 is therefore referred to as the weighted residual  $R(u_0, \cdot)$ . Figure 5.6 shows for

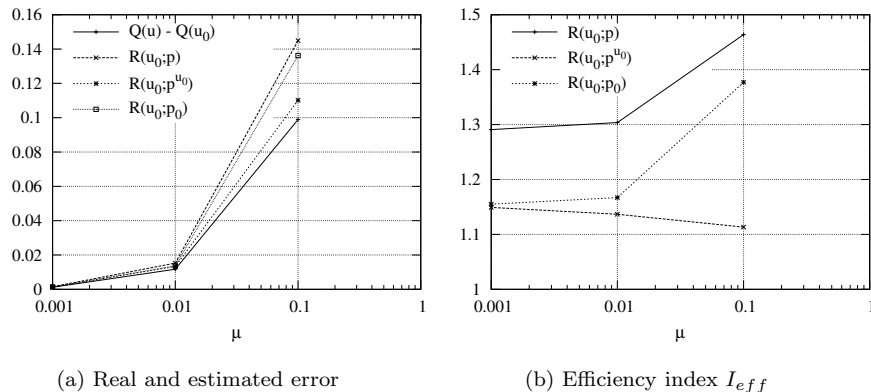


Figure 5.5: The error estimators and efficiency index as function of  $\mu$ , case 1.

the fine-dual weighted residual estimator, that the boundary contribution in the modelling-error estimator is larger than the domain contribution. This emphasises, again, the importance of a separate treatment of boundaries in singularly perturbed problems.

### The Influence of high-order terms from the inner domain

A striking observation from figure 5.5, is that the fine dual-weighted error-estimator  $R(u_0; p)$  that should be most accurate of all, is the most inaccurate and the coarse dual-weighted residual estimator  $R(u_0; p_0)$  is the most accurate one. This is explained by the fact that the dual error is neglected, but also by the effect of cancellation of the domain integrals in the high-order terms  $\Delta R$  and  $r(e_0, \epsilon_0)$ . Therefore we evaluate, based on the numerical solutions, the following two integrals from  $\Delta R$  (given by (5.14)) for  $\mu = .1$

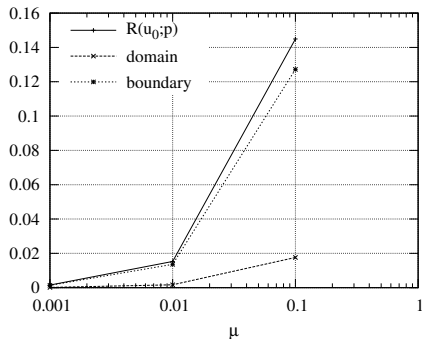


Figure 5.6: Domain and boundary contributions of the error, case 1.

where the integrals are largest (remind that the domain integrals vanish for  $\mu \rightarrow 0$ ):

$$I_1 = \int_0^T \int_{\Omega} \frac{\partial(e_0^2)}{\partial x} p_0 dx dt \approx 2.991e - 2, \quad (5.32)$$

$$I_2 = \int_{\Omega} e_0^2(x, T) dx \approx 3.876e - 2. \quad (5.33)$$

In these integrals the dual error  $\epsilon_0$  is neglected. The estimator then becomes:

$$Q(u) - Q(u_0) \approx R(u_0; p) - \frac{1}{2}(I_1 + I_2). \quad (5.34)$$

In table 5.1, the efficiency index is given for the original estimator as shown in figure 5.5, and for the estimator with the high-order terms included as in equation (5.34). The table shows that the estimator based on  $p$  as well as

$Q(u) - Q(u_0)$	$I_{eff}$
$R(u_0; p)$	1.46
$R(u_0; p) - \frac{1}{2}(I_1 + I_2)$	1.12
$R(u_0; p^{u_0})$	1.11
$R(u_0; p^{u_0}) - \frac{1}{2}(I_1 + I_2)$	1.03
$R(u_0; p_0)$	1.38
$R(u_0; p_0) - \frac{1}{2}(I_1 + I_2)$	.77

Table 5.1: Effect of high-order domain contributions on the estimator.

$p^{u_0}$  improves ( $I_{eff}$  closer to unity), but the estimator based on  $p_0$  does not



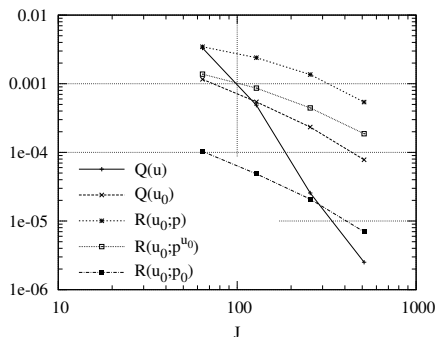


Figure 5.7: Discretisation errors for case in 1 in  $Q$  and  $R(u_0, \cdot)$ ,  $\mu = .01$

improve; in fact the over-estimation changes to under-estimation. Therefore, one can conclude that the better performance of  $R(u_0; p_0)$  in figure 5.5, is a coincidence due to cancellation of the boundary integrals as they appear in  $\Delta R$  and  $r(e_0, \epsilon_0)$ .

### The discretisation error

Besides the influence of the high-order terms and the neglected dual error  $\epsilon_0$ , also discretisation errors have an effect on the accuracy of the goal-oriented modelling-error estimator. The discretisation error in the quantity of interest and the modelling-error estimators however, decreases for increasing number of cells as shown by figure 5.7. The errors in this figure are computed on a uniform mesh with respect to the reference solutions on a mesh with 1024 cells. All quantities shown are at least first-order accurate. Among the error-estimators, the coarse dual-based estimator  $R(u_0; p_0)$  shows the lowest discretisation error. This is caused by the lack of boundary layers in both primal and dual solutions.

The discretisation error in the primal solutions at  $t = T$  and the dual solutions at  $t = 0$ , given in the  $L_0$  and  $L_2$  norm, are shown in figure 5.8. The errors are computed with respect to a reference solution on a mesh with 1024 cells. Although the third-order accurate  $\kappa = 1/3$  scheme is applied, the order of accuracy of the primal solutions becomes lower than three for decreasing number of cells. This is caused by the flux limiter.

The order of accuracy of the dual solutions is even lower than the primal solutions. This is explained by the effect of the flux limiter that comes into play, due to the discontinuity introduced initially at the boundary  $x = 1$ .

Furthermore, the use of the primal solution as coefficient in the dual equation influences the discretisation error in the dual solution. The error estimators as shown in figure 5.7, are nevertheless at least first-order accurate.

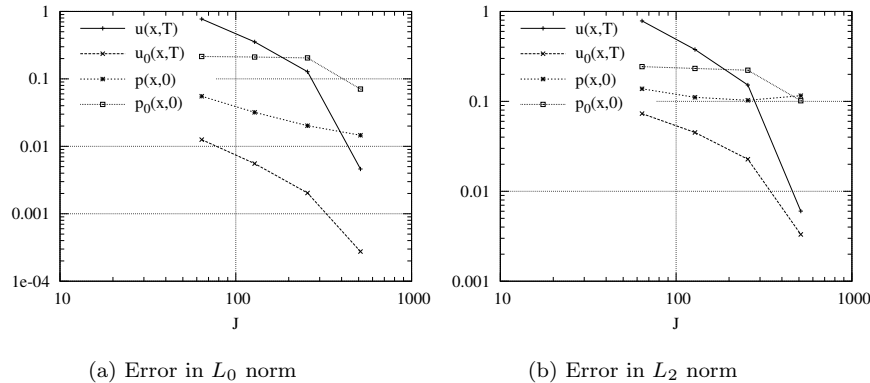


Figure 5.8: Discretisation errors for case 1 in  $L_0$  and  $L_2$  norm,  $\mu = .01$ .

### Comment on the application in adaptive modelling

When the modelling-error estimator is applied in an adaptive modelling strategy, the localised modelling error (see section 2.5.2) is used to determine where the model should be adapted from the coarse to the fine model. When in the present case the model is adapted to the fine model near the boundary  $x = 1$ , a boundary layer will occur in the solution. This solution is then determined by a mix of the coarse and fine model. To capture the new boundary layer properly, a refinement of the mesh in the boundary layer is required. This illustrates the reason why adaptive modelling is often combined with mesh refinement, see for instance [12, 13, 14]).

An important aspect of the application of the DWR method in adaptive modelling is the efficiency of the method. As mentioned before, it is essential for the efficiency to apply the coarse dual solution in the estimator, since solving the fine dual problem requires the same computational effort as solving the fine primal problem. The total computational time required to solve both the coarse primal and coarse dual problems and to compute the error estimator, should be lower than solving the fine primal problem. In table 5.2 the computational time is given in seconds for the primal and dual

problems, indicated by their solutions, for  $\mu = .01$  and a mesh based on  $J = 128$  cells (with mesh refinement in the boundary layer). The table confirms that the computational time required for the fine dual solution  $p$  is the same as for the fine primal solution  $u$ . Also the computational time required to compute the modelling-error estimator  $R(u_0; p_0)$  is given in the table. Table 5.2 shows that the total computational time of 234.9 seconds, required

$u$	$u_0$	$p$	$p_0$	$R(u_0; p_0)$	$u_0 + p_0 + R(u_0; p_0)$
177.6	99.9	176.6	98.9	36.1	234.9

Table 5.2: Computational time in seconds for  $\mu = .01$ .

to compute the coarse primal and dual solutions  $u_0$  and  $p_0$  and the error estimator  $R(u_0; p_0)$ , is more than the 177.6 seconds necessary to solve the fine primal problem. Therefore it can be concluded that employing adaptive modelling to save computational time for the present Burgers problem is a waste of time.

### 5.3.2 Case 2

Case 2 implies the formation of a stationary shock, as shown in the primal solutions in figure 5.9. In the viscous Burgers solution in figure 5.9(a), the smearing of the shock due to diffusion is clearly visible. The fine and coarse solutions at the final time  $T$  are given in figure 5.10. Due to the incoming primal characteristics the dual characteristics are outgoing. This means no dual boundary conditions are required. The fine and coarse dual solutions are shown in figure 5.11.

#### The error estimator

Since we have incoming characteristics on both boundaries  $x = 0$  and  $x = 1$ , there are no boundary residuals such that the modelling-error estimator, shown in figure 5.13(a), only has a contribution from the inner domain. The fine dual solutions  $p$  and  $p^{u_0}$ , have viscous layers emanating from the shock (see figures 5.11(a) and 5.12, respectively) that move towards the boundaries where new boundary layers arise. Therefore the whole mesh is refined uniformly for decreasing  $\mu$ . As can be expected *a-priori*, the modelling error vanishes for  $\mu \rightarrow 0$ . The efficiency index for  $R(u_0; p^{u_0})$  and  $R(u_0; p_0)$  shows a dip for  $\mu = .01$ , for which no explanation is found. It is probably due to discretisation errors.

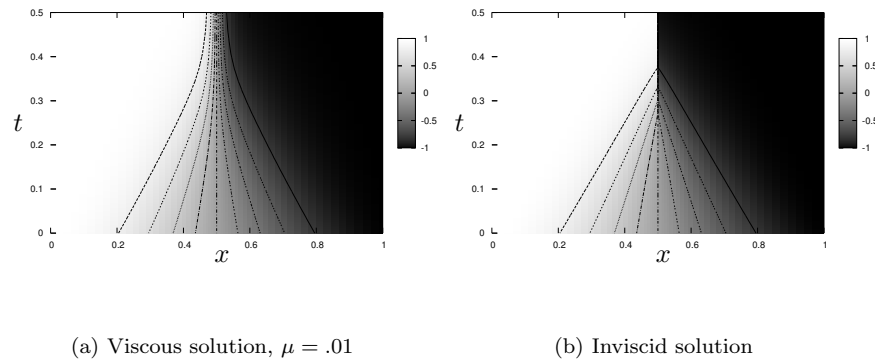


Figure 5.9: Primal solutions of the viscous and inviscid Burgers equation, case 2.

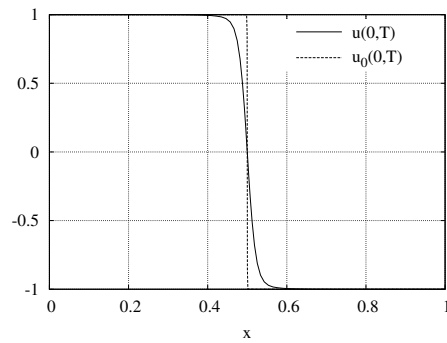
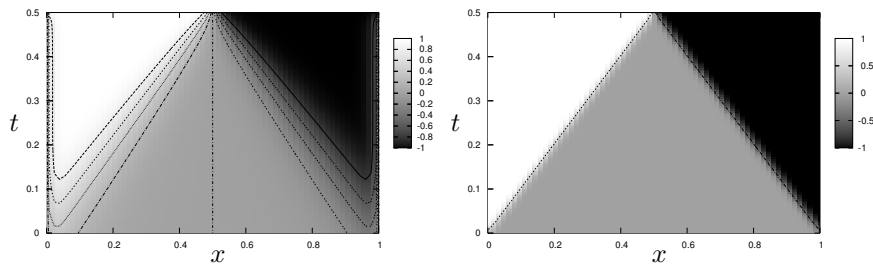


Figure 5.10: Final solutions  $u(x, T)$  and  $u_0(x, T)$ .

### The discretisation error

The discretisation errors in the  $L_0$  and  $L_2$  norms for the primal and dual solutions, are shown in figure 5.14. For the solutions on the meshes with less than 256 cells, the order of accuracy of the fine model solutions decreases, due to the effect of the flux limiter. This effect is even higher for the coarse model solution. The discretisation error in the quantity of interest and the modelling-error estimators shown in figure 5.15, is of at least first order accuracy.

(a) Fine dual solution,  $\mu = .01$ 

(b) Coarse dual solution

Figure 5.11: Dual solutions of the viscous and inviscid Burgers equation, case 2.

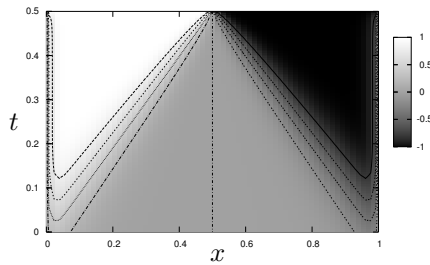


Figure 5.12: Fine dual solution  $p^{u_0}$  (based on  $u_0$ ) for  $\mu = .01$

### Remarks on shocks in the solution

When a shock occurs in the primal solution that has not left the domain before the final time  $T$ , and the quantity of interest is the energy measure (5.27), the dual initial condition  $p(x, T) = u(x, T)$  contains a shock as well. Giles shows in [68, 69] that for the Burgers problem, besides the dual initial condition  $p(x, T)$ , an additional shock boundary condition has to be

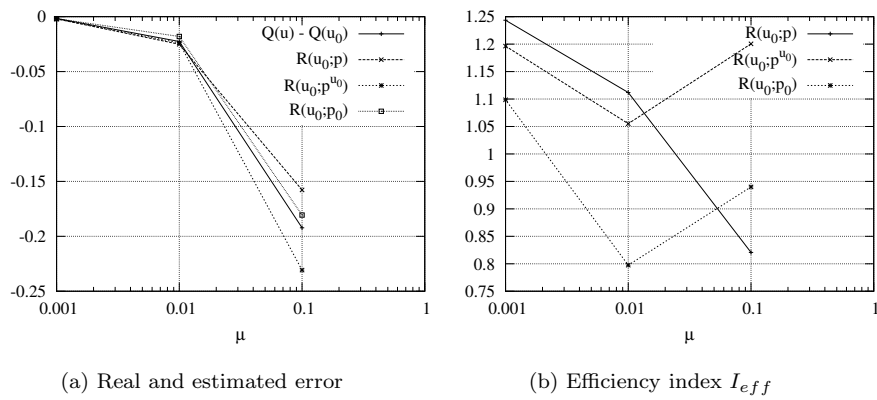


Figure 5.13: The error estimators and efficiency index as function of  $\mu$ , case 2.

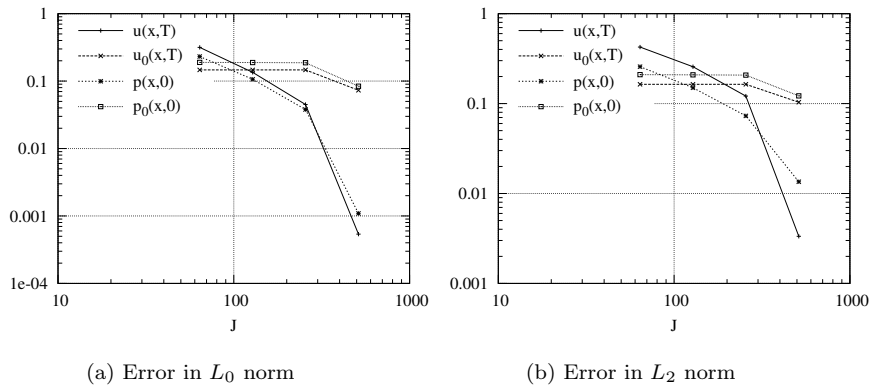


Figure 5.14: Discretisation errors for case 2 in  $L_0$  and  $L_2$  norm,  $\mu = .01$ .

applied, given by:

$$p_s(T) = \frac{[G]}{[u]}. \tag{5.35}$$

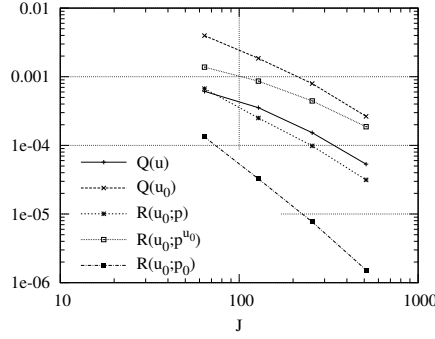


Figure 5.15: Discretisation errors for case in 2 in  $Q$  and  $R(u_0, \cdot)$ ,  $\mu = .01$

Here,  $[\cdot]$  denotes the jump in the quantity across the shock and  $G(u)$  is the function integrated in the quantity of interest:

$$Q(u) = \int_{\Omega} G(u) dx. \quad (5.36)$$

For the energy measure (5.27),  $G(u)$  is equal to  $u^2/2$ . Defining  $u_-$  and  $u_+$  as the values of  $u(x, T)$  on either side of the shock,  $[G]$  is given by:

$$[G] = \int_{u_-}^{u_+} \frac{dG}{du} du. \quad (5.37)$$

For the energy measure, this results in the following shock boundary condition:

$$p_s(T) = \frac{u_+^2/2 - u_-^2/2}{u_+ - u_-} = 0. \quad (5.38)$$

This means the dual solution  $p(x, t)$  is zero along all characteristics emanating from the shock at  $t = T$ .

In Giles [68, 70] it is shown that correct values of the dual solution can be obtained without inclusion of the shock boundary condition, depending on the applied discretisation scheme. Giles shows that the numerical flux scheme and, in particular for a Riemann flux scheme, the shock location on the mesh, has a large impact on the dual solution. In case of a Riemann flux scheme, the shock is contained in one cell and an incorrect dual solution is computed. It is shown that a diffusive scheme which smears a shock over several cells, is beneficial for a correct dual solution.

For the applied Engquist-Osher scheme (C.3), one can show that the shock is always contained in at least two cells. This is an advantage when

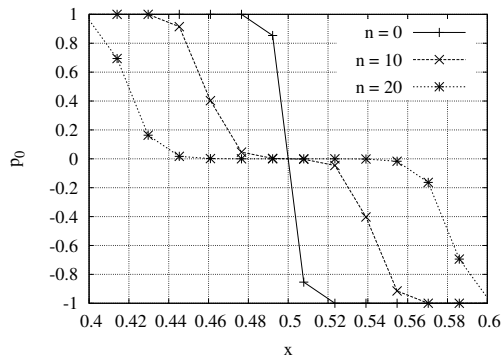


Figure 5.16: Dual solution  $p_0^h$  at different time levels.

applying the scheme to a dual problem with a discontinuous dual initial condition, as shown in figure 5.9 for case 2. This is confirmed by figure 5.16, which shows a close-up of the coarse dual initial condition  $p_0^h = u_0^h(x, T)$  at the dual initial time  $n = 0, 10$  and  $20$  ( $n = 0$  means:  $t = T$  for the dual problem). In the computations performed to obtain the solutions as shown in figure 5.11, no additional shock boundary conditions are imposed. Nevertheless, figure 5.16 shows the dual shock boundary condition (5.38) is satisfied, without imposing it explicitly which confirms the statements by Giles in [68, 70].

## 5.4 Conclusions

The application of the DWR method to the nonlinear Burgers problem is presented in which the viscous Burgers equation (the fine model) is approximated by the inviscid Burgers equation (the coarse model). Satisfying results are obtained using the DWR method for goal-oriented modelling-error estimation for two cases: case 1 with a boundary layer and case 2 with a stationary shock. For both cases the nonlinear energy measure at the final time is studied as quantity of interest. Due to the nonlinearity of the model equations, high-order terms arise in the modelling-error estimator. These high-order terms are analysed for the unsteady 1-D case, which reveals that an additional boundary term arises. This term is computable based on the given boundary conditions, the coarse model solution and the dual solution. For a quantity of interest defined on a boundary however, this high-order boundary term is zero. Analysis of this additional bound-



ary term, shows that for  $e_0 \geq 0$  it is at least of the same magnitude as the convective contribution in the error-estimator and should therefore be included.

For the discrete solutions a finite volume approach is used, where high-order discretisation is applied and a flux limiter to prevent spurious oscillations in the solutions.

### Case 1

For case 1 with the boundary layer, it is shown that incorporating the boundary residual is important, since the boundary contribution in the error estimator is larger than the contribution from the inner domain. This is similar to the discrete case studied for the linear convection-diffusion problem in the previous chapter.

In this nonlinear problem, the primal solution is required as coefficient for the convective term and as dual initial condition. The purpose of goal-oriented modelling-error estimator however, is based on the fact that the fine model solution  $u(x, t)$  is not available. Therefore the fine dual solution is computed as well using the coarse model solution  $u_0(x, t)$  as coefficient for the convective term and as dual initial condition. The error estimator based on this dual solution performs good.

The efficiency index for case 1 suggests that the coarse dual-weighted residual estimator  $R(u_0; p_0)$ , performs better than the fine dual weighted estimator  $R(u_0; p)$ . Making an explicit evaluation of the most important high-order terms, reveals that this is a coincidence. For  $\mu = 0.1$ , it is shown that the fine dual-based estimator improves more than the coarse dual-based estimator, when incorporating the evaluated high-order terms. For decreasing  $\mu$ , the goal-oriented modelling error estimator improves.

### Case 2

Case 2 implies a stationary shock in the primal solution which enables to study the modelling-error estimator for strongly nonlinear problems. The situation is not a singularly perturbed problem as in case 1, since the modelling error goes to zero for vanishing  $\mu$ . Therefore the modelling error  $Q(u) - Q(u_0)$  and the high-order terms approach zero as well.

Also for case 2, the fine dual solution  $p$  is computed using the fine and the coarse model solutions  $u$  and  $u_0$ , as coefficient in the dual equation and as initial condition. This estimator performs fine.

In case of shocks in the primal solution, attention should be paid to solving the dual problem. For certain quantities of interest a discontinuous dual initial condition may arise, for which analytically an additional shock

boundary condition needs to be applied. For the case studied and the applied discretisation scheme however, the proper dual solution emanates from the shock, without imposing the additional shock boundary condition explicitly.

## Chapter 6

# An approach for steady 2-D flow problems

In this chapter, an approach is described and studied to derive a goal-oriented modelling-error estimator for a 2-D flow problem. In this case the Navier-Stokes equations represent the fine model and the Euler equations the coarse model, which is obtained by omitting diffusion and heat conduction in the Navier-Stokes equations. This model simplification is similar to the (nonlinear) convection-diffusion problems described in the previous chapters, where the coarse model is also obtained by omitting the diffusion. In both cases the type of the equations changes, due to this simplification in the coarse model. The elliptic Navier-Stokes equations change type when diffusion and heat conduction are omitted.

Contrary to the convection-diffusion problems in the previous chapter where the variational approach is followed, in this chapter the linear differential approach as described in chapter 2 is followed. The linear differential approach followed for a 2-D flow, is based on the work of Giles and Pierce [36] for the thin-layer Navier-Stokes equations. The advantage of the linear differential approach in this 2-D problem, is that the formulation and derivation of boundary operators can be done in a more compact form than with the variational approach. However, due to the nonlinearity of the problem, the variational approach should also be applied to gain insight in high-order contributions in the error-estimator. Therefore this chapter should be considered as a preliminary study into the application of the DWR method in flow problems where model equations are of different type. The boundary operators for the dual problem and the error estimator that are derived by the linear differential approach are studied and described in

more detail.

The DWR method (in the variational approach) has been successfully applied to a flow problem by Oden and Prudhomme [27]. In this problem however, they consider the Stokes equations as approximating model. In the Stokes equations the convective instead of diffusive terms are omitted due to which the type of the equations remains the same and no boundary residuals arise.

In section 6.1 the model equations are given in conservative form and linearised form. The latter is required in order to derive the dual equations and dual boundary operators as will be shown in section 6.2. Using these boundary operators the goal-oriented modelling-error estimator is derived in section 6.3. Conclusions and recommendations are given in section 6.5.

## 6.1 The model equations

In this section the model equations are given for the fine and coarse model represented by the Navier-Stokes and the Euler equations, respectively. To apply the linear differential approach as given in chapter 2, the Navier-Stokes and Euler equations need to be linearised as shown in the following section.

### 6.1.1 The fine model: the Navier-Stokes equations

We first consider the compressible steady Navier-Stokes equations in 2-D:

$$\frac{\partial}{\partial x}(F_x(U) + F_x^v(U)) + \frac{\partial}{\partial y}(F_y(U) + F_y^v(U)) = 0, \quad (6.1)$$

where  $U = (\rho, \rho u_x, \rho u_y, \rho E)^T$  is the solution vector of conservative variables with  $\rho$  the density,  $u_x$  and  $u_y$  the velocity components of  $\vec{u} = (u_x, u_y)^T$  and  $E$  the total energy. The vectors  $F_i$  and  $F_i^v$  are the convective and viscous flux vectors in  $i$ -direction, respectively. For the convective fluxes we have:

$$F_x(U) = \begin{pmatrix} \rho u_x \\ \rho u_x^2 + p \\ \rho u_x u_y \\ \rho u_x H \end{pmatrix}, \quad F_y(U) = \begin{pmatrix} \rho u_y \\ \rho u_x u_y \\ \rho u_y^2 + p \\ \rho u_y H \end{pmatrix}, \quad (6.2)$$

with  $p$  the static pressure and  $H = \frac{\gamma}{\gamma-1} \frac{p}{\rho} + |\vec{u}|^2/2$  the total enthalpy in which  $\gamma$  is the ratio of specific heats. For the viscous fluxes we have:

$$F_x^v(U) = \begin{pmatrix} 0 \\ \tau_{xx} \\ \tau_{xy} \\ u\tau_{xx} + v\tau_{xy} + k\frac{\partial T}{\partial x} \end{pmatrix}, \quad F_y^v(U) = \begin{pmatrix} 0 \\ \tau_{yx} \\ \tau_{yy} \\ u\tau_{yx} + v\tau_{yy} + k\frac{\partial T}{\partial y} \end{pmatrix}. \quad (6.3)$$

The stress tensor  $\tau_{ij}$ , ( $i, j = x, y$ ) given by:

$$\tau_{ij} = \delta^{ij} \lambda (\nabla \cdot \vec{u}) + 2\mu \left( \frac{\partial u_j}{\partial x_i} + \frac{\partial u_i}{\partial x_j} \right), \quad i, j = x, y, \quad (6.4)$$

where  $\lambda = -2/3\mu$  is the bulk viscosity coefficient and  $\delta^{ij}$  the Kronecker delta. To apply the linear differential approach, the Navier-Stokes equations (6.1) are linearised around a steady state solution. In linearised form, with  $u = (\tilde{\rho}, (\tilde{\rho}u_x), (\tilde{\rho}u_y), (\tilde{\rho}E))^T$  the solution vector of perturbed conservative variables, equation (6.1) becomes:

$$Lu \equiv \frac{\partial}{\partial x} \left( (A_x - A_x^v)u - D_{xx} \frac{\partial u}{\partial x} - D_{xy} \frac{\partial u}{\partial y} \right) + \frac{\partial}{\partial y} \left( (A_y - A_y^v)u - D_{yx} \frac{\partial u}{\partial x} - D_{yy} \frac{\partial u}{\partial y} \right) = 0. \quad (6.5)$$

The convective and viscous Jacobians in  $i$ -direction are:

$$A_i = \frac{\partial F_i}{\partial U} \Big|_{U(x,y)}, \quad A_i^v = \frac{\partial F_i^v}{\partial U} \Big|_{U(x,y)}, \quad i = x, y. \quad (6.6)$$

The matrices  $D_{ij}$  are the Jacobians with respect to the derivatives in  $i, j$ -directions:

$$D_{ij} = \frac{\partial F_i^v}{\partial (\frac{\partial U}{\partial x_j})} \Big|_{U(x,y)}, \quad i, j = x, y. \quad (6.7)$$

A detailed discussion on boundary conditions for the Navier-Stokes and Euler equations is beyond the scope of this thesis, see the numerous literature available on the subject, e.g. [64, 66, 71, 72].

### 6.1.2 The coarse model: the Euler equations

To obtain the approximating Euler equations, all viscous and heat conducting terms in the (linearised) Navier-Stokes equations (6.5) are dropped. This yields:

$$L_0 u_0 \equiv \frac{\partial}{\partial x} (A_x u_0) + \frac{\partial}{\partial y} (A_y u_0) = 0, \quad (6.8)$$

where  $u_0$  is the solution vector with conservative variables (with the subscript ‘0’ indicating the coarse model solution) and  $A_x$  and  $A_y$  are the same convective Jacobians as in (6.5). For the derivation of the dual boundary conditions for the Euler equations, the reader is referred to Giles and Pierce [36] and Soemarwoto [38]. To derive the goal-oriented modelling-error estimator in the following sections, the dual boundary operators for the Navier-Stokes equations are required.

## 6.2 Dual boundary operators

To find the dual equation, the inner product (defined in (2.4)) of the linearised Navier-Stokes equations (6.5) with the vector of dual variables  $v^1$  is taken and integration by parts is performed as in (2.9):

$$\begin{aligned}
(v, Lu)_\Omega &= \left( - (A_x - A_x^v)^T \frac{\partial v}{\partial x} - \frac{\partial}{\partial x} \left( D_{xx}^T \frac{\partial v}{\partial x} + D_{yx}^T \frac{\partial v}{\partial y} \right), u \right)_\Omega \\
&\quad + \left( - (A_y - A_y^v)^T \frac{\partial v}{\partial y} - \frac{\partial}{\partial y} \left( D_{xy}^T \frac{\partial v}{\partial x} + D_{yy}^T \frac{\partial v}{\partial y} \right), u \right)_\Omega \\
&\quad + \left( v, n_x \left( (A_x - A_x^v)^T - D_{xx} \frac{\partial u}{\partial x} - D_{xy} \frac{\partial u}{\partial y} \right) \right)_\Gamma \\
&\quad + \left( v, n_y \left( (A_y - A_y^v)^T - D_{yx} \frac{\partial u}{\partial x} - D_{yy} \frac{\partial u}{\partial y} \right) \right)_\Gamma \\
&\quad + \left( \frac{\partial v}{\partial x}, (n_x D_{xx} + n_y D_{yx}) u \right)_\Gamma \\
&\quad + \left( \frac{\partial v}{\partial y}, (n_x D_{xy} + n_y D_{yy}) u \right)_\Gamma.
\end{aligned} \tag{6.9}$$

Here,  $n_x$  and  $n_y$  are the components of the outward pointing unit normal on the boundary  $\vec{n} = (n_x, n_y)^T$ . The inner product of the dual equation and the primal solution  $u$ , i.e.  $(L^*v, u)$ , is given by the first two lines in (6.9). This yields for the dual problem:

$$\begin{aligned}
L^*v &= - (A_x - A_x^v)^T \frac{\partial v}{\partial x} - \frac{\partial}{\partial x} \left( D_{xx}^T \frac{\partial v}{\partial x} + D_{yx}^T \frac{\partial v}{\partial y} \right) \\
&\quad + \left( - (A_y - A_y^v)^T \frac{\partial v}{\partial y} - \frac{\partial}{\partial y} \left( D_{xy}^T \frac{\partial v}{\partial x} + D_{yy}^T \frac{\partial v}{\partial y} \right) \right) = g,
\end{aligned} \tag{6.10}$$

where  $g$  depends on the quantity of interest considered, as described in chapter 2. For a quantity of interest defined on a boundary, we have  $g = 0$ .

---

<sup>1</sup>To prevent confusion with the pressure  $p$  it is chosen to use  $v$  for the vector of dual variables.

The remaining terms in equation(6.9) are the boundary integrals, which shows that the matrices  $A_i$ ,  $A_i^v$  and  $D_{ij}$  given in (6.6) and (6.7) are present in the dual problem. There are several approaches to obtain these matrices in discrete computations, such as explicit evaluation of the derivatives [43, 44, 73, 74, 75] or automatic differentiation [25, 76, 77, 78] of which the last is more accurate and less time consuming.

Before proceeding, we switch from conservative variables  $u \equiv (\tilde{\rho}, (\rho\tilde{u}_x), (\rho\tilde{u}_y), (\rho\tilde{E}))^T$  to primitive variables  $u_p \equiv (\tilde{\rho}, \tilde{u}_x, \tilde{u}_y, \tilde{T})^T$ , with  $\tilde{T}$  the perturbed temperature. Computing the Jacobians (6.6)–(6.7) with respect to primitive variables yields a more synoptic derivation of boundary operators than using Jacobians with respect to the conservative variables. The switch to primitive variables is achieved by  $u = Su_p$ , where  $S$  is the transformation matrix  $S = \partial u / \partial u_p$ .

In order to derive the dual boundary operators, the boundary terms in (6.9) are written in compact form as in (2.11). Therefore the following extended vectors  $\mathbf{u}_p$  and  $\mathbf{v}_p$  are introduced containing the vector itself and the derivatives with respect to its normal:

$$\mathbf{u}_p = \begin{pmatrix} u_p \\ \frac{\partial u_p}{\partial n} \end{pmatrix} = \begin{pmatrix} S^{-1}u \\ \frac{\partial(S^{-1}u)}{\partial n} \end{pmatrix}, \quad \mathbf{v}_p = \begin{pmatrix} S^T v \\ S^T \frac{\partial v}{\partial n} \end{pmatrix}, \quad (6.11)$$

with  $\frac{\partial}{\partial n} = \vec{n} \cdot \nabla$  the directional derivative. The boundary integrals in (6.9) are then written in matrix form as  $\mathbf{v}_p^T \mathbf{A}_p \mathbf{u}_p$ . To construct the matrix  $\mathbf{A}_p$  with respect to the primitive variables, the matrices  $A_i$ ,  $A_i^v$  and  $D_{ij}$  from (6.6) and (6.7) are given with respect to the primitive variables, indicated by the subscript ‘ $p$ ’. Derivatives in (6.9) with respect to  $x$  and  $y$ , are rewritten in terms of the directional derivative by  $\frac{\partial}{\partial x} = n_x \frac{\partial}{\partial n}$  and  $\frac{\partial}{\partial y} = n_y \frac{\partial}{\partial n}$ . To have the energy equation in terms of the temperature  $\tilde{T}$ , it

is divided by  $\rho c_v$ . The resulting matrices are:

$$\mathbf{A}_{x,p} = \begin{bmatrix} u_x & \rho & 0 & 0 \\ u_x^2 + RT & 2\rho u_x & 0 & \rho R \\ u_x u_y & \rho u_y & \rho u_x & 0 \\ u_x \left( \frac{\gamma R}{\gamma-1} T + \frac{|\bar{u}|^2}{2} \right) & \rho \left( \frac{\gamma R}{\gamma-1} T + \frac{|\bar{u}|^2}{2} + u_x^2 \right) & \rho u_x u_y & \frac{\rho \gamma R}{\gamma-1} u_x \end{bmatrix} \quad (6.12a)$$

$$\mathbf{A}_{y,p} = \begin{bmatrix} u_y & 0 & \rho & 0 \\ u_x u_y & \rho u_y & \rho u_x & 0 \\ u_y^2 + RT & 0 & 2\rho u_y & \rho R \\ u_y \left( \frac{\gamma R}{\gamma-1} T + \frac{|\bar{u}|^2}{2} \right) & \rho u_x u_y & \rho \left( \frac{\gamma R}{\gamma-1} T + \frac{|\bar{u}|^2}{2} + u_y^2 \right) & \frac{\rho \gamma R}{\gamma-1} u_y \end{bmatrix} \quad (6.12b)$$

and

$$\mathbf{A}_{x,p}^v = \begin{bmatrix} 0 & 0 & 0 & 0 \\ 0 & 0 & 0 & 0 \\ 0 & 0 & 0 & 0 \\ 0 & \tau_{xx} & \tau_{xy} & 0 \end{bmatrix}, \quad \mathbf{A}_{y,p}^v = \begin{bmatrix} 0 & 0 & 0 & 0 \\ 0 & 0 & 0 & 0 \\ 0 & 0 & 0 & 0 \\ 0 & \tau_{yx} & \tau_{yy} & 0 \end{bmatrix}. \quad (6.13)$$

The convective matrices  $\mathbf{A}_{x,p}$  and  $\mathbf{A}_{y,p}$  and the viscous matrices  $\mathbf{A}_{x,p}^v$  and  $\mathbf{A}_{y,p}^v$ , together with their corresponding normal components  $n_x$  and  $n_y$ , form the Jacobian of the normal flux defined at the boundaries:

$$\frac{\partial(\vec{F} \cdot \vec{n})}{\partial U_p} = (\mathbf{A}_{x,p} + \mathbf{A}_{x,p}^v) n_x + (\mathbf{A}_{y,p} + \mathbf{A}_{y,p}^v) n_y \quad (6.14)$$

where  $\vec{F}$  is given by:

$$\vec{F} = \begin{pmatrix} F_x + F_x^v \\ F_y + F_y^v \end{pmatrix}.$$



For the viscous derivative matrices  $\mathbf{D}_{ij,p}$  we have:

$$\mathbf{D}_{xx,p} = \frac{\partial F_x^v}{\partial(\frac{\partial U}{\partial x})} \Big|_{U(x,y)} = \begin{bmatrix} 0 & 0 & 0 & 0 \\ 0 & 2\mu + \lambda & 0 & 0 \\ 0 & 0 & \mu & 0 \\ 0 & (2\mu + \lambda)u_x & \mu u_y & k \end{bmatrix}, \quad (6.15a)$$

$$\mathbf{D}_{xy,p} = \frac{\partial F_x^v}{\partial(\frac{\partial U}{\partial y})} \Big|_{U(x,y)} = \begin{bmatrix} 0 & 0 & 0 & 0 \\ 0 & 0 & \lambda & 0 \\ 0 & \mu & 0 & 0 \\ 0 & \mu u_y & \lambda u_x & 0 \end{bmatrix}, \quad (6.15b)$$

$$\mathbf{D}_{yx,p} = \frac{\partial F_y^v}{\partial(\frac{\partial U}{\partial x})} \Big|_{U(x,y)} = \begin{bmatrix} 0 & 0 & 0 & 0 \\ 0 & 0 & \mu & 0 \\ 0 & \lambda & 0 & 0 \\ 0 & \lambda u_y & \mu u_x & 0 \end{bmatrix}, \quad (6.15c)$$

$$\mathbf{D}_{yy,p} = \frac{\partial F_y^v}{\partial(\frac{\partial U}{\partial y})} \Big|_{U(x,y)} = \begin{bmatrix} 0 & 0 & 0 & 0 \\ 0 & \mu & 0 & 0 \\ 0 & 0 & 2\mu + \lambda & 0 \\ 0 & \mu u_x & (2\mu + \lambda)u_y & k \end{bmatrix}. \quad (6.15d)$$

Using the convective and viscous matrices given in (6.12a)–(6.15d), the matrix  $\mathbf{A}_p$  can finally be constructed:

$$\mathbf{A}_p = \begin{bmatrix} \vec{u} \cdot \vec{n} & \rho n_x & \rho n_y & 0 & 0 & 0 & 0 & 0 \\ \frac{RTn_x}{\rho} & \vec{u} \cdot \vec{n} & 0 & Rn_x & 0 & A_p^{2,6} & A_p^{2,7} & 0 \\ \frac{RTn_y}{\rho} & 0 & \vec{u} \cdot \vec{n} & Rn_y & 0 & A_p^{3,6} & A_p^{3,7} & 0 \\ 0 & A_p^{4,2} & A_p^{4,3} & \vec{u} \cdot \vec{n} & 0 & A_p^{4,6} & A_p^{4,7} & -\frac{k}{\rho c_v} \\ 0 & 0 & 0 & 0 & 0 & 0 & 0 & 0 \\ 0 & A_p^{6,2} & A_p^{6,3} & 0 & 0 & 0 & 0 & 0 \\ 0 & A_p^{7,2} & A_p^{7,3} & 0 & 0 & 0 & 0 & 0 \\ 0 & A_p^{8,2} & A_p^{8,3} & \frac{k}{\rho c_v} & 0 & 0 & 0 & 0 \end{bmatrix}, \quad (6.16)$$

with the shorted entries given by:

$$A_p^{4,2} = -\frac{\tau_{xy}}{\rho c_v} n_y + \left( (\gamma - 1) T - \frac{\tau_{xx}}{\rho c_v} \right) n_x, \quad (6.17a)$$

$$A_p^{4,3} = \left( (\gamma - 1) T - \frac{\tau_{yy}}{\rho c_v} \right) n_y - \frac{\tau_{xy}}{\rho c_v} n_x, \quad (6.17b)$$

$$A_p^{6,2} = -A_p^{2,6} = \frac{1}{\rho} \{ (2\mu + \lambda) n_x^2 + \mu n_y^2 \}, \quad (6.17c)$$

$$A_p^{7,3} = -A_p^{3,7} = \frac{1}{\rho} \{ (2\mu + \lambda) n_y^2 + \mu n_x^2 \}, \quad (6.17d)$$

$$A_p^{6,3} = A_p^{7,2} = -A_p^{2,7} = -A_p^{3,6} = \frac{(\lambda + \mu)}{\rho} n_x n_y, \quad (6.17e)$$

$$A_p^{8,2} = -A_p^{4,6} = \frac{1}{\rho} \{ (2\mu + \lambda) u_x n_x^2 + (\mu + \lambda) u_y n_x n_y + \mu u_x n_y^2 \}, \quad (6.17f)$$

$$A_p^{8,3} = -A_p^{4,7} = \frac{1}{\rho} \{ (2\mu + \lambda) u_y n_y^2 + (\mu + \lambda) u_x n_x n_y + \mu u_y n_x^2 \}. \quad (6.17g)$$

With matrix  $\mathbf{A}_p$  given, it is now possible to derive the dual boundary operators  $\mathbf{B}_p^*$  and  $\mathbf{C}_p^*$  as defined in (2.11), following the approach described in section 2.2. In short, this means that the following relation must hold:

$$\mathbf{A}_p = (\mathbf{B}_p^*)^T \mathbf{C}_p - (\mathbf{C}_p^*)^T \mathbf{B}_p. \quad (6.18)$$

This can be reformulated by:

$$\mathbf{A}_p = (\mathbf{T}^*)^T \mathbf{T}, \quad (6.19)$$

when defining the matrices  $\mathbf{T}$  and  $\mathbf{T}^*$  as:

$$\mathbf{T} = \begin{bmatrix} \mathbf{B}_p \\ \mathbf{C}_p \end{bmatrix}, \quad \mathbf{T}^* = \begin{bmatrix} -\mathbf{C}_p^* \\ \mathbf{B}_p^* \end{bmatrix}. \quad (6.20)$$

This means that  $\mathbf{T}^*$  needs to be resolved to determine  $\mathbf{B}_p^*$  and  $\mathbf{C}_p^*$ .

In the following sections, the boundary operators  $\mathbf{B}_p^*$  and  $\mathbf{C}_p^*$  are determined for a solid wall and for outflow boundaries. To do so, the primal boundary conditions are rewritten in matrix form by  $\mathbf{B}_p$  and  $\mathbf{C}_p$ . A similar procedure can be followed for the inflow boundary, but this is not discussed here, since the purpose is to derive the goal-oriented modelling-error estimator. Boundary residuals on the inflow boundary are zero, therefore they do not contribute to the modelling-error estimator (similar to the (nonlinear) convection-diffusion problems described in the previous chapters).



which illustrates that the quantities, represented by (a combination of) the rows of  $\mathbf{C}_p$ , are sensible choices for the quantity of interest: the wall shear stress formed by the first row, the normal stress (including the static pressure) formed by the second row and the heat flux formed by the third row. When the heat flux is used as boundary condition in combination with the no-slip condition, one finds from  $\mathbf{C}_p$  that the wall temperature is a sensible choice as quantity of interest.

The dual operators  $\mathbf{B}_p^*$  and  $\mathbf{C}_p^*$  can now be found by solving system (6.19), where  $\mathbf{T}$  and  $\mathbf{T}^*$  are determined by the definitions (6.20). For  $\mathbf{B}_p^*$  this yields:

$$\mathbf{B}_p^* = \begin{bmatrix} 0 & -\frac{n_y}{\rho} & \frac{n_x}{\rho} & 0 & 0 & 0 & 0 & 0 \\ 0 & \frac{n_x}{\rho} & \frac{n_y}{\rho} & 0 & 0 & 0 & 0 & 0 \\ 0 & 0 & 0 & \frac{1}{\rho c_v} & 0 & 0 & 0 & 0 \end{bmatrix}. \quad (6.24)$$

When solving the dual equation with respect to the primitive variables, the dual boundary conditions are:

$$\mathbf{B}_p^* \mathbf{v}_p = \begin{bmatrix} \frac{\vec{v} \cdot \vec{s}}{\rho} \\ \frac{\vec{v} \cdot \vec{n}}{\rho} \\ \frac{v_4}{\rho c_v} \end{bmatrix}, \quad (6.25)$$

where  $\vec{v} = (v_2, v_3)$  is the dual velocity and  $\vec{s}$  the unit tangential vector. This shows that the boundary conditions for the fine dual problem are comparable to those for the primal problem (the Navier-Stokes equations), where the no-slip condition and zero flow through the solid wall, are in fact conditions on the tangential and normal component of the velocity vector.

For the matrix  $\mathbf{C}_p^*$ , required for the modelling-error estimator, we have:

$$\mathbf{C}_p^* = \begin{bmatrix} -\rho n_x & 0 & 0 & -A_p^{4,2} & 0 & -A_p^{6,2} & -A_p^{7,2} & 0 \\ -\rho n_y & 0 & 0 & -A_p^{4,3} & 0 & -A_p^{7,2} & -A_p^{7,3} & 0 \\ 0 & 0 & 0 & 0 & 0 & 0 & 0 & -\frac{k}{\rho c_v} \end{bmatrix}, \quad (6.26)$$

in which the  $A_p$  entries are given in (6.17). These matrices can be converted back into the original conservative variables using the relations in equation (6.11). We continue by using the primitive variables and the corresponding matrices.

Note that the entries of  $\mathbf{C}_p^*$  are based on the solution  $u$  of the Navier-Stokes equations, the fine model. Since  $u$  is not available, the coarse solution  $u_0$  needs to be used instead. This aspect is comparable to the Burgers problem in the previous chapter, where the fine model solution  $u$  appears in the fine dual problem as coefficient for the convective term and as dual initial condition. In that case the fine model solution is also replaced by coarse model solution  $u_0$ .

The  $\mathbf{C}_p^*$ -entries  $A_p^{4,2}$  and  $A_p^{4,3}$ , given in (6.17), reveal that stress terms appear in the error estimator. The stress terms as given in equation (6.4), require the gradients of the velocity  $\vec{u}$  from the Navier-Stokes solution. Since the fine model solution  $u$  is not at hand, the coarse model solution  $u_0$  has to be used. This means that the velocity gradients, as they appear in  $\mathbf{C}_p^*$ , are based on the coarse model velocity  $\vec{u}_0$  instead of the fine model velocity  $\vec{u}$ . Due to the boundary layer in the fine model solution which lacks in the coarse model solution, the gradients of  $\vec{u}$  at the solid wall are much larger than the gradients of  $\vec{u}_0$ . This difference in velocity gradients has an effect on the accuracy of the estimator that can be quite large.

### Boundary conditions for a quantity of interest on a solid wall

Consider as quantity of interest the following force exerted on the solid wall  $\Gamma_S$  (for instance the lift of an airfoil):

$$Q(u) = \int_{\Gamma_S} \tilde{p} - (2\mu + \lambda) \left( \frac{\partial \tilde{u}_x}{\partial x} + \frac{\partial \tilde{u}_y}{\partial y} \right) ds. \quad (6.27)$$

Remind that the general form of a quantity of interest is given by (2.3):

$$Q(u) = (g, u)_\Omega + (h, Cu)_\Gamma.$$

Since the quantity of interest (6.27) has zero inner domain contribution ( $g = 0$ ), it can be written as:

$$Q(u) = h^T \mathbf{C}_p \mathbf{u}_p. \quad (6.28)$$

With  $\mathbf{C}_p$  given in (6.23) this becomes:

$$\begin{aligned} Q(u) &= h_1 \mu \left( n_y \frac{\partial \tilde{u}_x}{\partial n} + n_x \frac{\partial \tilde{u}_y}{\partial n} \right) \\ &\quad - h_2 \left( RT \tilde{\rho} + \rho R \tilde{T} - (2\mu + \lambda) \left( n_x \frac{\partial \tilde{u}_x}{\partial n} + n_y \frac{\partial \tilde{u}_y}{\partial n} \right) \right) \\ &\quad - h_3 k \frac{\partial \tilde{T}}{\partial n}, \end{aligned} \quad (6.29)$$

where the perturbed pressure  $\tilde{p}$  is rewritten in terms of the primitive variables  $\tilde{\rho}$  and  $\tilde{T}$ , using the equation of state  $p = \rho R T$  as:

$$\tilde{p} = (\tilde{\rho} R T + \rho R \tilde{T}). \quad (6.30)$$

Equation (6.29) in combination with equation (6.27), implies  $h_1 = 0$ ,  $h_2 = 1$  and  $h_3 = 0$ . Since the dual boundary conditions are defined according to  $B^*v = h$  from (2.5b), this gives for the dual boundary conditions on  $\Gamma_S$  using (6.25):

$$\begin{aligned} \frac{\vec{v} \cdot \vec{s}}{\rho} &= h_1 = 0, \\ \frac{\vec{v} \cdot \vec{n}}{\rho} &= h_2 = 1, \\ \frac{v_4}{\rho c_v} &= h_3 = 0. \end{aligned} \quad (6.31)$$

### 6.2.2 Outflow boundary operators

For a subsonic outflow boundary  $\Gamma_O$  (which is an inflow boundary for the dual problem), Neumann boundary conditions are applied on the stress and temperature (see Wesseling [64] and Hirsch [66]):

$$\tau_{\alpha\beta} n_\beta - p \delta_{\alpha\beta} n_\beta = -p_\infty n_\alpha, \quad \text{with } \alpha, \beta = x, y, \quad (6.32a)$$

$$k \frac{\partial T}{\partial n} = 0. \quad (6.32b)$$

which yields in terms of primitive variables:

$$(2\mu \frac{\partial u_x}{\partial x} + \lambda (\frac{\partial u_x}{\partial x} + \frac{\partial u_y}{\partial y}) - p) n_x = -p_\infty n_x, \quad (6.33a)$$

$$(2\mu \frac{\partial u_y}{\partial y} + \lambda (\frac{\partial u_x}{\partial x} + \frac{\partial u_y}{\partial y}) - p) n_y = -p_\infty n_y, \quad (6.33b)$$

$$\mu (\frac{\partial u_x}{\partial y} + \frac{\partial u_y}{\partial x}) n_x = \mu (\frac{\partial u_x}{\partial y} + \frac{\partial u_y}{\partial x}) n_y = 0, \quad (6.33c)$$

$$k \frac{\partial T}{\partial n} = 0. \quad (6.33d)$$

These conditions also apply to the equations in linearised form. Note that in (6.33a) and (6.33b) the terms  $(\partial u_y / \partial y) n_x$  and  $(\partial u_x / \partial x) n_y$  are zero. Taking together (6.33a) and (6.33b) and rewriting the pressure  $\tilde{p}$  using (6.30), yields:

$$(R T \tilde{\rho} + \rho R \tilde{T}) - (2\mu + \lambda) (\frac{\partial \tilde{u}_x}{\partial n} n_x + \frac{\partial \tilde{u}_y}{\partial n} n_y) = p_\infty. \quad (6.34)$$

Similar to the solid wall boundary conditions in the previous section the outflow boundary conditions should be defined in terms of rows that form a basis for  $\mathbf{A}_p$  as given in equation (6.16), in order to find the dual boundary operators. In its full form  $\mathbf{A}_p$  is of rank 7, since each of its rows can be written as a combination of the following rows:

$$\begin{aligned}
& \left( \begin{array}{ccccccccc} 1 & 0 & 0 & 0 & 0 & 0 & 0 & 0 & 0 \end{array} \right) \\
& \left( \begin{array}{ccccccccc} 0 & 1 & 0 & 0 & 0 & 0 & 0 & 0 & 0 \end{array} \right) \\
& \left( \begin{array}{ccccccccc} 0 & 0 & 1 & 0 & 0 & 0 & 0 & 0 & 0 \end{array} \right) \\
& \left( \begin{array}{ccccccccc} 0 & 0 & 0 & 1 & 0 & 0 & 0 & 0 & 0 \end{array} \right) \quad (6.35) \\
& \left( \begin{array}{ccccccccc} RT & 0 & 0 & \rho R & 0 & -(2\mu + \lambda) n_x & -(2\mu + \lambda) n_y & 0 & 0 \end{array} \right) \\
& \left( \begin{array}{ccccccccc} 0 & 0 & 0 & 0 & 0 & \mu n_y & -\mu n_x & 0 & 0 \end{array} \right) \\
& \left( \begin{array}{ccccccccc} 0 & 0 & 0 & 0 & 0 & 0 & 0 & 0 & -k \end{array} \right)
\end{aligned}$$

which corresponds to perturbations in  $\rho$ ,  $u_x$ ,  $u_y$ ,  $T$ , the normal stress, the shear stress and the heat flux, respectively.

With (6.34) and (6.37), the primal outflow boundary operator  $\mathbf{B}_p$  is then constructed from the appropriate rows from (6.35):

$$\mathbf{B}_p = \begin{bmatrix} 0 & 0 & 0 & 0 & 0 & \mu n_y & -\mu n_x & 0 \\ RT & 0 & 0 & \rho R & 0 & -(2\mu + \lambda) n_x & -(2\mu + \lambda) n_y & 0 \\ 0 & 0 & 0 & 0 & 0 & 0 & 0 & -k \end{bmatrix}. \quad (6.36)$$

The first row of  $\mathbf{B}_p$  comes from the condition (6.33c) and is found by rearrangement:

$$\mu \frac{\partial \tilde{u}_x}{\partial y} n_y - \mu \frac{\partial \tilde{u}_y}{\partial x} n_x = \mu \frac{\partial \tilde{u}_x}{\partial y} n_x - \mu \frac{\partial \tilde{u}_y}{\partial x} n_y = 0,$$

which is equal to:

$$\mu n_y \frac{\partial \tilde{u}_x}{\partial n} - \mu n_x \frac{\partial \tilde{u}_y}{\partial n} = 0. \quad (6.37)$$

For  $\mathbf{C}_p$  we choose the rest of the rows (6.21) that form, together with  $\mathbf{B}_p$ , a complete basis for the rows of  $\mathbf{A}_p$ :

$$\mathbf{C}_p = \begin{bmatrix} 1 & 0 & 0 & 0 & 0 & 0 & 0 & 0 & 0 \\ 0 & 1 & 0 & 0 & 0 & 0 & 0 & 0 & 0 \\ 0 & 0 & 1 & 0 & 0 & 0 & 0 & 0 & 0 \\ 0 & 0 & 0 & 1 & 0 & 0 & 0 & 0 & 0 \end{bmatrix}. \quad (6.38)$$

Now the dual operators  $\mathbf{B}_p^*$  and  $\mathbf{C}_p^*$  are determined by solving system (6.19) with  $\mathbf{T}$  and  $\mathbf{T}^*$  given by (6.20). Splitting the Dirichlet and Neumann parts in  $\mathbf{B}_p^*$ , yields:

$$\mathbf{B}_p^* \mathbf{v}_p = \begin{bmatrix} \vec{u} \cdot \vec{n} & 0 & 0 & -\frac{TR}{\rho} \vec{u} \cdot \vec{n} \\ \rho n_x & \vec{u} \cdot \vec{n} & 0 & A_p^{4,2} \\ \rho n_y & 0 & \vec{u} \cdot \vec{n} & A_p^{4,3} \\ 0 & 0 & 0 & (1-R)\vec{u} \cdot \vec{n} \end{bmatrix} v + \begin{bmatrix} 0 & 0 & 0 & 0 \\ 0 & A_p^{6,2} & A_p^{7,2} & A_p^{8,2} \\ 0 & A_p^{6,3} & A_p^{7,3} & A_p^{8,3} \\ 0 & 0 & 0 & \frac{k}{\rho c_v} \end{bmatrix} \frac{\partial v}{\partial n}, \quad (6.39)$$

and for  $\mathbf{C}_p^*$  one finds:

$$\mathbf{C}_p^* = \begin{bmatrix} 0 & \frac{n_y}{\rho} & -\frac{n_x}{\rho} & \frac{\vec{u} \cdot \vec{s}}{\rho} & 0 & 0 & 0 & 0 \\ 0 & -\frac{n_x}{\rho} & -\frac{n_y}{\rho} & \frac{-\vec{u} \cdot \vec{n}}{\rho} & 0 & 0 & 0 & 0 \\ 0 & 0 & 0 & \frac{1}{\rho c_v} & 0 & 0 & 0 & 0 \end{bmatrix}. \quad (6.40)$$

The required dual boundary conditions on a dual inflow boundary, determined by  $\mathbf{B}_p^* \mathbf{v}_p$  given in (6.39), are rather complicated. Instead, the boundary conditions for the Euler case on far-field boundaries (the inflow and outflow boundaries) can be applied, see also Soemarwoto [38]. When the quantity of interest is defined on a solid wall, far-field boundary conditions have low influence on the dual solution near that wall (see [38]).

When the quantity of interest is defined on a solid wall, all dual outflow boundary conditions are homogeneous on  $\Gamma_O$ :

$$B^* v = h \Rightarrow \mathbf{B}_p^* \mathbf{v}_p = h, \quad (6.41)$$

with  $h_1 = h_2 = h_3 = 0$  and  $\mathbf{B}_p^*$  given in (6.39).

### 6.3 The error estimator

The error estimator in general form is defined by equation (2.18). In the chapters 4 and 5 it is explained that the error estimator has no contributions



from the inflow boundary, since the fine and coarse model have the same boundary conditions. For the 2-D flow problem considered with  $f = 0$ , the estimator in terms of the boundary matrices with respect to the primitive variables is given by:

$$\begin{aligned} Q(u) &= (v, -Lu_0)_\Omega + (a_S - \mathbf{B}_p \mathbf{u}_{0,p})^T \mathbf{C}_p^* \mathbf{v}_p|_{\Gamma_S} \\ &\quad + (a_O - \mathbf{B}_p \mathbf{u}_{0,p})^T \mathbf{C}_p^* \mathbf{v}_p|_{\Gamma_O}. \end{aligned} \quad (6.42)$$

In the following sections, the individual contributions from the inner domain, the solid wall and the outflow boundary are discussed. Applying the coarse dual solution  $v_0$  as weighting function in the error estimator, means that  $v$  should be replaced by  $v_0$ . Also in the dual boundary operator  $\mathbf{C}_p^*$  the primal variables  $u_p \equiv (\tilde{\rho}, \tilde{u}_y, \tilde{u}_y, \tilde{T})^T$  should be replaced by the coarse model variables  $u_{0p} \equiv (\tilde{\rho}_0, \tilde{u}_{0x}, \tilde{u}_{0y}, \tilde{T}_0)^T$ .

### 6.3.1 Inner domain contribution

The contribution from the inner domain  $(v, -Lu_0)$  is found by substituting the Euler solution  $u_0$  into the Navier-Stokes equations (6.5). To simplify the expression, the coarse model is used. This is allowed when the right-hand-side of the model equations is equal (zero in this case). This yields:

$$\begin{aligned} (v, -Lu_0) &= (v, L_0 u_0 - Lu_0) \\ &= (v, \frac{\partial}{\partial x} \left( (A_x^v) u_0 + D_{xx} \frac{\partial u_0}{\partial x} + D_{xy} \frac{\partial u_0}{\partial y} \right) \\ &\quad + \frac{\partial}{\partial y} \left( (A_y^v) u_0 + D_{yx} \frac{\partial u_0}{\partial x} + D_{yy} \frac{\partial u_0}{\partial y} \right)). \end{aligned} \quad (6.43)$$

Note that the modelling residual can also be evaluated in nonlinear form by:

$$(v, -Lu_0) = \left( v, -\frac{\partial F_x^v(U)}{\partial x} - \frac{\partial F_y^v(U)}{\partial y} \right), \quad (6.44)$$

with  $F_x^v(U)$  and  $F_y^v(U)$  given in (6.3). This allows to use the viscous flux evaluation routines in case of numerical computations.

### 6.3.2 Solid wall contribution

For the modelling residual on a solid wall  $a - Bu_0$ , the no-slip condition on the wall for the Navier-Stokes equations is used, i.e.  $\tilde{u}_x = \tilde{u}_y = 0$ . Since the wall temperature is considered to be a given boundary condition, it is equal for both the fine and the coarse model, i.e.  $\tilde{T} = \tilde{T}_0$ . With the matrices  $\mathbf{C}_p^*$

and  $\mathbf{B}_p$  given in (6.26) and (6.22), respectively, the contribution from the solid wall  $\Gamma_S$  can be computed from:

$$\begin{aligned}
(a_S - \mathbf{B}_p \mathbf{u}_{0p})^T \mathbf{C}_p^* \mathbf{v}_p|_{\Gamma_S} &= \\
&= \begin{pmatrix} 0 - \tilde{u}_{0,x} \\ 0 - \tilde{u}_{0,y} \\ \tilde{T} - \tilde{T}_0 \end{pmatrix}^T \left( \begin{bmatrix} -\rho n_x & 0 & 0 & -A_p^{4,2} \\ -\rho n_y & 0 & 0 & -A_p^{4,3} \\ 0 & 0 & 0 & 0 \end{bmatrix} v \right. \\
&\quad \left. + \begin{bmatrix} 0 & -A_p^{6,2} & -A_p^{7,2} & 0 \\ 0 & -A_p^{7,2} & -A_p^{7,3} & 0 \\ 0 & 0 & 0 & -\frac{k}{\rho c_v} \end{bmatrix} \begin{bmatrix} \frac{\partial v}{\partial \vec{n}} \\ \frac{\partial v}{\partial \vec{n}} \end{bmatrix} \right). \quad (6.45)
\end{aligned}$$

Note that the  $\mathbf{C}_p^*$ -entries  $A_p^{4,2}$  and  $A_p^{4,3}$  that are given in (6.17), involve derivatives of the velocity components  $u_x$  and  $u_y$ . Since the fine model solution is not available, the coarse model solution should be used to evaluate the entries of  $\mathbf{C}_p^*$ . This has consequences for the accuracy of the error-estimator, as described in section 6.2.1

### 6.3.3 Outflow boundary contribution

For the outflow boundary, the residual  $(a_O - \mathbf{B}_p \mathbf{u}_O)$  is derived first with  $a_O = \mathbf{B}_p \mathbf{u}_p$  and  $\mathbf{B}_p$  given in (6.36):

$$\begin{aligned}
(a_O - \mathbf{B}_p \mathbf{u}_O) &= (\mathbf{B}_p \mathbf{u}_p - \mathbf{B}_p \mathbf{u}_{0p}) = \mathbf{B}_p (\mathbf{u}_p - \mathbf{u}_{0p}) \\
&= \begin{bmatrix} 0 & 0 & 0 & 0 & 0 & \mu n_y & -\mu n_x & 0 \\ RT & 0 & 0 & \rho R & 0 & -(2\mu + \lambda) n_x & -(2\mu + \lambda) n_y & 0 \\ 0 & 0 & 0 & 0 & 0 & 0 & 0 & -k \end{bmatrix} (\mathbf{u}_p - \mathbf{u}_O) \\
&= \begin{pmatrix} \mu \left( \frac{\partial \tilde{u}_x}{\partial y} - \frac{\partial \tilde{u}_y}{\partial x} \right) - \mu \left( \frac{\partial \tilde{u}_{0x}}{\partial y} - \frac{\partial \tilde{u}_{0y}}{\partial x} \right) \\ \tilde{p} - \tilde{p}_0 - (2\mu + \lambda) \left( \frac{\partial \tilde{u}_x}{\partial y} - \frac{\partial \tilde{u}_{0x}}{\partial y} \right) - (2\mu + \lambda) \left( \frac{\partial \tilde{u}_y}{\partial x} - \frac{\partial \tilde{u}_{0y}}{\partial x} \right) \\ -k \left( \frac{\partial \tilde{T}}{\partial \vec{n}} - \frac{\partial \tilde{T}_0}{\partial \vec{n}} \right) \end{pmatrix}. \quad (6.46)
\end{aligned}$$

The residual (6.46) is multiplied by  $\mathbf{C}_p^* \mathbf{v}_p$  with  $\mathbf{C}_p^*$  given in (6.40):

$$\mathbf{C}_p^* \mathbf{v}_p = \begin{bmatrix} 0 & \frac{n_y}{\rho} & -\frac{n_x}{\rho} & \frac{\vec{u} \cdot \vec{s}}{\rho} \\ 0 & -\frac{n_x}{\rho} & -\frac{n_y}{\rho} & \frac{-\vec{u} \cdot \vec{n}}{\rho} \\ 0 & 0 & 0 & \frac{1}{\rho c_v} \end{bmatrix} v. \quad (6.47)$$

## 6.4 Overview of the approach

Goal-oriented modelling-error estimation for a 2-D flow problem with the Navier-Stokes and the Euler equations as fine and coarse models, can be summarised by the following steps.

When the Euler equations (6.8) are solved, the quantity of interest expressed in terms of  $\mathbf{C}_p$ , can be computed. For a solid wall,  $\mathbf{C}_p$  is given by (6.23) and for an outflow boundary by (6.38). Then the dual problem (6.10) is solved with the boundary conditions determined by  $\mathbf{B}_p^*$ . For a solid wall and an outflow boundary,  $\mathbf{B}_p^* \mathbf{v}_p$  is given by (6.25) and (6.39), respectively.

To compute the goal-oriented modelling-error estimator, firstly the modelling residuals are required. The residual on the inner domain can be computed by substituting the Euler solution into the Navier-Stokes equations. With the boundary conditions for the Navier-Stokes equations known, the modelling residuals on the boundaries can also be computed. Then, these modelling residuals are multiplied by the weighting term  $\mathbf{C}_p^* \mathbf{v}_p$ . For the inner domain contribution we obtain the weighted residual (6.43). For the solid wall and outflow boundaries, we obtain the weighted residuals (6.45) and (6.46), respectively. Summing these inner domain and boundary contributions, yields the goal-oriented modelling-error estimator for a 2-D flow problem.

A drawback of the application of the linear differential approach to non-linear flow problems, is that high-order terms in the primal and dual error are neglected. These high-order terms originate from nonlinear terms such as the convective term and a nonlinear quantity of interest. In the previous chapter concerning the Burgers problem, it is shown that a computable high-order term on a boundary can be of significant size. Therefore, neglecting this term may have a negative effect on the accuracy of the error estimator.

## 6.5 Conclusions and recommendations

In this chapter, a possible approach is given for the application of the DWR method to 2-D flow problems based on the linear differential approach described in chapter 2. To derive the dual boundary operators by the linear differential approach, the primal fine and coarse problems are linearised. The resulting dual boundary operators yield an estimator without high-order terms, inherent to the linear differential approach.

The boundary conditions for the fine dual problem on a solid wall also yield a condition for the tangential and normal component of the dual velocity vector  $\vec{v} = (v_1, v_2)^T$ , similar to the conditions for the fine model. For the outflow boundary however, the derived dual boundary conditions for an outflow boundary are rather complex. Therefore, often the outflow boundary conditions for the coarse dual problem are applied for the fine dual problem. This approach is similar to the application of far-field boundary conditions for the Euler equations to the Navier-Stokes equations.

Some of the entries of the boundary operator for a solid wall are based on the primal solution. Since the fine model solution is not available, an error is introduced when applying the coarse model solution. It is explained that the gradients of the velocity at a solid wall based on the coarse model solution can differ a lot from the gradients based on the fine model solution, due to the boundary layer behaviour in the latter. Possible ways to improve the estimator can be the addition of an artificial boundary layer using Blasius theory and re-compute the gradients, or change the model type of the cells adjacent to the solid wall in case of discrete computations. This has to be evaluated by performing numerical tests.

The variational approach should be applied as well, in order to derive computable high-order contributions in the error-estimator. In the previous chapter concerning the nonlinear Burgers problem, it is found that high-order terms on a boundary can be of at least the same magnitude as convective contributions. These computable high-order boundary terms should therefore be included in the error estimator.

For the outflow boundary contribution in the error estimator with the quantity of interest defined on a solid wall, it should be investigated how large the outflow boundary contribution in the error estimator is with respect to the wall boundary contribution.

## Chapter 7

# Conclusions and recommendations

In this thesis it is shown that the Dual-Weighted Residual (DWR) method is a suitable method to perform goal-oriented modelling-error estimation in a class of hierarchical models in which the model equations are of different type. In this case, the type concerns the characterisation of the partial differential equation or the order of the equation. The error estimator for a modelling error in a quantity of interest in such a class, needs an explicit treatment of the boundaries. An example of hierarchical models of different type are the singularly perturbed convection-diffusion problems, where the coarse model is reduced problem in which diffusion is omitted. An expression for the modelling error is derived for (non-linear) convection-diffusion problems in which inner domain and boundary contributions occur.

### 7.1 Conclusions

To employ the DWR method, a dual problem is solved of which the solution acts as weighting function for the modelling residual. This residual is found by substituting the coarse model solution into the fine model equations. To obtain the goal-oriented modelling-error estimator according to the DWR method, a so-called linear differential approach and a variational approach are followed. The first approach is also applicable to non-linear problems, but since the model equations are first linearised before the error estimator is derived, all information contained in high-order contributions is discarded. Therefore, the variational approach, in which the model equations are con-

sidered in a weak formulation, is more suitable for non-linear problems since it allows to analyse contributions from non-linear terms (coming from the quantity of interest as well as the model equations).

### **Boundary residual inclusion**

For both the linear differential and the variational approach, it is shown to be essential to include boundary residuals explicitly in the modelling-error estimator when boundary conditions for the fine and coarse model differ, or when these models are of a different type. In the variational approach, this is achieved by imposing boundary and initial conditions weakly. The importance of boundary residual inclusion is illustrated by cases where the quantity of interest is defined on the whole domain, whilst the error estimator has only contributions from the boundaries. In convection-diffusion problems, both the convection and the diffusion term have a boundary contribution in the error estimator.

### **Applying the coarse dual solution in the estimator**

When the computation of the fine dual solution and the computation of the fine primal solution are equally expensive in terms of computational time, it is essential for the efficiency of the DWR method to employ the coarse dual solution instead of the fine dual solution. This introduces an additional dual error in the estimator which causes the quality of the estimator to decrease. The quality of the goal-oriented modelling-error estimator is indicated by the efficiency index, which is defined as the ratio between the estimator and the real error. A perfect estimator has an efficiency index of unity. In the (nonlinear) convection-diffusion cases considered, the efficiency index approaches unity for decreasing diffusion coefficient. This is also the case for both the fine and coarse dual-weighted residual estimators.

In the linearised dual problem, the quantity of interest appears in a weak formulation on the right-hand side. In some cases this leads to an ill-posed dual problem. This is demonstrated for a diffusion-related quantity of interest on a boundary that cannot be represented by the coarse model without a diffusive operator. A possible remedy for the ill-posed coarse dual problem is to apply domain decomposition, and use the fine dual equation in a small part of the domain. Applying the fine dual equation in a small region near that boundary yields a well-posed approximating dual problem.

### Application to nonlinear problems

Analysis of the high-order terms derived by the variational approach for the nonlinear Burgers problem, shows that the high-order terms also involve a computable boundary term that can be of the same magnitude as the convective boundary contribution. This illustrates the importance of analysing the high-order terms for nonlinear problems when the hierarchical models are of a different type.

It is also found that the fine model solution appears in the fine dual problem as a coefficient for the convective term and, in case of a nonlinear quantity of interest defined on the domain, also in the initial dual solution. Since the fine model solution is not provided, one can apply the coarse model solution in case one wants to use the fine dual solution in the error estimator. However, this introduces an additional error in the estimator.

### Violation of solution restrictions

Application of the DWR method to a Burgers problem in which a shock occurs in the inviscid Burgers solution, shows that the DWR method results in a reliable estimator, despite the restriction on the coarse model solution. This restriction is inherent to the variational approach and means that only sufficiently smooth solutions should be considered. The studied Burgers problem shows that for vanishing diffusion, the local modelling error vanishes, and consequently the modelling error in the quantity of interest.

In unsteady problems, when a discontinuity occurs between the initial dual condition and dual boundary conditions, the restriction that only sufficiently smooth solution should be considered, is violated. Despite this violation, the unsteady convection-diffusion problems studied in this thesis show good results for the goal-oriented modelling-error estimator.

### Aspects of numerical computations

The unsteady (nonlinear) convection-diffusion problems in this thesis are studied by numerical approximations in which difficulties arise when a discontinuity is introduced. A Spectral Element Method (SEM) and a Finite Volume Method (FVM) are applied to a linear convection-diffusion and a nonlinear Burgers problem, respectively. To deal with the initial discontinuity introduced in the dual problem at the boundary in the SEM approximations, the solution is locally smoothed near the boundary. In case of the FVM approximations, a flux limiter is applied to prevent spurious ‘wiggles’ in the solution.

It is important to have a good approximation of the dual solution near the boundaries, since its derivative there appears in the error estimator in both the linear and nonlinear problems. As mentioned before, good results for the error estimator are obtained for both problems.

Besides the efficiency gain when using the coarse dual problem, another advantage is that no mesh refinement is required to capture possible viscous layers in the dual solution. This is not necessarily the case however, when the coarse model is locally adapted to the fine model, since viscous layers may be introduced.

In unsteady problems, when a quantity of interest is defined on the final time, the DWR method is expensive in the sense of computational time since the dual problem must be solved backward in time to the initial time. This is a major drawback of the DWR method when applied to unsteady problems for the purpose of driving an adaptive modelling algorithm.

### **Preliminary study for application of DWR method to 2-D flow problems**

The linear differential approach is applied to derive a goal-oriented modelling error estimator in 2-D flow problems, where the Navier-Stokes equations represent the fine model and the Euler equations the coarse model. The fine model solution appears in the dual boundary operator matrix that is used in the error estimator. Since the fine model solution is not available, the coarse model solution needs to be used to evaluate the entries of the dual boundary operator matrix. This introduces an additional error in the error estimator, as was described previously for nonlinear problems.

## **7.2 Recommendations**

The work presented in this thesis is a first step towards the application of the DWR method to classes of hierarchical problems in which the models are of a different type. Illustrations are given for some simple problems in which the approach to apply the DWR method to different type of models yields satisfactory results. More research should be performed however, for more complex problems such as (nonlinear) convection-diffusion problems in multi-dimensions to study the behaviour near solid wall boundaries and quantities of interest defined on a boundary. Then flow problems can be a next step for which also the variational approach should be used in order to incorporate high-order terms. Analysis of high-order terms for the Burgers problem, reveals computable high-order terms of the same magnitude as



convective contributions. It is expected this is the case for flow problems as well.

The application to flow problems requires a computer code that is able to solve the Navier-Stokes equations (the fine model), the Euler equations (the coarse model), as well as their dual problems. When such a code is provided it enables the implementation of a goal-oriented modelling-error estimator based on both the fine and coarse dual solutions. Using the same code (and thus the same discretisation schemes) for the fine, as well as coarse model, is essential to prevent the discretisation error from interfering with the modelling error.

When the error estimator is used to drive an adaptive modelling algorithm, also adaptive meshing should be incorporated. When the error estimator is used to drive an adaptive modelling algorithm, viscous layers may arise when the coarse model is locally adapted to the fine model. To capture such a layer it may be necessary to refine the mesh.

When the dual problem is ill-posed as discussed before, a possible remedy is to apply domain decomposition. In numerical problems, this can be achieved by applying the fine model in cells adjacent to the boundary where the quantity of interest is defined. Whether or not this is a feasible solution to ill-posed dual problems, needs to be studied by numerical problems.

Since the dual boundary conditions on an outflow boundary for Navier-Stokes equations are rather complex, often the far-field boundary conditions for the dual problem of the Euler equations are applied. When doing so, its effect on the quality of the error estimator should be studied.

The mesh used to solve a discrete problem depends on the applied model. Problems in which boundary layers are present, often require refinement of the mesh in order to capture a boundary layer properly. When boundary layers are not present in the solution of a coarse -reduced- model and the model is (locally) adapted to the fine model, this might result in the need to refine the mesh. Therefore, adaptive modelling is often combined with adaptive meshing (both goal-oriented) to balance modelling and discretisation errors.



# Bibliography

- [1] W.L. Oberkampf, M.M. Sindir, and A.T. Conlisk. Guide for the Verification and Validation of Computational Fluid Dynamics Simulations. Technical Report AIAA-G-077-1998, AIAA, 1998.
- [2] P. J. Roache. *Verification and validation in computational science and engineering*. Hermosa, 1998.
- [3] J. Ambrosiano and M-M. Peterson. Research software development based on exploratory workflows: the exploratory process model (ExP). Technical Report LA-UR-00-3697, Los Alamos National Laboratory, 2000.
- [4] F. Stern, R.V. Wilson, H.W. Coleman, and E.G. Paterson. Comprehensive approach to verification and validation of CFD simulations-Part 1: methodology and procedures. *Journal of fluids engineering*, 123:793–802, December 2001.
- [5] F. Stern, R.V. Wilson, H.W. Coleman, and E.G. Paterson. Comprehensive approach to verification and validation of CFD simulations-Part 2: application for RANS simulation of a cargo/container ship. *Journal of fluids engineering*, 123:803–810, December 2001.
- [6] C.J. Roy, M.A McWherter-Payne and W.L. Oberkampf. Verification and Validation for Laminar Hypersonic Flowfields, Part 1: Verification. *AIAA Journal*, 41(10):1934–1943, 2003.
- [7] C.J. Roy, M.A McWherter-Payne and W.L. Oberkampf. Verification and Validation for Laminar Hypersonic Flowfields, Part 2: Validation. *AIAA Journal*, 41(10):1944–1954, 2003.
- [8] S. Schlesinger. Terminology for Model Credibility. *Simulation*, 32(3):103–104, 1979.

- 
- [9] W.L. Oberkampf, S.M. DeLand, B.M. Rutherford, K.V. Diegert and K.F. Alvin. Estimation of Total Uncertainty in Modeling and Simulation. Technical Report SAND2000-0824, Sandia National Laboratories, 2000. Reprint 2005.
- [10] W.L. Oberkampf, S.M. DeLand, B.M. Rutherford, K.V. Diegert and K.F. Alvin. Error and uncertainty in modeling and simulation. *Reliability Engineering & System Safety*, 75:333–357, 2002.
- [11] W.L. Oberkampf and T.G. Trucano. Verification and validation in computational fluid dynamics. *Progress in Aerospace Sciences*, 38:209–272, 2002.
- [12] M. Braack and A. Ern. A posteriori control of modeling errors and discretization errors. *Multiscale Modeling & Simulation, SIAM*, 1(2):221–238, 2003.
- [13] M. Braack and A. Ern. Coupling multimodelling with local mesh refinement for the numerical computation of laminar flames. *Combustion Theory and Modelling*, 8(4):771–788, 2004.
- [14] G. Carey. A perspective on adaptive modeling and meshing (AM&M). *Computer Methods in Applied Mechanics And Engineering*, 195:214–235, 2005.
- [15] J.T. Oden, S. Prudhomme and P. Bauman. On the extension of goal-oriented error estimation and hierarchical modeling to discrete lattice models. *Computer Methods in Applied Mechanics and Engineering*, 194(34–35):3668–3688, 2005.
- [16] J.T. Oden, I. Babuska, F. Nobile, Y.S. Feng and R. Tempone. Theory and methodology for estimation and control of errors due to modeling, approximation, and uncertainty. *Computer Methods in Applied Mechanics and Engineering*, 2005.
- [17] J.T. Oden, S. Prudhomme, D.C. Hammerand and M.S. Kuczma. Modeling error and adaptivity in nonlinear continuum mechanics. *Computer Methods in Applied Mechanics and Engineering*, 190:6663–6684, 2001.
- [18] R. Becker and R. Rannacher. A feed-back approach to error control in finite element methods: basic analysis and examples. *East-West Journal of Numerical Mathematics*, 4:237–264, 1996.
- [19] R. Becker and R. Rannacher. An optimal control approach to a posteriori error estimation in finite element methods. In *Acta Numerica*, volume 10, pages 1–102. Cambridge University Press, 2001.

- 
- [20] C. Johnson. On computability and error control in CFD. *International Journal for Numerical Methods in Fluids*, 20(8–9):777–788, 1995.
- [21] J.T. Oden and S. Prudhomme. On goal-oriented error estimation for elliptic problems: application to the control of pointwise errors. *Computer Methods in Applied Mechanics and Engineering*, 176:313–331, 1999.
- [22] P. Houston and R. Hartmann. Goal-oriented a posteriori error estimation for compressible fluid flows. In F. Brezzi, A. Buffa, S. Corsaro, and A. Murli, editors, *Numerical Mathematics and Advanced Applications*, pages 775–784. Springer, 2003.
- [23] R. Hartmann and P. Houston. Goal-oriented a posteriori error estimation for multiple target functionals. In Thomas Y. Hou and Eitan Tadmor, editors, *Hyperbolic problems: theory, numerics, applications*, pages 579–588. Springer, 2003.
- [24] P. Houston, R. Hartmann, and E. Süli. Adaptive discontinuous Galerkin finite element methods for compressible fluid flows. In M. Baines, editor, *Numerical methods for Fluid Dynamics VII, ICFD*, pages 347–353, 2001.
- [25] B. Mohammadi and O. Pironneau. Mesh adaption and automatic differentiation in a CAD-free framework for optimal shape design. *International Journal for Numerical Method in Fluids*, 30(2):127–136, 1999.
- [26] M.B. Giles and E. Süli. Adjoint methods for PDEs: a posteriori error analysis and postprocessing by duality. In *Acta Numerica*, volume 11, pages 145–236. Cambridge University Press, 2002.
- [27] J.T. Oden and S. Prudhomme. Estimation of modeling error in computational mechanics. *Journal of Computational Physics*, 182:496–515, 2002.
- [28] R. Courant and D. Hilbert. *Methods of Mathematical Physics, vol I & II*. Wiley-Interscience, New York, 1962.
- [29] D. Zwillinger. *Handbook of Differential Equations*. Academic Press, Boston, 3 edition, 1997.
- [30] Y. Pinchover and J. Rubinstein. *An Introduction to Partial Differential Equations*. Cambridge University Press, Cambridge, 2005.

- 
- [31] J.T. Oden and K.S. Vemaganti. Estimation of local modeling error and goal-oriented adaptive modeling of heterogeneous materials, I. Error estimates and adaptive algorithms. *Journal of Computational Physics*, 164:22–47, 2000.
- [32] E. Stein, M. Ruter and S. Ohnibus. Adaptive finite element analysis and modelling of solids and structures. findings, problems and trends. *International Journal for Numerical Methods in Engineering*, 60:103–138, 2004.
- [33] S. Perotto. Adaptive modeling for free-surface flows. *ESAIM-Mathematical modelling and numerical analysis*, 40(3):469–499, 2006.
- [34] R.S. Johnson. *Singular Perturbation Theory: Mathematical and Analytical Techniques with Applications to Engineering*. Springer, 2004.
- [35] F. Verhulst. *Methods and Applications of Singular Perturbations, Boundary Layers and Multiple Timescale Dynamics*. Springer, 2005.
- [36] M.B. Giles and N.A. Pierce. Adjoint equations in CFD: duality, boundary conditions and solution behaviour. In *AIAA Computational Fluid Dynamics Conference, 13th, Snowmass Village, CO, June 29-July 2, 1997, Collection of Technical Papers. Pt. 1*, number A97-32424, pages 182–198. American Institute of Aeronautics and Astronautics, 1997.
- [37] W.K. Anderson and V. Venkatakrisnan. Aerodynamic Design Optimization on Unstructured Grids with a Continuous Adjoint Formulation. Number AIAA-97-0643. American Institute of Aeronautics and Astronautics, Inc., 1997.
- [38] B.I. Soemarwoto. *Multi-point aerodynamic design by optimization*. PhD thesis, Delft University of Technology, 1996.
- [39] E.J. Nielsen and W.K. Anderson. Recent Improvements in Aerodynamic Design Optimization On Unstructured Grids. *AIAA journal*, 40(6):1155–1163, 2002.
- [40] L. Xie. *Gradient-Based Optimum Aerodynamic Design Using Adjoint Methods*. PhD thesis, Virginia Polytechnic Institute and State University, 2002.
- [41] J.M. Cnossen, H. Bijl, B. Koren and E.H. van Brummelen. Model error estimation in global functionals based on adjoint formulation. In N.-E. Wiberg and P. Díez, editors, *Adaptive Modeling and Simulation*. ECCOMAS, CIMNE, 2003.

- [42] J.M. Cnossen, H. Bijl, B. Koren and E.H. van Brummelen. Adjoint based model adaptation for a linear problem. In *Proceedings of the 4<sup>th</sup> European Congress on Computational Methods in Applied Sciences and Engineering*, volume I, Jyväskylä, Finland, July 2004. ECCOMAS.
- [43] D.A. Venditti and D.L. Darmofal. Adjoint error estimation and grid adaptation for functional outputs: Application to quasi-one-dimensional flow. *Journal of Computational Physics*, 164:204–227, 2000.
- [44] D.A. Venditti and D.L. Darmofal. Grid adaptation for functional outputs: Application to two-dimensional inviscid flows. *Journal of Computational Physics*, 176:40–69, 2002.
- [45] C. Johnson, J.Hoffman and A. Logg. Topics in adaptive computational methods for differential equations. In *Congreso de Ecuaciones Diferenciales y Aplicaciones*, 2001.
- [46] J.T. Oden and T.I. Zohdi. Analysis and adaptive modeling of highly heterogeneous elastic structures. *Computer Methods in Applied Mechanics and Engineering*, (148):367–391, 1997.
- [47] L.M. Perko. A method of error estimation in singular perturbation problems with application to the restricted three body problem. *SIAM Journal on Applied Mathematics*, 15(3):738–753, 1967.
- [48] M.S. Krol. On the averaging method in nearly time-periodic advection-diffusion problems. *SIAM Journal on Applied Mathematics*, 51(6):1622–1637, 1991.
- [49] M. Ainsworth and I. Babuska. Reliable and robust a posteriori error estimation for singularly perturbed reaction-diffusion problems. *SIAM Journal on Numerical Analysis*, 36(2):331–353, 1999.
- [50] R. Vulcanovic and G. Hovhannisyanyan. A posteriori error estimates for one-dimensional convection-diffusion problems. *Computers & Mathematics with Applications*, 51(6–7):915–926, 2006.
- [51] R. Verfürth. Robust a posteriori error estimators for a singularly perturbed reaction-diffusion equation. *Numerische Mathematik*, 78(3):479–493, 1998.
- [52] H.-G. Roos, M. Stynes and L. Tobiska. *Numerical Methods for Singularly Perturbed Differential Equations, Convection-Diffusion and Flow Problems*. Springer, 1996.

- [53] A. Ern and J.-L. Guermond. *Theory and Practice of Finite Elements*. Springer, 2004.
- [54] G.E. Karniadakis and S.J. Sherwin. *Spectral/hp Element Methods for CFD*. Oxford University Press, 2005.
- [55] Y. Maday and A.T. Patera. Spectral element methods for the incompressible Navier-Stokes equations. *State-of-the-art surveys on computational mechanics*, pages 71–143, 1989.
- [56] M.O. Deville, P.F. Fischer and E.H. Mund. *High-Order Methods for Incompressible Fluid Flow*. Cambridge University Press, 2002.
- [57] C. Canuto, M. Hussaini, A. Quarteroni and T. Zang. *Spectral Methods in Fluid Dynamics*. Springer Verlag, 1990.
- [58] T.J.R. Hughes, M. Mallet and A. Mizukami. A new finite element formulation for computational fluid dynamics: II, beyond SUPG. *Computer Methods in Applied Mechanics and Engineering*, 54:341–355, 1986.
- [59] J.M. Cnossen, H. Bijl, M.I. Gerritsma and B. Koren. Goal-oriented model-error estimation in linear convection-diffusion problems. In P. Wesseling, E. O nate, and J. Périaux, editors, *Proceedings of the European Conference on Computational Fluid Dynamics*. ECCOMAS, 2006.
- [60] A. Griewank and A. Walther. Algorithm 799: Revolve: An implementation of checkpoint for the reverse or adjoint mode of computational differentiation. *ACM Transactions on Mathematical Software*, 26(1):19–45, 2000.
- [61] B. van Leer. On the relation between the upwind-differencing schemes of Godunov, Engquist-Osher and Roe. *SIAM Journal on Scientific and Statistical Computing*, 5:1–19, 1984.
- [62] B. van Leer. Towards the ultimate conservative difference scheme iii. upstream-centered finite-difference schemes for ideal compressible flow. *Journal of Computational Physics*, 23:263–275, 1977.
- [63] B. Koren. A robust upwind discretization method for advection, diffusion and source terms, volume 45: *Notes on Numerical Fluid Mechanics of Numerical Methods for Advection-Diffusion Problems* (C.B. Vreugdenhil and B. Koren, eds.), pages 117–138. Vieweg, Braunschweig, 1993.



- [64] P. Wesseling. *Principles of computational fluid dynamics*. Springer, 2000.
- [65] C. Hirsch. *Numerical computation of internal and external flows*, volume 1: Fundamentals of Numerical discretization. John Wiley & Sons, Chichester, 1988.
- [66] C. Hirsch. *Numerical computation of internal and external flows*, volume 2: Computational Methods for Inviscid and Viscous Flows. John Wiley & Sons, Chichester, 1988.
- [67] J.H. Ferziger and M. Perić. *Computational Methods for Fluid Dynamics*. Springer, 2002.
- [68] M.B. Giles. Discrete adjoint approximations with shocks. Report 02/10, Oxford University Computing Laboratory, 2002.
- [69] M.B. Giles and N.A. Pierce. Analytic adjoint solutions for the quasi-one-dimensional euler equations. *Journal of Fluid Mechanics*, 426:327–345, 2001.
- [70] M.B. Giles. Discrete adjoint approximations with shocks. In T. Hou and E. Tadmor, editors, *Proceedings of HYP2002*. Springer-Verlag, 2002.
- [71] P.M. Gresho. Incompressible fluid-dynamics - some fundamental formulation issues. *Annual Review of Fluid Dynamics*, 23:413–453, 1991.
- [72] K. Demirdzic, Z. Lilek and M. Peric. A collocated finite-volume method for predicting flows at all speeds. *International Journal for Numerical Methods in Fluids*, 16(12):1029–1050, 1993.
- [73] W.K. Anderson and D.L. Bonhaus. Airfoil design on unstructured grids for turbulent flows. *AIAA Journal*, 37(2):185–191, 1999.
- [74] J. Elliott and J. Peraire. Practical Three-Dimensional Aerodynamic Design and Optimization Using Unstructured Meshes. *AIAA Journal*, 35(9):1479–1485, 1997.
- [75] A.L. Moigne and N. Qin. Variable-Fidelity Aerodynamic Optimization for Turbulent Flows Using a Discrete Adjoint Formulation. *AIAA Journal*, 42(7):1281–1292, 2004.
- [76] G. Corliss, C. Faure, A. Griewank, L. Hascoët, and U. Naumann, editors. *Automatic Differentiation: From Simulation to Optimization*. Computer and Information Science. Springer, New York, NY, 2001.

- [77] M.B. Giles, M.C. Duta, J-D. Müller and N.A. Pierce. Algorithm developments for discrete adjoint methods. *AIAA Journal*, 41(2):198–205, 2003.
- [78] R. Giering and T. Kaminski. Recipes for adjoint code construction. *ACM Transactions on Mathematical Software*, 24(4):437–474, 1998.

# Appendix A

## Differentiation and linearisation of functionals

Let  $V$  denote a Banach space and  $N(\cdot; \cdot)$  and  $Q(\cdot)$  differentiable semilinear and possibly nonlinear differential functional, respectively, defined on  $V$ :

$$\begin{aligned} N &: V \times V \rightarrow \mathbb{R}, \\ Q &: V \rightarrow \mathbb{R}. \end{aligned}$$

$N$  is linear in all arguments following the semicolon. Differentiability of  $N(\cdot; \cdot)$  means that the following limits of Gâteaux derivatives exist:

$$N'(u; p, v) = \lim_{\theta \rightarrow 0} \theta^{-1} [N(u + \theta p; v) - N(u; v)], \quad (\text{A.1a})$$

$$N''(u; p, q, v) = \lim_{\theta \rightarrow 0} \theta^{-1} [N'(u + \theta q; p, v) - N'(u; p, v)], \quad (\text{A.1b})$$

$$N'''(u; p, q, r, v) = \lim_{\theta \rightarrow 0} \theta^{-1} [N''(u + \theta r; p, q, v) - N''(u; p, q, v)], \dots \quad (\text{A.1c})$$

For  $Q(\cdot)$  differentiability is also defined in the sense of an existing limit of the Gâteaux derivative:

$$Q'(u; p) = \lim_{\theta \rightarrow 0} \theta^{-1} [Q(u + \theta p) - Q(u)], \quad (\text{A.2a})$$

$$Q''(u; p, q) = \lim_{\theta \rightarrow 0} \theta^{-1} [Q'(u + \theta q; p) - Q'(u; p)], \quad (\text{A.2b})$$

$$Q'''(u; p, q, r) = \lim_{\theta \rightarrow 0} \theta^{-1} [Q''(u + \theta r; p, q) - Q''(u; p, q)], \dots \quad (\text{A.2c})$$

Since for fixed  $u$   $N(\cdot; \cdot)$  is a semilinear form in the argument following the semicolon, its derivatives such as  $N'(u; p, v)$  and  $N''(u; p, q, v)$  are bilinear or trilinear forms in the arguments following the semicolon. Derivatives of  $Q$ , for instance  $Q'(u; p)$  and  $Q''(u; p, r)$ , are semilinear and bilinear forms in its arguments following the semicolon.

With the derivatives defined, Taylor expansions with integral remainders can be constructed for functionals such as  $N$  and  $Q$ . Many forms of the expansions are possible, but the ones used in the derivation of the DWR modelling-error estimation are for the semilinear form  $N(\cdot; \cdot)$ :

$$N(u + v; w) - N(u; w) = \int_0^1 N'(u + s v; v, w) ds \quad (\text{A.3a})$$

$$N(u + v; w) - N(u; w) = N'(u; v, w) + \int_0^1 N''(u + s v; v, v, w)(1 - s) ds, \quad (\text{A.3b})$$

and for  $Q(\cdot)$ :

$$Q(u + v) - Q(u) = \int_0^1 Q'(u + s v; v) ds, \quad (\text{A.4a})$$

$$Q(u + v) - Q(u) = Q'(u; v) + \int_0^1 Q''(u + s v; v, v)(1 - s) ds, \quad (\text{A.4b})$$

$$Q(u + v) - Q(u) = \frac{1}{2}Q'(u; v) + \frac{1}{2}Q'(u + v; v) + \int_0^1 Q'''(u + s v; v, v, v)(1 - s)s ds. \quad (\text{A.4c})$$

## Appendix B

# The Galerkin spectral element method

In this appendix a short overview of some basic aspects of the Galerkin spectral element method (SEM) are given. A Galerkin spectral element approximation is used in space-time formulation to compute both the primal and dual solutions of the convection-diffusion and the convection equation (i.e. the fine and coarse model, respectively). For more details on Spectral Element Methods the reader is referred to the numerous literature on SEM, such as [54, 55, 56, 57].

The domain is divided into space-time slaps  $\Omega_n$  which are again divided into  $N_{el}$  non-overlapping subdomains  $\Omega_e$ :

$$\Omega_n = \bigcup_{e=1}^{N_{el}} \Omega_e.$$

With the finite dimensional subspace  $U^h \subset U$  with basis  $\phi_i$ , the approximating solution  $u^h \in U^h$  (as well as the dual solution  $p^h \in U^h$ ) can be written as the expansion:

$$u^h(x, t) = \sum_i^{N_{el}} u_i \phi_i(x, t) \quad (\text{B.1})$$

For the basis functions  $\phi_i$  two-dimensional Legendre polynomials are used, defined using the local element coordinates  $\boldsymbol{\xi} = (\xi, \eta)$ . The order of the polynomials are indicated by  $P$  and  $Q$  for the order in space and time, respectively, so the elemental degree of freedom is  $(P + 1)(Q + 1)$ .

**Numerical integration** Numerical integration is done through Gaussian quadrature based on the Gauss-Lobatto-Legendre roots. The weights for numerical integration are the corresponding Gauss-Lobatto-Legendre weights (GLL-weights). Gaussian quadrature is a very accurate integration method to compute integrals where the integrand is smooth. The evaluation of an integral using Gaussian quadrature in one dimension, for example in  $\xi$ , is done through the finite summation:

$$\int_{-1}^1 f(\xi) d\xi \approx \sum_{p=1}^{P+1} w_p f(\xi_p), \quad (\text{B.2})$$

where  $w_p$  is the GLL-weight factor and  $\xi_p$  the  $p$ -th GLL-root. To evaluate the integral in global coordinates  $(x, t)$ , equation (B.2) is multiplied by the determinant  $\frac{\partial x}{\partial \xi}$ . A similar expression can be derived for integrals with respect to  $\eta$ .

In constructing the spectral element matrices and computing the modelling error, the inner product of two functions needs to be evaluated over an elemental region  $\Omega_e$ . For two functions  $u(x, t)$  and  $v(x, t)$ , the inner product is computed using Gaussian quadrature:

$$\begin{aligned} (u, v)_{\Omega_e} &= \int \int_{\Omega_e} u(\xi, \eta) v(\xi, \eta) |J^e| d\xi d\eta \\ &\approx \sum_{p=1}^{P+1} \sum_{q=1}^{Q+1} w_p w_q u(\xi_p, \eta_q) v(\xi_p, \eta_q) |J_{pq}^e| = \mathbf{u}^T \mathbf{W} \mathbf{v}, \end{aligned} \quad (\text{B.3})$$

where  $\mathbf{u}$  and  $\mathbf{v}$  are the vectors containing the values of  $u$  and  $v$  evaluated in the GLL-roots. The weight matrix  $\mathbf{W}$  contains the GLL-weights  $w_p$  and  $w_q$ :

$$W_{ii} = w_p w_q |J^e(\xi_i)|, \quad (\text{B.4})$$

where  $J_{pq}^e$  is the Jacobian determinant.

**Numerical differentiation** Differentiation of  $u^h$  (and  $p^h$ ) with respect to the global coordinates  $x$  and  $t$  is achieved by applying the differentiation matrices  $D_x$  and  $D_t$ . These matrices are defined in terms of the local coordinates  $\xi$  and  $\eta$  by:

$$D_x = \Lambda \left( \frac{\partial \xi}{\partial x} \right) D_\xi + \Lambda \left( \frac{\partial \eta}{\partial x} \right) D_\eta, \quad (\text{B.5})$$

$$D_t = \Lambda \left( \frac{\partial \xi}{\partial t} \right) D_\xi + \Lambda \left( \frac{\partial \eta}{\partial t} \right) D_\eta, \quad (\text{B.6})$$

where  $\Lambda(\cdot)$  is a diagonal matrix that evaluates the function between brackets at the GLL-points. The local differentiation matrices  $D_\xi$  and  $D_\eta$  contain the derivatives of the Legendre polynomials with respect to the local coordinates  $\xi$  and  $\eta$ , respectively.





# Appendix C

## The finite volume method for the Burgers problem

In this appendix the discrete primal and dual problems are discussed. The discrete approach for the dual problem differs from the primal problem, due to the linearisation inherent to the dual problem.

### C.1 The discrete primal problem

For the inviscid Burgers problem the convective part is discretised explicitly in time with a non-linear flux evaluation:

$$\mathcal{L}_0^{k-1}(u^h) = \frac{u_i^k - u_i^{k-1}}{\Delta t} + \frac{\Delta F_i^{k-1}}{h} = 0, \quad 1 \leq i \leq J, \quad 0 < k \leq N, \quad (\text{C.1})$$

where  $u^h$  is the discrete solution vector,  $i$  the cell index,  $J$  = number of cells,  $h$  the cell size,  $k$  the time-level and  $\Delta t$  the time step,  $i, k \in \mathbb{N}$ . The initial time-level is  $k = 0$ . The flux residual  $\Delta F_i$  in a cell centre  $i$  is computed using the fluxes through neighbouring cell faces (indicated by  $i \pm 1/2$ ):

$$\Delta F_i = \begin{cases} F_{3/2} - \frac{1}{2}(a^0)^2 & i = 1, \\ F_{i+1/2} - F_{i-1/2} & 2 \leq i \leq J-1, \\ \frac{1}{2}(a^1)^2 - F_{J-1/2} & i = J, \end{cases} \quad (\text{C.2})$$

with  $a^0$  and  $a^1$  the values on the boundary conditions for the viscous case. In case of the inviscid Burgers equation  $a^0$  and  $a^1$  are replaced by the extrapolated values in case of an outflow boundary.

The flux  $F$  through a cell face is computed by means of the non-linear Engquist-Osher scheme, see [61], with left and right states  $u_L$  and  $u_R$ :

$$F(u_L, u_R) = \frac{1}{2} \left( \frac{1}{2} u_L^2 + \frac{1}{2} u_R^2 \right) - \frac{1}{2} \int_{u_L}^{u_R} |u| du. \quad (\text{C.3})$$

This can also be written as:

$$F(u_L, u_R) = \frac{1}{2} (u_L^+)^2 + \frac{1}{2} (u_R^-)^2, \quad (\text{C.4})$$

where:

$$u^- = \min(u, 0), \quad (\text{C.5a})$$

$$u^+ = \max(u, 0). \quad (\text{C.5b})$$

High-order accuracy is achieved by applying the so called  $\kappa$ -scheme, introduced by Van Leer [62] and extensively discussed in literature, for instance [64]. A value of  $\kappa = 1/3$  is applied, which yields a third-order upwind biased scheme. To prevent spurious oscillations in the solutions, the so called Koren flux limiter [63] is applied such that the resulting discretisation is monotonicity preserving (see, e.g., Wesseling [64]).

The dissipative operator on a non-uniform mesh is discretised by:

$$\mathcal{L}_d u^h = \mu \frac{h_- u_{i+1} - (h_+ + h_-) u_i + h_+ u_{i-1}}{\frac{1}{2} h_+ h_- (h_+ + h_-)}, \quad 1 \leq i \leq J, \quad (\text{C.6})$$

which can be derived from Taylor series for  $u_{i-1}$  and  $u_{i+1}$  considering the three grid points  $x_-$ ,  $x_i$  and  $x_+$  from figure C.1 with:

$$h_- = (h_{i-1} + h_i)/2 \quad \text{and} \quad h_+ = (h_i + h_{i+1})/2. \quad (\text{C.7})$$

For discretisation in the cells adjacent to the boundaries,  $u_{i-1}$  and  $u_{i+1}$  are replaced by  $a^0$  and  $a^1$ , respectively. For the viscous Burgers equation (5.1) with implicit discretisation of the dissipative operator we then obtain:

$$\mathcal{L}_0^{n-1}(u^h) + \mathcal{L}_d^n u^h = 0, \quad 1 \leq i \leq J, \quad 0 < n \leq N. \quad (\text{C.8})$$

## C.2 The discrete dual problem

The reason to discuss the discrete dual problem explicitly here, contrary to the discrete linear convection-diffusion case in section (4.5), is the linearisation required for the dual problem. In the linear convection-diffusion



Figure C.1: Unstructured triple grid

problem the dual equation is in fact the same as the primal equation, but it is solved backward in time with different boundary conditions and initial solution. For the discrete approach this has no significant consequences.

Two different approaches can be followed to find the discrete dual problems: the 'analytic' approach in which the analytical dual problems are discretised. The other approach is the 'discrete' approach in which the discrete dual operator is the transpose of the corresponding linear operator of the linearised primal problem, see for instance [36, 77, 37]. The latter approach is preferred since numerical equivalence between the linearised primal and dual problems is maintained, see also [77].

Since the primal equation is solved by a non-linear flux evaluation (C.2), the discrete primal equation (C.8) needs to be linearised. Therefore the Engquist-Osher scheme (C.3) is linearised by substituting  $u_L = \tilde{u}_L + u'_L$  and  $u_R = \tilde{u}_R + u'_R$  in (C.3):

$$\begin{aligned}
 F(u_L, u_R) &= \frac{1}{2} \left( \frac{1}{2} (\tilde{u}_L + u'_L)^2 + \frac{1}{2} (\tilde{u}_R + u'_R)^2 \right) - \frac{1}{2} \int_{\tilde{u}_L + u'_L}^{\tilde{u}_R + u'_R} |u| du \\
 &= \frac{1}{2} \left( \frac{1}{2} (\tilde{u}_L + u'_L)^2 + \frac{1}{2} (\tilde{u}_R + u'_R)^2 \right) \\
 &\quad - \frac{1}{2} \left\{ \int_{\tilde{u}_L}^{\tilde{u}_R} |u| du + (|\tilde{u}_R| u'_R - |\tilde{u}_L| u'_L) \right\}. \tag{C.9}
 \end{aligned}$$

For the coarse model equation we can have:

$$\tilde{F}(\tilde{u}_L, \tilde{u}_R) = \frac{1}{2} \left( \frac{1}{2} \tilde{u}_L^2 + \frac{1}{2} \tilde{u}_R^2 \right) - \frac{1}{2} \int_{\tilde{u}_L}^{\tilde{u}_R} |u| du. \tag{C.10}$$

Neglecting high-order terms in  $u'$  and subtracting the coarse model flux function (C.10) from equation (C.9) gives the flux function for the perturbation  $u'$ :

$$F'(u'_L, u'_R) = \frac{1}{2} (\tilde{u}_L u'_L + \tilde{u}_R u'_R) - \frac{1}{2} (|\tilde{u}_R| u'_R - |\tilde{u}_L| u'_L), \tag{C.11}$$

which can be rewritten using (C.5) as:

$$F'(u'_L, u'_R) = \tilde{u}_L^+ u'_L + \tilde{u}_R^- u'_R. \tag{C.12}$$

Linearising the full equation and subtracting  $\mathcal{L}_0^{n-1}(\tilde{u}^h) = 0$  yields for cell  $i$  at time-level  $n$ :

$$\frac{u_i^n - u_i^{n-1}}{\Delta t} + \frac{1}{h}(\tilde{u}_i^+ u_i' + \tilde{u}_{i+1}^- u_{i+1}' - \tilde{u}_{i-1}^+ u_{i-1}' + \tilde{u}_i^- u_i')^{n-1} - \mathcal{L}_d^n u_i^h = \mathcal{L}_d^n \tilde{u}^h. \quad (\text{C.13})$$

In a space-time system equation (C.13) is written as:

$$\mathbf{L}_h \mathbf{U}'_h = \mathbf{f}_h, \quad (\text{C.14})$$

with  $\mathbf{L}_h$  the discrete space-time operator of size  $(NJ) \times (NJ)$ ,  $\mathbf{U}'_h$  the solution vector of size  $(NJ)$  containing the solution at all time-levels and  $\mathbf{f}_h$  the discrete model residual. With zero initial perturbation,  $\mathbf{L}_h$  looks like:

$$\mathbf{L}_h = \begin{pmatrix} \mathbf{D}^1 & 0 & \dots & & \\ \mathbf{C}^1 & \mathbf{D}^2 & 0 & \dots & \\ 0 & \mathbf{C}^2 & \mathbf{D}^3 & 0 & \dots \\ & & \ddots & \ddots & \\ \dots & 0 & \mathbf{C}^{N-1} & \mathbf{D}^N & \end{pmatrix}. \quad (\text{C.15})$$

where  $\mathbf{C}$  is the convective matrix with the flux Jacobian entries and  $\mathbf{D}$  the matrix containing the discrete dissipative operator. At a specific time-level  $k$ , the system looks like:

$$\mathbf{C}^{k-1} u'^{k-1} + \mathbf{D}^k u'^k = \mathbf{f}_h^k, \quad (\text{C.16})$$

The dual operator is found by transposing the matrix  $\mathbf{L}_h$ , see also [36, 77, 37], and yields:

$$\mathbf{L}_h^T = \begin{pmatrix} \mathbf{D}^1 & \mathbf{C}^{T,1} & 0 & \dots & \\ 0 & \mathbf{D}^2 & \mathbf{C}^{T,2} & 0 & \dots \\ & 0 & \mathbf{D}^3 & \mathbf{C}^{T,3} & 0 \\ & & \ddots & \ddots & \\ & & 0 & \mathbf{D}^{N-1} & \mathbf{C}^{T,N-1} \\ \dots & & \dots & 0 & \mathbf{D}^N \end{pmatrix}. \quad (\text{C.17})$$

Since the dissipative matrix  $\mathbf{D}$  is symmetric, we have  $\mathbf{D}^T = \mathbf{D}$  and therefore the boundary condition implementation from the primal problem is maintained in the dual problem. On a specific time level  $k$  the dual operator is given by:

$$\mathbf{C}^{T,k} p_h^{k+1} + \mathbf{D}^k p_h^k = g_h^k. \quad (\text{C.18})$$

with  $p_h$  the discrete dual solution and  $g_h^k$  the linearised quantity of interest, as in (2.5) for linear systems<sup>1</sup>. Time integration of the convective term in the dual problem is again explicit, since the dual problem is solved backward in time. Likewise, the dissipative operator is discretised implicitly. Transposing the convective matrix  $\mathbf{C}$  yields for the dual flux functions the following formulation:

$$F_{i-1/2}^* = (u_0^-)_i p_{i-1} + (u_0^+)_i p_i, \quad (\text{C.19a})$$

$$F_{i+1/2}^* = (u_0^-)_i p_i + (u_0^+)_i p_{i+1}. \quad (\text{C.19b})$$

Here, the convective velocity  $u_0$  is not included in the upwinding, contrary to the primal linearised flux function (C.12). The dual flux residual  $\Delta F_i^*$  is defined in the same way as the primal flux residual (C.2), with a similar boundary condition treatment. The discrete dual equation for a certain cell  $i$  at time level  $k$ , can now be written as:

$$\frac{p_i^k - p_i^{k+1}}{\Delta t} - \frac{(\Delta F_i^*)^{k+1}}{h} - \mathcal{L}_d^k p^h = 0. \quad (\text{C.20})$$

High-order accuracy for the dual solution is achieved by employing the same  $\kappa$ -scheme as used for the primal problem. To prevent spurious oscillation in the dual solution, also the Koren flux limiter from the primal problem is used.

---

<sup>1</sup>When the quantity of interest is defined on a boundary we have  $g_h = 0$  and the quantity of interest appears as boundary condition for the dual problem



# Dankwoord

Dit proefschrift is mede tot stand gekomen door de ondersteuning van de Technologie Stichting STW, waarvoor veel dank. Verder wil ik mijn dank betuigen aan iedereen die mij heeft geholpen bij het onderzoek en het schrijven van dit proefschrift.

In het bijzonder wil ik mijn ouders Wybe en Jans en mijn zus Hester bedanken voor de liefde en steun tijdens de meer, maar ook minder voortvarende periodes van mijn promotie. Met trots kan zeggen dat ik een familie heb die ook tot mijn beste maatjes behoren. Verder dank ik al mijn andere vrienden voor alle positieve energie en goede afleiding die zij me gaven tijdens mijn promotieonderzoek en hopelijk blijven geven. TSJOCH!





# Curriculum Vitae

- May 23, 1975 Born in Nijland, The Netherlands.
- 1987 – 1993 Bogerman College, Sneek, The Netherlands.  
Secondary school, Atheneum.
- 1993 – 1998 Hogeschool van Amsterdam, The Netherlands.  
Bachelor's degree in Operational Technology, direction  
of Aircraft Operations.  
Research subject: 'Development and testing of  
an artificial stall warning device for sailplanes'.
- 1998 – 2002 Delft University of Technology, The Netherlands.  
Master's degree in Aerospace Engineering.  
Research subject: 'Numerical computation of the flow  
inside an industrial transport blower'.
- 2002 – 2007 Delft University of Technology, The Netherlands.  
Ph.D. student at Faculty of Aerospace Engineering,  
Aerodynamics Group.  
Funded by the Dutch Technology Foundation STW.  
Research subject: 'Goal-oriented modelling-error  
estimation for hierarchical models of a different type'.